

**DYNAMIC BEHAVIOUR OF UNREINFORCED
MASONRY BUILDING**

Md. Aminul Islam

MASTER OF SCIENCE IN CIVIL ENGINEERING (STRUCTURAL)

DEPARTMENT OF CIVIL ENGINEERING
BANGLADESH UNIVERSITY OF ENGINEERING AND TECHNOLOGY
DHAKA-1000, BANGLADESH

DECEMBER 2018

Dynamic Behaviour of Unreinforced Masonry Building

by

Md. Aminul Islam
(Student No: 1014042239 P)

A thesis Submitted to the Department of Civil Engineering, Bangladesh University of Engineering and Technology, Dhaka, in partial fulfillment of the degree for Masters of Science in Civil Engineering (Structural)



Department of Civil Engineering
Bangladesh University of Engineering and Technology
Dhaka-1000, Bangladesh

December 2018

The thesis titled "Dynamic Behaviour of Unreinforced Masonry Building", submitted by Md. Aminul Islam, Roll No. 1014042239P, Session October 2014, to the Department of Civil Engineering, Bangladesh University of Engineering and Technology, has been accepted as satisfactory in partial fulfillment of the requirements for the degree of Master of Science in Civil Engineering (Structural) on December 17, 2018.

Board of Examiners



Dr. Raquib Ahsan
Professor
Department of Civil Engineering
Bangladesh University of Engineering & Technology, Dhaka-1000

Chairman
(Supervisor)



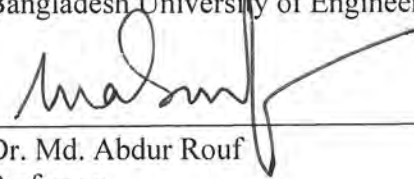
Dr. Ahsanul Kabir
Professor and Head
Department of Civil Engineering
Bangladesh University of Engineering & Technology, Dhaka-1000

Member
(Ex-Officio)



Dr. Shohel Rana
Associate Professor
Department of Civil Engineering
Bangladesh University of Engineering & Technology, Dhaka-1000

Member



Dr. Md. Abdur Rouf
Professor
Department of Civil Engineering
Ahsanullah University of Science & Technology
74/A, Green Road, Farmgate, Dhaka-1215

Member
(External)

DECLARATION

This is hereby declared that the work titled "Dynamic Behaviour of Unreinforced Masonry Building" is the outcome of research carried out by me under the supervision of Dr. Raquib Ahsan, Professor in the Department of Civil Engineering, Bangladesh University of Engineering and Technology, Dhaka-1000. It is also declared that this thesis or any part of it has not been submitted elsewhere for the award of any degree or diploma.



Md. Aminul Islam

ACKNOWLEDGEMENT

All praise is due to the Almighty, the most Merciful.

I would like to express my heart-felt gratitude to my supervisor, Dr. Raquib Ahsan, Professor, Department of Civil Engineering, BUET, Dhaka for his constant supervision of this work. He helped me a lot in every aspect of this work and guided me with proper directions.

I would like to thank Dr. Shohel Rana, Associate Professor, Department of Civil Engineering, BUET, Dhaka for his valuable suggestion in this research work. I would also like to thank Dr. M.A. Ansary, Professor, Department of Civil Engineering, BUET, Dhaka for his support in this research work.

My sincere thank goes to faculty members and technical personnel of BUET-JIDPUS who have helped me during this study. Finally, I am greatly thankful to my family who have always paved the way to reach my goal with their unfailing love and support.

ABSTRACT

Unreinforced masonry (URM) buildings represent a large portion of the buildings stock around the world and in Bangladesh. During the construction of those buildings very little or no seismic design requirements are considered. Recent earthquakes e.g. Gorkha earthquake in 2015 have shown that many such buildings are seismically vulnerable; therefore, the demand for dynamic analysis and upgrading strategies of these buildings has become increasingly stronger in the last few years. Moreover, no dynamic test on unreinforced masonry building made by Bangladeshi indigenous material is done yet. Therefore, the objective of this study is to understand the dynamic behavior of a typical unreinforced masonry (URM) building of Bangladesh. For this purpose, a half-scale URM room having dimension of 6' x 5' (length x width) with 5' height and 2.5" wall thickness, were built using M2 type mortar (c:s=1:4) and half-scale brick units. Time history of Imperial Valley Earthquake was chosen as an input motion because pre-dominant frequency (5Hz) of Scaled Imperial Valley earthquake is close to the model's pre-dominant frequency (6Hz). The URM model was tested as reference specimen. Then, the reference specimen was retrofitted on all faces using 18 gauge wire mesh (12mm x 12mm (1/2" x 1/2") opening), which is locally available and retested again. The tests were conducted on a uni-directional earthquake simulator. The tests show that wire mesh may be used as a retrofitting material for URM buildings. The retrofitting measure decreased the specimens' lateral deflection by a factor of 4.3 to 4.8 times compared to the reference (URM) specimen for different intensities of earthquake. In addition, the upgrading enhanced the cracking resistance and the energy dissipation of the upgraded specimen. The upgraded specimen is able to undergo 1.42 times more acceleration than reference specimen. Lateral load of the reference model is compared with the prescribed shear force (capacity) as per Bangladesh National Building Code (BNBC 1993). The reference model failed after reaching the capacity. Therefore, the code is conservative in terms of lateral load resistance capacity.

Table of Contents

ACKNOWLEDGEMENTS	i
ABSTRACT	ii
List of Figures	vi
List of Tables	ix
Chapter 1 INTRODUCTION	1
1.1 General	1
1.2 Background of the Study	2
1.3 Specific Objectives of the Study	3
1.4 Organization of the Thesis	4
Chapter 2 LITERATURE REVIEW	5
2.1 Introduction	5
2.2 Tectonics and Seismicity of Bangladesh	5
2.3 Historical Earthquakes around Bangladesh	8
2.3.1 Regional earthquakes	8
2.3.2 Earthquakes and masonry buildings	11
2.4 URM Building stock in Bangladesh	15
2.5 Type, Joint and Bond of Masonry Wall	15
2.6 Mechanical Properties of Masonry Materials	17
2.7 Research Conducted Using Bangladeshi Indigenous Masonry	19
2.8 Review of Experimental Work on Masonry Walls and Buildings	19
2.8.1 Review of the dynamic experiments	19
2.8.2 Review of the in-plane behavior	22
2.8.3 Review of the out of plane behavior	24
2.9 Summary	27
Chapter 3 EXPERIMENTAL PROGRAM	28
3.1 Introduction	28
3.2 Material Properties	28
3.2.1 Properties of bricks	28
3.2.2 Properties of sand	29
3.2.3 Properties of cement	31
3.2.4 Properties of mortar	31
3.2.5 Prism test	31

3.3	Specimen Preparation	32
3.3.1	Foundation pad casting and curing	32
3.3.2	Masonry room construction	33
3.3.3	Diaphragm design	34
3.3.4	Retrofitting of the masonry model	35
3.4	Experimental Setup	36
3.4.1	Axial load estimation	36
3.4.2	Instrumentation	38
3.4.2.1	Accelerometers	38
3.4.2.1	Laser displacement sensors	39
3.4.3	Earthquake simulator	40
3.4.4	Selection of time history	40
3.5	Simulation of the Seismic Action and Procedure	41
3.6	Dynamic Testing	43
Chapter 4 EXPERIMENTAL RESULTS AND DISCUSSION		45
4.1	Introduction	45
4.2	Observations	45
4.2.1	Input acceleration comparison	46
4.2.2	Damage pattern	46
4.3	Displacement Characteristics	53
4.3.1	Displacement characteristics of reference model	53
4.3.2	Displacement characteristics of retrofitted model	55
4.4	Load Characteristics	56
4.4.1	Load characteristics of reference model	56
4.4.2	Load characteristics of retrofitted model	60
4.4.3	Tested lateral force and calculated lateral force comparison	64
4.5	Sine Wave Excitation	64
4.5.1	Sine wave excitation of reference model	64
4.5.2	Sine wave excitation of retrofitted model	65
Chapter 5 CONCLUSIONS AND SUGGESTIONS		67
5.1	Introduction	67
5.2	Conclusions	67
5.3	Suggestions	68

5.4	Limitations	69
	REFERENCES	70

List of Figures

Figure 1.1 Common Failure of Unreinforced Masonry Building	3
Figure 2.1 Plate Boundary between Indian and Eurasian Plate (CDMP, 2009)	6
Figure 2.2 Historical Earthquakes along Indian and Eurasian Plate Boundary (CDMP, 2009)	7
Figure 2.3 Seismicity classified in Magnitude in and around Bangladesh (Data is offered with courtesy of Dr. T. M. Al-Hussaini)	12
Figure 2.4 Components of unreinforced brick (left) and unreinforced concrete block (right) walls	12
Figure 2.5 Typical Construction of Unreinforced Masonry Building (Ansary, 2003)	13
Figure 2.7 URM damage in USA (FEMA P-774, 2009)	14
Figure 2.8 URM Buildings in the major city Dhaka, Chittagong and Sylhet (Shaw et.al., 2013)	16
Figure 2.9 Joints in brick wall	17
Figure 2.10 Different type of bond in brick wall	18
Figure 2.11 Process of specimen collapse in the shaking table test (Nakagawa et.al., 2012)	20
Figure 2.12 Damage Mechanism of Tested Building Model (Ali et. al., 2012)	21
Figure 2.13 In-plane failure modes of a laterally loaded URM wall	23
Figure 2.14 Test Setup for out of plane test of masonry wall (Derakhshan and Ingham, 2008)	25
Figure 2.15 Specimen on the shake table for out of plane test (Simsir et.al., 2004)	26
Figure 3.1 Dimensions of reduced scale brick	29
Figure 3.2 Gradation curve of Local Sand	30
Figure 3.3 Gradation curve of Sylhet Sand	30
Figure 3.4 Detailing of foundation pad and cross section	33

Figure 3.5 Foundation pad on shake table	33
Figure 3.6 Unreinforced Masonry Room	35
Figure 3.7 Reinforcement in Slab	37
Figure 3.8 Retrofitting Procedure	37
Figure 3.9 Weights on the slab	38
Figure 3.10 Locations of LDSs	39
Figure 3.11 Instruments used in the test	40
Figure 3.12 Pre-Dominant Frequencies of model structure	42
Figure 3.13 time history and Pre-Dominant Frequencies of scaled Imperial Valley earthquake	42
Figure 3.14 Complete Experimental Setup	43
Figure 4.1 Input Motion in Reference Model (1.05g)	47
Figure 4.2 Input Motion in Retrofitted Model (1.49g)	48
Figure 4.3 First crack develop at 0.83g in east wall (out of plane wall)	48
Figure 4.4 Cracks develop at 0.92g ((a) horizontal crack in out plane wall (b) horizontal and zigzag cracks in-plane wall)	49
Figure 4.5 Horizontal Cracks develop at 0.92g (south wall)	50
Figure 4.6 Cracks developed at 1.05g in east wall (out-of-plane wall) ((a) south-east face (b) north-east face)	51
Figure 4.7 Cracks developed at 1.05g in north wall (in-plane wall) ((a) north-east face (b) north-west face)	51
Figure 4.8 Cracks developed at 1.05g in south wall (in-plane wall)	52
Figure 4.9 Cracks developed at 1.05g in west wall (out of plane wall)	52
Figure 4.10 Crack developed in Retrofitted Model ((a) vertical crack in north wall (b) separation of wall from base)	53
Figure 4.11 Position of Sensors measuring displacements of walls	54
Figure 4.12 Approximate deflected shape of In-Plane wall for maximum top deflection	54

Figure 4.13 Approximate deflected shape of Out-of-Plane wall for maximum top deflection	55
Figure 4.14 Approximate Deflected shape of In-Plane wall for maximum top deflection	55
Figure 4.15 Approximate Deflected shape of Out-of-Plane wall for maximum top deflection	56
Figure 4.16 Input acceleration vs normalized lateral force and displacement of Reference Model	58
Figure 4.17 Lateral Force vs. Relative Lateral Displacement of in-plane wall for different input acceleration	59
Figure 4.18 Roof Acceleration vs. Relative Lateral Displacement of out-of-plane wall for different input acceleration	60
Figure 4.19 Input acceleration vs normalized lateral force and displacement of Retrofitted Model	62
Figure 4.20 Force-Displacement relationship for in-plane wall of Retrofitted Model	63
Figure 4.21 Force-Displacement relationship for out-of-plane wall of Retrofitted Model	63
Figure 4.22 Acceleration at Roof Level for Sine Wave Excitation	65
Figure 4.23 In-plane and Out of plane displacement of Reference Model for Sine wave excitation	65
Figure 4.24 In-plane and Out of plane displacement of Retrofitted Model for Sine wave Excitation	66

List of Tables

Table 2.1 List of Historical Earthquake (CDMP, 2009)	9
Table 2.2 Earthquake Epicenter Location (Chakravorti et.al., 2015)	9
Table 3.1 Compressive strength of reduced scale brick (127mm x 57mm x 38mm)	29
Table 3.2 Properties of Sand used for the construction purpose	30
Table 3.3 Compressive Strength of Mortar	31
Table 3.4 Compressive Strength of scaled masonry unit (127mm x 57mm x 191mm)	32
Table 3.5 Compressive Strength of real size masonry unit (241mm x 114mm x 349mm)	32
Table 3.6 Scale factors of the Cauchy similitude	36
Table 3.7 Accelerometer locations	39
Table 3.8 Accelerometer locations	39
Table 3.9 Specification of Shake Table of BUET-JIDPUS	41
Table 4.1 Seismic Input and corresponding Peak Acceleration at Shake Table	46
Table 4.2 Crack Distribution in different acceleration of Reference Model	49
Table 4.3 Maximum displacement and maximum lateral force of Reference Model	57
Table 4.4 Maximum displacement and maximum lateral force of Retrofitted Model	61

Chapter 1

INTRODUCTION

1.1 General

The oldest material, which is widely used in the construction industry, is masonry (Moffet, 2016). Even now a day, in different parts of the world including Bangladesh, people are constructing masonry buildings. There some of the inherent advantages of masonry construction e.g. low construction cost, pleasant aesthetics, and good heat and sound insulation properties, which have made it the material of choice for home construction. In Bangladesh, masonry buildings are integral and very important part of housing infrastructure and there are some important historical heritages.

However, URM structures are very much vulnerable when it is subjected to lateral forces, especially those located in seismically active parts of the world such as Bangladesh. Failure of URM structures is reported as one of the main causes of human casualties during earthquakes. Masonry is a non-homogeneous and anisotropic composite structural material, consisting of masonry units and mortar (Elgwady et. al., 2002). Due to this complex brick-mortar interface behavior, the accurate prediction of lateral load resistance or seismic load resistance capacity of unreinforced masonry (URM) wall is very difficult. This heterogeneity in a masonry structure makes for complex seismic behavior. To determine the strength, stiffness and dynamic characteristics of masonry, experimental research is of great importance because of the complex behavior of such composite structures.

Since Bangladesh situated in the high seismic zone, those buildings including the historical heritages are in very high risk. For simulation of structural behavior of such buildings, performance of embedded joint (bed joints and head joints) is important from the point of view of seismic design. Mostly vertical loading is considered during the design of masonry. While, the structural elements such as walls in URM buildings which were designed for vertical loads only, have to carry lateral load as well during an earthquake. As a result, those structures are vulnerable to earthquake because there is no ductility provision, which is necessary to withstand a certain level of earthquake. The heavy damage inflicted on masonry structures by the some historic earthquake such as earthquake in 1987 in Srimangal, Bangladesh; 1997 in Umbria-Marche, Italy; 2005 in Kashmir, Pakistan; 2008 in Wenchuan, China; 2010 in Darfield, New Zealand; 2015 in

Gorkha, Nepal all especially emphasized the high seismic vulnerability of unreinforced masonry structures. Both experimentally and theoretically have gained much attention since the 1990s in different countries. But in Bangladesh, there are very few experimental evidence/results of lateral load resistance capacity of URM wall/buildings and no actual dynamic loading test have been conducted yet now. So, complicated and intensive research on the seismic behavior of masonry structures is essential. Therefore, the objective of this research is to understand the failure mode of unreinforced masonry structures with particular material properties, aspect ratio and boundary conditions under dynamic loading.

1.2 Background of the Study

One of the prime causes of mass casualties in an earthquake around the world is collapse of the non-engineered structures (Macabuag et. al., 2012). Many advanced researches have been conducted in the field of earthquake engineering; yet non-engineered structures often remain outside the scope. Along with many architectural heritage structures, there are many residential buildings in Bangladesh, which are non-engineered unreinforced masonry (URM) buildings. Those buildings are vulnerable due to lack of lateral load resisting system. Figure 1.1 shows some common failure of URM in Bangladesh. Rather than demolishing those URM buildings, we need to seek a favorable option for the improvement of their seismic performance. However, before adopting any retrofitting or rehabilitation technique, it is essential to understand the seismic behavior of URM buildings. A number of experimental researches e.g. In-plane tests (Elgwady et. al., 2002; Russwill et. al., 2007; Fam et. al., 2002; Capozucca, 2011), out of plane tests (Derakhshan and Ingham, 2008; Simsir et. al., 2004) and shake table tests (Elgwady et. al., 2002; Simsir et. al., 2004; Hanazato et. al., 2008; Ersubasi and Korkmaz, 2010) were conducted in different countries using their indigenous materials and testing equipment. In these researches, particular construction technique, aspect ratio, boundary condition, brick-mortar interface and axial loading have been focused. Findings from the researches reveal that use of improper masonry units, formation of inappropriate wall cross sections, inadequate or no connection of crossing walls, irregular wall openings, improper roofing and lack of continuity in seismic load path are the main cause of damage of URM buildings.



a) Damage at Rangpur, 1897 earthquake



b) Damage due to 2003 Rangamati Earthquake

Figure 1.1 Common Failure of Unreinforced Masonry Building

In Bangladesh, there are very few (Das, 2016; Asif et. al., 2017) experimental evidence of lateral load resistance capacity of URM wall and no actual dynamic loading test have been conducted. The exact crack pattern will, of course, depend on the wall boundary conditions and the aspect ratio of the URM elements. Seismic actions are bidirectional and the URM can perform in both in-plane and out-of-plane direction. Therefore, the objective of this research is to understand the overall dynamic behavior, in-plane and out of plane behavior of walls as well as the failure pattern of masonry structures with retrofit (using wire mesh) and without retrofit under shaking table tests in context of Bangladesh.

1.3 Specific Objectives of the Study

The total analysis on the dynamic behavior of masonry building/room is done based on the experimental results. Shaking table test is carried out with the following specific objectives:

1. Investigation of the system (overall building) response of bare masonry building/room and retrofitted masonry building/room over a range of real earthquake scenario in shaking table.
2. Investigation of in-plane deformation characteristics of URM building/room for bare model and retrofitted model.
3. Investigation of out-of-plane deformation characteristics of URM building/room for bare model and retrofitted model.

4. Investigation of the lateral load resistance capacity of URM building/room and comparison with Bangladesh National Building Code (BNBC 1993).
5. Investigation of lateral load variation with deformation for both in-plane and out-of-plane wall (for bare model and retrofitted model).
6. Investigation of behavior of URM building for sine (various frequency) wave excitation.

1.4 Organization of the Thesis

The full thesis is organized as follows:

Chapter 2, based on a literature study, gives an overview of past research on the dynamic behavior, in-plane and out of plane behavior of masonry structures.

In Chapter 3, the masonry model construction and experimental test setup are presented where includes material properties, specimens preparation. This chapter presents the step by step construction procedure of base, building and slab, retrofitting process as well as adopted procedure for testing under dynamic loading in detail. It includes the details of the time history selection, test instrumentation, specification of shake table, testing procedure and data acquisition process.

Chapter 4 presents the results from the experimental program of this research. The experimental results and observation for different earthquake loading are also included in this chapter. General dynamic behavior mechanisms for common masonry structures in Bangladesh are presented. In-plane, out of plane behavior, lateral load characteristics, deflection characteristics etc. of masonry wall are also presented in this chapter.

A summary of the results drawn from the whole research work, limitation of the research and recommendation for future research are included in Chapter 5.

Chapter 2

LITERATURE REVIEW

2.1 Introduction

Masonry, a material as old as the civilizations, due to relatively low capacity in tension and shear it performs poorly in seismic events. Lang (2000) carried out vulnerability analysis of existing masonry buildings on a target area in Basel, Switzerland; the study shows that between 45% and 80% of the existing URM buildings will experience heavy damage or destruction during an earthquake of intensity VIII (MSK). In context of Bangladesh, condition of masonry building is much more severe, approximately 50% of the private housing units have no lateral load resisting system e.g. continuous lintel, in the earthquake prone areas like Chittagong, Sylhet (Ansary, 2003). Those masonry buildings may create much more casualties during earthquakes as seen in the 2015 Gorkha earthquake in Nepal and because of this the performance of masonry buildings need to be known before taking any precautionary measures like retrofitting. It is miserable but true that no dynamic test is done on masonry buildings in Bangladesh.

The aim of this chapter is to present a conceptual framework for the present research problem. A thorough and extensive literature review of seismicity around Bangladesh, masonry buildings stock in Bangladesh and review of different studies incorporating the dynamic performances of unreinforced masonry buildings is undertaken. This study also provides a brief review of literature regarding the in-plane and out-of-plane behavior of unreinforced masonry. Experimental investigations reported in the literature are included.

2.2 Tectonics and Seismicity of Bangladesh

Bangladesh is in high seismic zone and the Indian Plate, Eurasian Plate and Burma Plate are in the around of Bangladesh which is shown in Figure 2.1. The Indian Plate is subducting under the Eurasian Plate and moving towards the north with slip rate of 6 cm/year (CDMP, 2009). Figure 2.2 shows the number of large earthquakes generated along the plate boundary under the compressive condition. The northern extension of the subduction fault and the Sagaing Fault System for a right-lateral fault, from off Sumatra which are the two subduction fault on the eastern edge of the Indian Plate. The average slip rate of the Sagaing Fault is 6 cm / year (Yeats et. al., 1997), and many historical earthquakes occurred along this fault. Along the northern extension of the

subduction fault, the historical earthquake is inferred to be only the 1762 event with the recurrence period of about 900 years (CDMP, 2009). The recurrence period of this subduction fault is too long. Along the Sagaing Fault, most of the strain along the plate boundary on the north of Sumatra may be consumed.



Figure 2.1 Plate Boundary between Indian and Eurasian Plate (CDMP, 2009)

The East-West trending Dauki Fault goes through on the southern fringe of Shillong Plateau shown in Figure 2.1. In the north of Bangladesh, Shillong Plateau is located and the Dauki Fault may cross to the northern extension of the subduction fault in Sylhet. But the relationship between the Dauki Fault and plate boundary fault is not understood now (CDMP, 2009).

The earthquake occurred in and around Bangladesh (seismicity classified in magnitude) is shown in Figure 2.3. As shown in these figures, the seismicity in Bangladesh is high along the plate boundary between the Indian and Eurasian Plate and the Dauki Fault. In the last 150 years, Bangladesh experienced damages of five earthquakes having magnitude over 7.0 (Richter scale) (Shaw et al. 2013). Shaw et al. (2013) revealed that there are subduction zones in the east and north of Bangladesh in which three major active faults have been studied so far having potential to generate 7.0 to 8.5 magnitude earthquake.

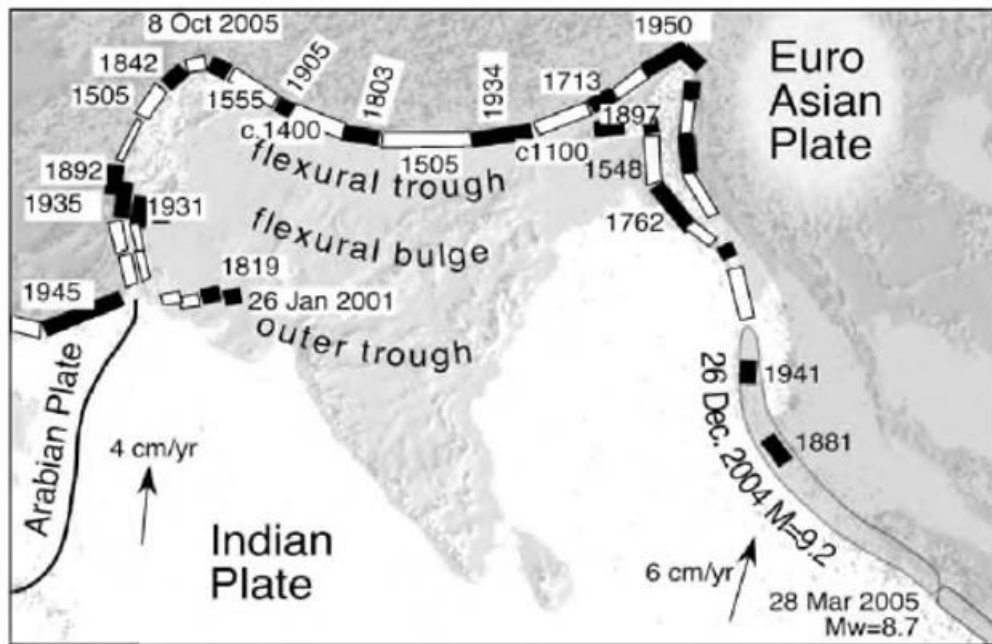


Figure 2.2 Historical Earthquakes along Indian and Eurasian Plate Boundary (CDMP, 2009)

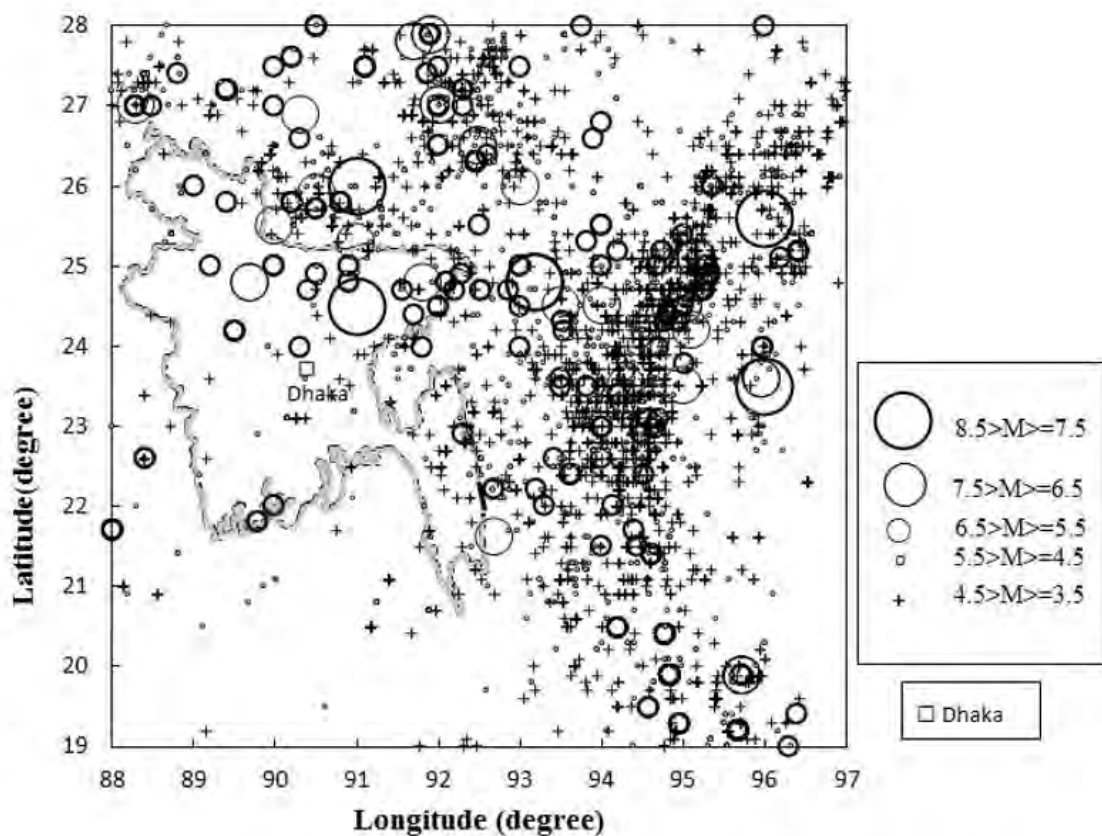


Figure 2.3 Seismicity classified in Magnitude in and around Bangladesh (Data is offered with courtesy of Dr. T. M. Al-Hussaini)

2.3 Historical Earthquakes around Bangladesh

Bangladesh is directly joined with Calcutta, Assam, Tripura in the Northern, Western and North-Eastern part respectively which are the most earthquake prone regions. From the perspective of the geological location, five major faults are significant for the occurrences of devastating earthquakes (Al Zaman and Monira, 2017) and those are:

- Bogra fault zone
- Tripura fault zone
- Sub-Dauki fault zone
- Shillong plateau and
- Assam plateau

In the last 250 years, there are available information of earthquakes occurrence in and around Bangladesh. The earthquake record reveals that after 1900 more than 100 moderate to large earthquakes occurred in Bangladesh, out of which more than 65 events occurred after 1960 (Chakravorti et.al., 2015). Table 2.1 shows some historic earthquake occurred in and around Bangladesh. From the earthquake record, it is clear that the frequency of earthquakes in the last 30 years is increased. This increase in earthquake activity is an indication of propagation of fractures from the adjacent seismic zones. From the previous earthquake records, it is obviously known that these boundaries are the most dangerous zone for occurring earthquake.

Bangladesh faced a large numbers of earthquakes in past and still continued. The earthquakes that occurred in Bangladesh and its surrounding area are large. Earthquakes having lower magnitudes ($M_s \leq 5.0$) bear less threat for us. But, those type earthquakes shown in Table 2.2, having higher magnitudes ($M_s \geq 7.0$) - are very destructive for any country.

2.3.1 Regional earthquakes

Historical earthquakes will help us to understand the seismicity of Bangladesh and ultimately it will help us to take necessary action for the built up earthquake resilience country. Brief description of earthquakes occurred in and around Bangladesh, are presented below:

(a) Great Bengal Earthquake, 1885: This earthquake also known as Manikganj Earthquake with a magnitude of 7.0 occurred on 14th July, 1885. The location of

epicenter was at Satura, Manikganj that is 170 km away from the capital Dhaka. The event was associated with the Jamuna fault. The people of Sirajganj, Bogra, Rangpur, Sherpur, Mymensingh, Jamalpur, Dhaka, Pabna, Bihar, Sikkim, Manipur (India) and Burma (Myanmar) felt this strong earthquake. The main shock was strong enough to destroy numerous residential buildings, important public buildings and great loss of life had occurred. Poor quality constructions were one of the main causes of damage. The main shock was followed by a series of aftershocks and the earthquake was associated with significant ground rupture. From the analysis of the macroseismic data, the isoseismal intensity at around 80 km distance was estimated as VII (Islam, 2010).

Table 2.1 List of Historical Earthquake (CDMP, 2009)

Year	Ms	Depth (km)	Source Area
1762	?	?	Chittagong-Arakan
1858	6.5	?	Sandway, Myanmar
1869	7.5	48	Cachar, India
1885	7	72	Sirajganj, Bangladesh
1897	8.1	60	Assam, India
1906	5.5	?	Calcutta, India
1912	7.9	25	Mandalay, Myanmar
1918	7.6	14	Srimangal, Bangladesh
1930	7.1	60	Dhubri, India
1934	8.3	33	Bihar, India-Nepal
1938	7.2	60	Mawlaik, Myanmar
1950	8.6	25	Assam, Himalaya
1954	7.4	180	Manipur, India
1975	6.7	112	Assam, India
1984	5.7	4	Cachar, India
1988	6.6	65	Bihar, India-Nepal
1997	5.6	35	Sylhet, Bangladesh
1997	5.3	56	Bangladesh-Myanmar
1999	4.2	10	Maheskhali, Bangladesh

? No Record

Table 2.2 Earthquake Epicenter Location (Chakravorti et.al., 2015)

Name of Earthquake	Fault Name	Time of Occurrence	Magnitude	Distance from Dhaka (in km)
Cachar Earthquake	Tripura	1869	7.5	250
Bengal Earthquake	Bogra	1885	7.0	170
Great Indian Earthquake	Assam	1897	8.7	230
Srimangal Earthquake	Sub-Dauki	1918	7.0	150
Dhubri Earthquake	Bogra	1930	7.1	250

(b) Meghalaya Earthquake, 1889: This earthquake with a magnitude of 7.5 occurred in Hills of Meghalaya State of India, on 10th January, 1889. There is no enough information about this earthquake. It affected the Sylhet town and its surrounding regions (Al Zaman and Monira, 2017).

(c) Great Indian Earthquake, 1897: The powerful Great Indian Earthquake occurred on 12th June 1897. The epicenter was 230 km away from Dhaka (Al Zaman and Monira, 2017) and located at 25.84N, 90.38E in Assam. The focal depth was reported to be 60 km (Islam et.al., 2010). Although the initial magnitude was reported to be 8.7, Ambraseys and Bilham (2003) later reported it as 8.0-8.1. The earthquake almost totally destroyed settlements and small towns on the western part of the Shillong Plateau, and caused heavy damage in surrounding districts, chiefly due to the extensive liquefaction of the ground (Islam et.al., 2010). Intensity in Dhaka for this earthquake was VI, which was re-estimated by Ambraseys and Bilham (2003). The large area over which loose deposits liquefied and the size of the area over which the shock was felt, are similar to those produced by other large earthquakes of New Madrid 1811, Bihar-Nepal 1934 and Assam 1950 (Islam et.al., 2010).

(d) The Sreemangal Earthquake, 1918: This earthquake of July 18, 1918 occurred at Moulavi Bazar, Sylhet which is 150 km from the capital Dhaka. Reported focal depth was around 14 km. Magnitude was reported to be 7.6. The main shock, which lasted about 12 secs, damaged almost every house in the epicentral area (Islam et.al., 2010). The greatest damage occurred in the tea garden areas of the Balisera, Doloi and Luskerpore valleys. The brick built buildings were severely destroyed within this area and minor effects were observed in Dhaka. Most of the area where the earthquake was violent enough damaged all or nearly all brick buildings.

(e) Dubri Earthquake, 1930: The Great Dhubri Earthquake of 3rd July 1930 occurred in Dubri, Assam. Reported focal depth was around 60 km. Magnitude was reported to be 7.1. Heavy damage and destruction of most of the constructions in the area around the villages of Dubri were occurred. Ground fissure and liquefaction-induced damages were majority in the zone covering the towns of Rangpur, Lalmanirhat, Cooch Bihar, Alipur Duar, eastern region of Brahmaputra River, and Tura town in Garo hills (Islam et.al., 2010). This earthquake had disastrous result in northern Bengal and in Western Assam and was felt very distinctly over a wide area, extending from Dibrugarh and

Manipur in the east to Chittagong and Calcutta in the South to Patna in the west and beyond the frontiers of Nepal, Sikkim and Bhutan in the North.

(f) Mikirhills Earthquake, 1945: The Earthquake occurred during 8th July, 1945 with magnitude to be 6.7. The epicentral distance of the third isoseist (IV-MMI) was considered as 260 km (Islam et.al., 2010).

(g) Medinipur Earthquake, 1964: The Earthquake was felt on 15th April, 1964. The magnitude of this earthquake was recorded to be 5.5. The mean epicentral distance of the third isoseist (III-MMI) was considered as 162 km (Islam et.al., 2010).

(h) Moheshkhali Earthquake, 1999: The Earthquake of magnitude 5.1 and focal depth 10 km occurred on 22th July, 1999. The Epicenter was 21.61N, 91.96E near Moheshkhali Island. The mean epicentral distance of the third isoseist (V-MMI) was considered as 17.5 km (Islam et.al., 2010).

(i) Bay of Bengal Earthquake, 2009: The earthquake occurred on 11th August 2009. The magnitude of this earthquake was 7.5. The epicenter of that earthquake was located at the North Andaman Islands of the Bay of Bengal and seacoast of Myanmar. It was strongly felt from Dhaka but fortunately, no heavy damages occurred.

(j) Myanmar Earthquake, 2016: This earthquake occurred on 24th August 2016. The magnitude of this earthquake was 6.8. The epicenter of this earthquake was in 25 kilometers west of Chauk in Myanmar. In Chittagong and Dhaka, this earthquake was strongly felt. Three people died in Myanmar but in Bangladesh, no casualties were reported but 20 people were seriously injured.

2.3.2 Earthquakes and masonry buildings

Unreinforced masonry can be defined generally as masonry in which no reinforcement is used. Earthen materials are the main component of masonry and the sub-types are listed below. The most common unreinforced masonry materials used for the walls of buildings are brick and hollow concrete block, which are illustrated in Figure 2.4.

- Brick: clay that is fired to a hard consistency.
- Hollow concrete block: “concrete masonry unit”, commonly known as “cinder block”.
- Hollow clay tile: similar to concrete block in shape, having hollow cells.

- Stone: can be “dressed” or cut into rectangular blocks, or used in its natural shape.
- Adobe: mud poured into the form of walls or made into sun-dried bricks.

The most common type of unreinforced masonry building in the Bangladesh is constructed of brick walls, shown in Figure 2.5. The masonry walls around the exterior, and sometimes similar walls in the interior, bear up under the weight that is delivered to them by floor or roof beams. For this reason, they are called bearing walls.

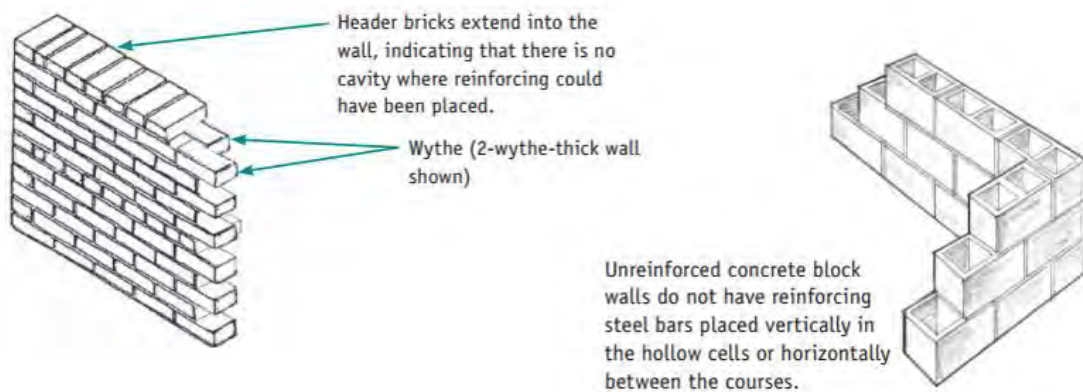


Figure 2.4 Components of unreinforced brick (left) and unreinforced concrete block (right) walls



Figure 2.5 Typical Construction of Unreinforced Masonry Building
(Ansary, 2003)

When the ground shakes during an earthquake, numerous examples from around the world show URM buildings are likely to partially or completely collapse. When they collapse, these buildings harm residents and people in the surrounding area.

Figure 2.6 illustrates the damage in masonry buildings in Bangladesh due to earthquake. During the 1897 Assam earthquake, almost 90% of masonry structure suffered some kind of damage (Ansary, 2003).



a) Sub-Divisional Officer's Bangalow, Kishorganj (Sreemangal Earthquake of July 8th, 1918)



b) Damage at Sirajganj, 1897 Earthquake

Figure 2.6 Damage of Unreinforced Masonry Building in Bangladesh
(Ansary, 2003)

Not only in Bangladesh, collapse of unreinforced masonry buildings are very common in the world. According to FEMA P-774, 2009, In USA, 82% percent of the brick buildings suffered more than minor damage, and 7% collapsed or were demolished during Charleston Earthquake (M 7.7), South Carolina in 1886. Forty percent of the unreinforced masonry buildings were severely damaged or collapsed at Santa Barbara Earthquake (M 6.2), Southern California in 1925. In the City of Long Beach (adjacent to the City of Los Angeles), 54% of the unreinforced masonry buildings ended up with damage that ranged from significant wall destruction to complete collapse at Long Beach Earthquake (M 6.3), Southern California in 1933. In 20% of the cases, damage fell in the categories of either damage to more than half the wall area, partial collapse, or complete collapse. In 1983, out of 37 unreinforced masonry buildings—the core of the Coalinga business district—only one escaped damage. Sixty percent were damaged to the extent of having more than half of their walls ruined, up to complete collapse at Coalinga Earthquake, Central California. In Loma Prieta Earthquake (M 7.1), Northern California, 374 (16%) of the 2,400 unreinforced masonry buildings in the region

experienced damage severe enough to require that they be vacated. Figure 2.7 illustrates the debris from collapsing second story masonry walls in USA.



a) Debris resulting from the 1886 Charleston, South Carolina Earthquake



b) Heavily damaged Hotel Californian, 1925 Santa Barbara, California earthquake.



c) URM building damage, 1933 Long Beach, California earthquake



d) Upper story wall collapse, with resulting fatalities

Figure 2.7 URM damage in USA (FEMA P-774, 2009)

Earthquakes destroyed Port-au-Prince in 1751, and again in 1770. As a result of these disasters the local authorities forbade building with masonry. The 2010 earthquake caused significant damage to Port-au-Prince and other cities. More than 200,000 structures were damaged or had collapsed, including many essential buildings, such as the Presidential Palace and the headquarters of the United Nations Stabilization Mission in Haiti (Nakagawa et. al., 2012). These buildings use a variation of confined masonry construction comprising weak hollow concrete blocks (HCBs) with lightly reinforced and non-ductile beams and columns (Nakagawa et. al., 2012).

Nepal about more than 5,000,000 buildings and houses were damaged and about half those which of had collapsed (Miyamoto and Amir, 2012) due to Gorkha earthquake in

2015. The adobe construction, wooden framed houses and rubble stone masonry constructions are more popular in villages of Nepal, meanwhile most of the urban and suburbs constitute majority fraction of stone or brick masonry buildings constituting around 20% of reinforced concrete (RC) construction (Miyamoto and Amir, 2012). The failure of masonry structures occur due to the following reasons: lack of anchorage, anchor failure, in-plane failures, out-of-plane failure, combined in-plane and out-of-plane effects and diaphragm-related failures. Many older URM-buildings lack positive anchorage of the floors and roof to the URM-walls, which contribute to sudden failure under seismic excitation.

2.4 URM Building stock in Bangladesh

It is estimated that there are 326,000, 182,000, and 52,000 buildings in Dhaka, Chittagong, and Sylhet City Corporation areas respectively (Shaw et.al., 2013). Figure 2.8 shows the percentage of unreinforced masonry buildings in Dhaka, Chittagong and Sylhet. Besides this data, in the rural area almost all of the buildings are made by brick or mud. Sometimes they use wood, bamboo and tin. CDMP (2009) conducted vulnerability assessment in three major cities e.g. Dhaka, Chittagong and Sylhet. They surveyed total 326825 buildings in Dhaka and 82629 of them are masonry buildings. In Chittagong, they found 39447 are masonry buildings among 182277 surveyed buildings. In addition, for Sylhet, it is 23827 out of 52176 surveyed buildings.

2.5 Type, Joint and Bond of Masonry Wall

Type of Masonry Walls

Type of masonry walls are listed below.

Cavity Wall: Comprising two limbs each built up as single or multi wythe units and separated by a 50 to 115 mm wide cavity. The limbs are tied together by metal ties or bonding units for structural integrity.

Curtain Wall: This wall subject to transverse lateral loads, and laterally supported by vertical or horizontal structural member where necessary. This is a non-load bearing and self-supporting wall.

Faced Wall: In this wall, facing and backing of two different materials are bonded together to ensure common action under load.

Load Bearing Wall: This wall is designed to carry an imposed vertical load in addition to its own weight, together with any lateral load.

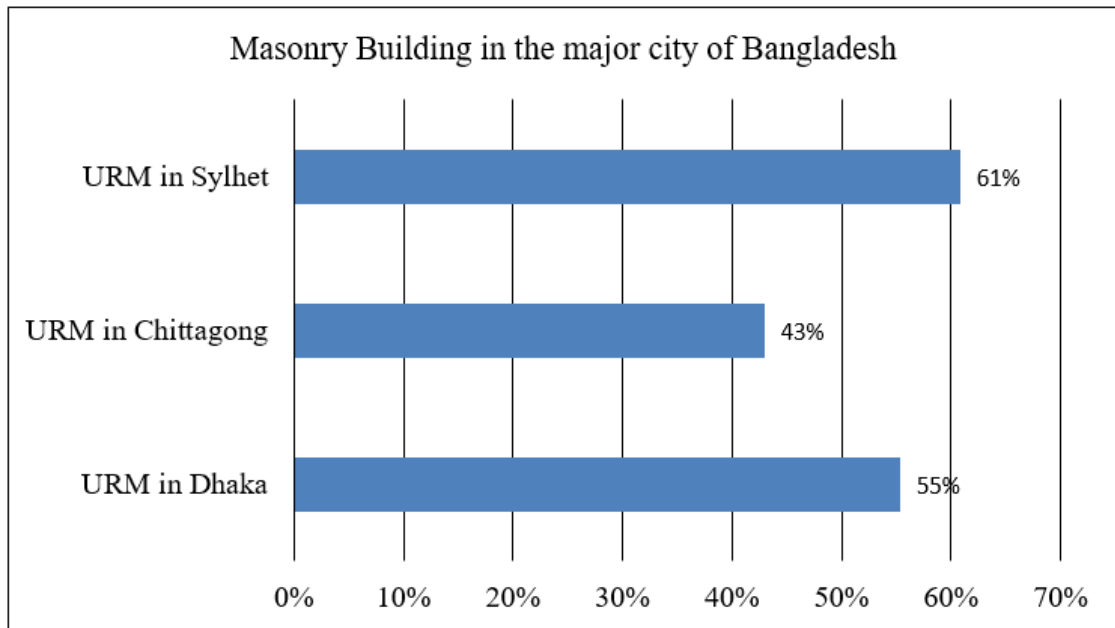


Figure 2.8 URM Buildings in the major city Dhaka, Chittagong and Sylhet (Shaw et.al., 2013)

Partition Wall: This is an interior non load bearing wall, one story or part story in height.

Panel Wall: This is an exterior non load bearing wall in framed structure, supported at each story but subject to lateral loads.

Shear Wall: This is a load bearing wall, designed to carry horizontal forces acting in its own plane with or without vertical imposed loads.

Veneered Wall: A wall in which the facing is attached to the backing but not so bonded as to result in a common action under load.

Joints on Masonry Wall

Bed joints: this is a horizontal joint in the masonry units

Collar joints: the vertical, longitudinal, mortar or grouted joints

Head joints: this is a vertical joint in the masonry units

Bond of Brick Wall

Stretcher Bond: The length of the brick is along with the face of the wall

Header Bond: The width of the bricks is along the direction of the wall

English Bond: This bond consists of alternate course of stretchers and headers. It is the most commonly used methods and considered the strongest

Flemish Bond: It comprises of alternative headers and stretchers

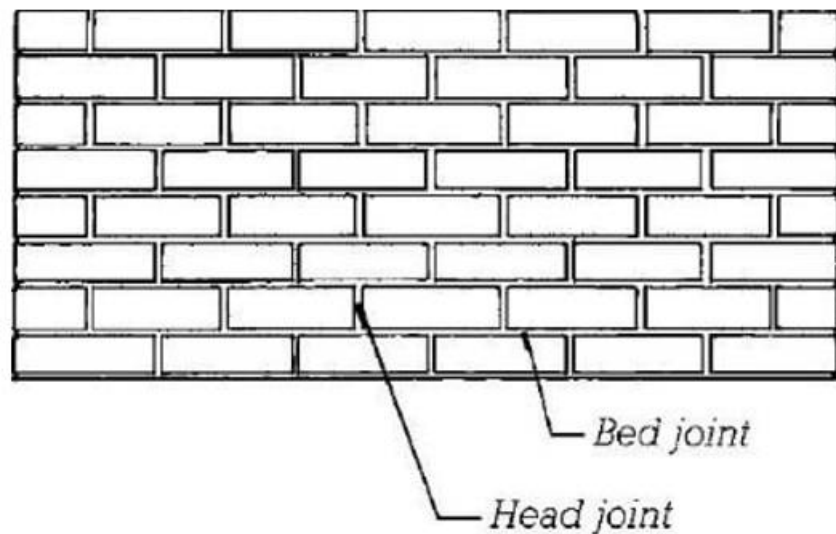


Figure 2.9 Joints in brick wall

2.6 Mechanical Properties of Masonry Materials

It is well known that, masonry is a nonhomogeneous material consisting of bricks and mortar. Both component have certain strength and deformation characteristics. Only a certain combination or quality of bricks and mortar can give a good result for bearing walls. The strength is also very much dependent on good workmanship. This section will cover properties of mortar and masonry units will be discussed.

Mortars

The characteristics of mortars have a big influence on the quality of brickwork. Both strength and workability of mortars are very much dependent on batching and mixing. For good bonding in between bricks and to take up all irregularities in the bricks, the workability of mortar must be well. Stiffness and plasticity are dependent on workability. The stiffness is dependent upon how much water there is added to the

mortar. How much water to add depends on purpose we are using mortar. The plasticity is a term for how easy the mortar can be formed. The grading of the aggregate also has a certain influence on the plasticity, the closer the grading is to the ideal curve the better the plasticity.

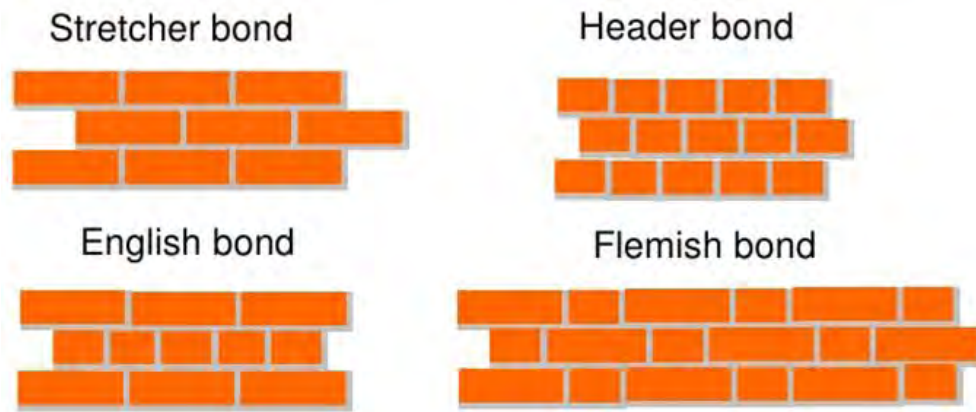


Figure 2.10 Different type of bond in brick wall

According to BNBC (1993), Mortar shall consist of a mixture of cementitious material. Cementitious materials for mortar shall be one or more of the following: lime, masonry cement, Portland cement and mortar cement should meet the specification in ASTM C150. Mortar for masonry construction other than the installation of ceramic tile shall conform to the requirements of ASTM C270. The sand for mortar should be clean, sharp and free from salt and organic contamination. Most natural sand contains a small quantity of silt or clay. A small quantity of silt improves the workability. Specifications of sand should conform to ASTM C144 standard. Mixing water for mortar should be clean and free from contaminants. Different mortar strengths are obtained by changing the aggregate ratio. Mortars, having lime as a binder normally, have a strength of 0.5 to 1 MPa, cement-lime mortars strength varies from 1 to 10 MPa and pure cement mortar strengths ranges from 10 to 20 MPa. For curing, instruction in ASTM C270 need to be followed.

Masonry

The tensile strength of masonry is very low, in the order of 1.5% to 2% of its compressive strength. Due to heavy specific gravity, it is capable of resisting axial load but is weak in resisting tensile and shear load and very weak in the level of ductility. As a result, it is no longer recommended to build unreinforced masonry buildings in

seismic prone regions. Because of specific characteristics of each constituent, especially the masonry unit, it is not easy to predict the mechanical characteristics of a specific masonry construction type by knowing only the characteristics of its constituent materials, mortar and masonry units. It is therefore important that, for each type of masonry, experiments should be carried out to correlate the strength characteristics of constituent materials with the characteristics of masonry.

2.7 Research Conducted Using Bangladeshi Indigenous Masonry

In Bangladesh, very few experimental researches is done on masonry. Some cyclic loading test (Das, 2016; Asif et. al., 2017) was done on masonry wall unit. In those experiments, lateral reverse cyclic loading was applied on masonry walls and the same walls retested after retrofitting using ferrocement. However, no dynamic test is done on masonry wall or buildings yet now. Therefore, the objective of this study is to conduct shaking table test on Unreinforced Masonry Building (URM).

2.8 Review of Experimental Work on Masonry Walls and Buildings

The main goal of this section is to review the experimental works have been done in the field of masonry structures. Experimental studies on masonry buildings/room show simpler and clearer damage patterns, which occur without the influences of other components. This can help to define the principal response of a complex masonry structure. Many experimental programme have been performed on this aspect, e.g. in-plane, out of plane and dynamic. Those three behavior will be explored and discussed in this section.

2.8.1 Review of the dynamic experiments

A dynamic collapse test was conducted on 3m x 3m brick masonry house using Pakistani bricks (Nakagawa et. al., 2012). The test was performed in a one-direction horizontal large-scale shaking table. The model structure exhibited a sufficient horizontal resistance to withstand the Bam and JMA Kobe earthquake excitations without developing cracks. A large pulse shock loading with a velocity of 40 cm/s and an acceleration of 1.7g, the structure develop cracks. Figure 2.11 shows the model building collapse. The tested structure was very strong compared to the structures in the developing countries. Therefore, it was anticipated that good workmanship could reduce the levels of damage of masonry-based houses in developing countries.



Figure 2.11 Process of specimen collapse in the shaking table test
(Nakagawa et.al., 2012)

In situ dynamic testing of masonry building model was conducted by means of underground explosions simulating earthquake ground motions (Ali et. al., 2012) for evaluating the seismic behavior (damage pattern and failure modes) and performance (lateral resistance capacity) of building models. Three different explosions were used with a peak ground acceleration of 0.15g, 0.48g and 0.70g. Figure 2.12 depicts the damage mechanism of tested building. Good performance of the structure was due to the good quality construction materials. Special type of constituent, which was used in mortar, called khaka. Which renders mortar with high strength, causing increase in the shear strength and tensile strength of masonry. Good behavior was also seen due to the global rocking.

A half-scale two-storey brick masonry house was tested for the investigation of seismic performance (Bothara et. al., 2010). The test was conducted under longitudinal and transverse shakings on a shake table. The building did not collapse under base excitations with PGA up to 0.8g. In-plane walls was mostly damaged in zones of high shear stress, notably the bottom storey and out-of-plane walls was damaged in zones of high response acceleration, starting from the top storey 1/3 scale 4 story unreinforced masonry buildings with masonry shear walls and wood-framed floors were tested on shaking table for quantification of vulnerability curves of typical Portuguese “gaioleiro” buildings (Candeisa et. al., 2004), before and after reinforcement.

Unidirectional shaking table test of two full-scale unreinforced masonry buildings - simulate the buildings in the Groningen region of the Netherlands - had been performed for assessing the seismic vulnerability of buildings (Guerrini et. al., 2004). Terraced house collapsed at a PGA of 0.31g and detached house collapsed state at a PGA of 0.68g. Detached house exhibits more than twice peak ground acceleration when reached to near collapse condition.

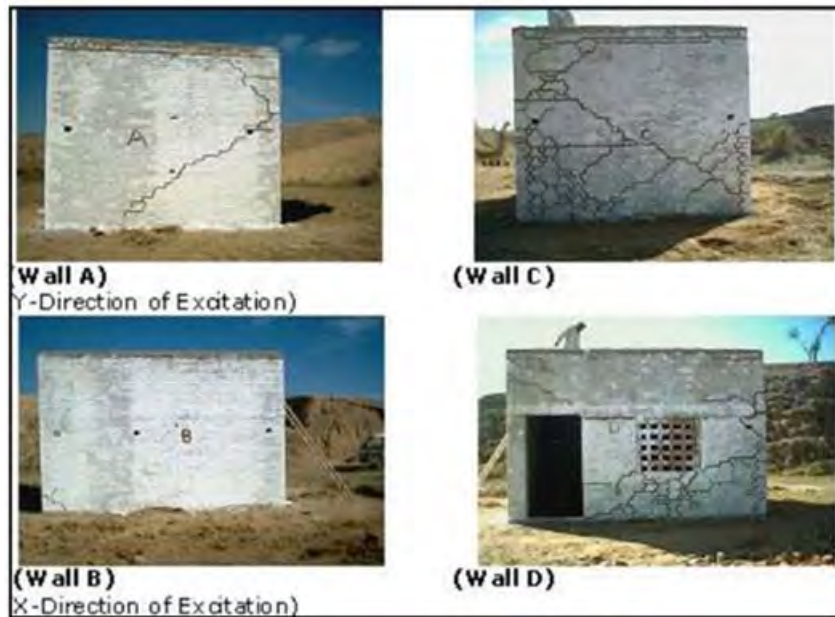


Figure 2.12 Damage Mechanism of Tested Building Model (Ali et. al., 2012)

Shaking table test on 1/3 scale four storey reinforced masonry building- made by construction waste recycled brick- was conducted (Hui Su et. al., 2014). To simulate the seismic response under different earthquake levels, three type of seismic wave e.g. EL-Centro seismic wave, Taft wave and artificial wave were used. The performance of the structure was good with certain seismic fortification requirement in the region of intensity VIII.

119 shaking table tests were carried out on 1:2 scaled, 24 masonry models and the tests were conducted on bared and strengthened (retrofitted by horizontal steel beam, horizontal tendons and wooden planks) structured (Benedetti et. al., 1998).

1/3-scale model of a two-story unreinforced masonry structure which was symmetric about the transverse axis but asymmetric to some degree about longitudinal axis, was tested in an earthquake simulator (Hong et. al., 2004). This type of structure is common in low seismicity region of Korea. The test result revealed that the overall torsional deformation was increased as the amplitude of the shaking table motion was increased and there was no out of bending failures in the walls perpendicular to the loading direction.

Dynamic shake table test on two 2/3 scale masonry building built in accordance with traditional construction codes of practice for the Italian Central and Southern Appenine Zones was conducted (Dlce et. al., 2008). The first model was tested in a base isolated

configuration and reinforced by the confinement of masonry (CAM) strengthening system and the second model was tested unstrengthened in a fixed base configuration. It is anticipated that, the CAM strengthened structure is five times more strength than its unreinforced counterpart.

The seismic behavior of mixed RC-URM buildings was observed by performing shaking table test (Tondelli et. al., 2013) on half-scaled four storey structure. The tested structure has shown a more evenly spread level of damage as the two lowest storeys.

Shaking table test on unreinforced masonry (URM) and reinforced masonry (RM) were conducted (Lourenco et. al., 2013) in which concrete blocks were used as construction materials. Crack patterns and deformation features of the tested buildings were compared. Great differences were observed in terms of cracking density and cracking path in which URM building represents only 62.5% of input energy attained by RM. In terms of displacement RM model exhibits much more homogeneous and ductile behavior than URM.

Partially grouted, nominally reinforced (PG-NR) concrete block walls were tested under in-plane seismic loading in a shake table (Kasparik et. al., 2014). This test was done in Meguro Lab, Tokyo University (Nesheli et al., 2006). Shaking table test on full-scale retrofitted and non-retrofitted masonry building were conducted using sinusoidal input motion, ranging from 2 Hz to 35 Hz with amplitude from 0.05g to 1.4g. For any given run, shake table acceleration was compared with the seismic intensity scale of Japan Meteorological Agency (JMA).

2.8.2 Review of the in-plane behavior

To establish the behavior of unreinforced masonry (URM) walls subjected to combined compression and shear, several studies were carried out in the past. The influence of some parameters on the shear strength of URM was investigated through a series of experimental researches. In-plane failure mechanisms of URM walls subjected to earthquake actions can be summarized as shown in Figure 2.13 (Elgawady et.al., 2007; Capozucca, 2011). These failure modes are as follows:

Shear failure: This kind of failure will occur in the walls with low aspect ratios and high axial loads. Diagonal cracks developed in the wall either follow the path of the bed

and head joints for relatively strong bricks and weak mortars or may go through the masonry units in case of relatively weak bricks and strong mortars, or both.

Sliding failure: In this kind of failure, the upper part of the wall will slides on the lower part of the wall. In the case of low vertical loads and/or low friction coefficient, which may be due to poor quality mortar, horizontal cracks in the bed joints can form a sliding plane extending along the wall length.

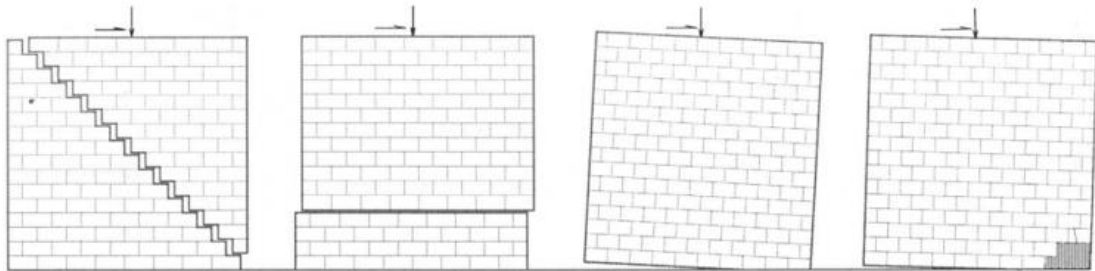


Figure 2.13 In-plane failure modes of a laterally loaded URM wall

Rocking and toe crushing failure: In the case of high moment/shear ratio or improved shear resistance, the wall may be set into rocking motion or toe crushing depending on the level of the applied normal force.

Many research on in-plane behavior of masonry wall was conducted in the past years. The behavior of masonry specimens before and after retrofitting using fiber-reinforced polymer (FRP) is investigated (Elgawady et.al., 2007) under constant gravity load and incrementally increasing in-plane loading cycles. It can be revealed from the test that the single-side retrofitting/upgrading significantly improved the lateral strength, stiffness, and energy dissipation of the test specimens. The reference specimen had mixed modes of failure, namely rocking, sliding, and toe crushing.

In-plane cycling loading test of historic unreinforced masonry (HURM) wall was performed strengthening by horizontal-vertical and diagonal using Carbon Fiber Reinforced Polymers (CFRP) after damage (Capozucca, 2011). In plane cyclic loading test of three type of load bearing wall with various types of head and bed joint was carried out [50]. Experimental behavior was modeled with four types of nonlinear finite-element models.

In-plane pseudo-static testing on a single unreinforced masonry wall, which was built to replicate typical New Zealand construction of the early 20th Century has been

conducted (Russell et. al., 2007). The results of this test was compared with the predicted performance calculated using existing New Zealand desktop assessment methods for unreinforced masonry. Currently available New Zealand guidelines successfully predicted the failure mode and limiting strength of a single URM wall with low axial load.

Indeed, the shaking-table tests on the in-plane seismic response of masonry walls conducted by Wight and Kowalsky (2007) demonstrated reduced structural stiffness and increased wall displacement at reduced loading levels. They also defined sliding as a typical, but small component of overall in-plane wall displacement.

A state of review of the existing models, which are used for the prediction of the in-plane load-bearing capacity of masonry piers, subjected to seismic actions, are analyzed (Calderini and Cattari, 2008). The aim of the review is to assess the reliability of those models, they are based on, by discussing the hypotheses. In this context, nonlinear finite element analyses are performed and different experimental data available in the literature are analyzed and compared.

In the last few years, several static cyclic and limited dynamic experimental tests have been carried out to investigate the in-plane behavior of URM walls retrofitted using FRP (Moon, 2004; Abrams and Lyncy, 2001).

2.8.3 Review of the out of plane behavior

Modelling the out-of-plane seismic behavior of masonry wall using the discrete element method and an SDOF analytic model was performed (Shawa et.al., 2011) and the obtained results compared with the shaking table test results. Both modelling approaches were capable to reproduce the experimental results in terms of maximum rotation and time history dynamic response.

A series of test e.g. static, free-vibration, dynamic tests using harmonic support and impulse support, and earthquake support motion were conducted on unreinforced brick masonry wall panels subjected to out of plane bending (Griffith et.al., 2004) and for the displacement based analysis, an empirical force-displacement relationship was proposed.

To delineate the nonlinear force-displacement relationship of out-of-plane behavior of unreinforced stone masonry walls, tri-linear force-displacement models (Ferreira et.al.,

2012) were constructed based on three different energy criteria and compared with experimental tests.

For in situ testing of abandoned traditional masonry houses, an experimental test setup was developed (Costa et.al., 2010). The aim of this test program was to characterize the out-of-plane behavior of unreinforced stone masonry walls and strengthening techniques recommended for post-earthquake interventions.

Uniform out-of-plane loading on New Zealand unreinforced masonry (URM) walls were applied to see the performance (Derakhshan and Ingham, 2008). The test was done on a full-scale URM wall with a slenderness ratio (h/t) of 16 with different levels of pre-compression (0 kPa, 20 kPa, 40 kPa). The tested simply supported wall is shown in Figure 2.14.



Figure 2.14 Test Setup for out of plane test of masonry wall
(Derakhshan and Ingham, 2008)

Out of plane behavior of masonry bearing wall was observed conducting a shaking table test (Simsir et.al., 2004) and the experimental results then compared with the SDOF and MDOF computational model. The tested wall is shown in Figure 2.15. The performance of the model was very well despite intense ground motion and slenderness ratio.

Pseudo static out of plane tilting test was carried out on dry masonry blocks with frictional behavior to study the out of plane behavior of masonry wall with different corner connection (Shi et.al., 2008). The comparison of the experimental results with the analytical predictions from the program FaMIVE was done. Figure 2.16 shows the collapse behavior of different out-of-plane damage mechanisms of dry masonry wall.

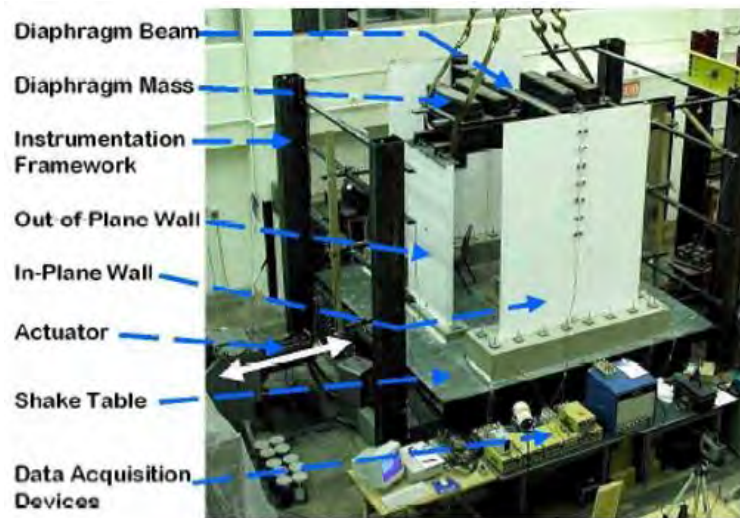


Figure 2.15 Specimen on the shake table for out of plane test (Simsir et.al., 2004)



(a) Mechanism A (b) Mechanism D (c) Mechanism B1 (d) Mechanism B2 (e) Mechanism G

Figure 2.16 Collapse behavior of different out-of-plane damage mechanisms

(Shi et.al., 2008)

Tri-linear force-displacement models were constructed for unreinforced masonry (URM) walls subjected to out-of-plane uniform loads (Derakhshan et.al., 2009). Uniform loading was applied on the surface of the walls using a system of airbags.

Out-of-plane uniform static loading on a full-scale URM wall with different levels of pre-compression was applied to investigate the basic characteristics of URM buildings in New Zealand (Derakhshan and Ingham, 2008). Tri-linear model was developed and it was found that the differing levels of overburden significantly changed the shape of the tri-linear model.

For the analysis of the nonlinear dynamic behavior of unreinforced masonry walls subjected to out-of-plane loads, a theoretical model has been developed (Hamed and Rabinovitch, 2008). The capabilities of the theoretical model have been examined through numerical examples and through comparison to test results available in the literature. A numerical study quantifies some aspects of the dynamic behavior of the masonry wall is presented. It is shown that the dynamic behavior of the wall is a nonperiodic or even chaotic one, which is influenced by the various physically and geometrically nonlinear effects.

2.9 Summary

Seismic behavior of unreinforced masonry is now the concerning topic because of the damage of masonry due to earthquake. On-site investigations, experimental and theoretical modeling are the three main way to identify the seismic behavior of unreinforced masonry. Among them, recently, experimental studies using dynamic loading have received more attention. This dynamic testing is the more practical way to obtain more understanding of practical dynamic collapse behavior and its development in masonry structures. These dynamic testing can provide much understanding regarding the development of stress, stiffness and displacement during the shaking of mechanical models. Most shaking-table, studies in the literature have focused on the mechanical status of the masonry structure and/or the dynamic responses of models of buildings typical of some local area of the world. These are too specific to be applied to masonry structures in general. The descriptions of damage mechanisms and their characteristics under dynamic loading still have no systematic basis. This situation rationalizes the aims of the experimental research on 3D masonry models described in this research in context of Bangladesh considering the seismicity of the country.

Chapter 3

EXPERIMENTAL PROGRAM

3.1 Introduction

In masonry buildings, walls are the main components carrying lateral loads produced by wind and earthquakes. Hence, when analyzing the seismic behavior of masonry structures, most attention should be paid to walls. Depending on the directions of the dominant forces they bear, masonry walls in a masonry structures may be damaged by earthquakes either as in-plane collapses or out-of-plane collapses. In practice, it is usual to happen both kinds of damages in different places in a building. It is therefore, necessary to investigate the in-plane collapses or out-of-plane collapses mechanism of a masonry wall of a masonry building. The behavior of the masonry wall is very much dependent on the material's properties, construction practices, properties of mortar and concrete etc. In this study, the conventional practice of masonry buildings construction of Bangladesh was followed.

This chapter presents material properties and the experimental program of this research consisting of sample preparation of half scale model of masonry wall. The chapter describes the method of the research work, design specification, casting, curing, axial load estimation, shake table specification, earthquake history selection and instrumentation.

3.2 Material Properties

Materials used for the construction of the model is presented in this section. Following subsection will cover the materials properties.

3.2.1 Properties of bricks

The bricks used in the test structure were sized to be 1/2 of Bangladeshi bricks taken as 241mm x 114mm x 70mm (9.5" x 4.5" x 2.75") (L x W x H). The dimensions of the scaled bricks are 127mm x 57mm x 38mm (5" x 2.25" x 1.5") (L x W x H) which is shown in Figure 3.1. The compressive strength of (machine made) the scaled bricks presented in Table 3.1 was evaluated using the standard test procedure. This involved loading the brick in compression with the brick located between the testing machine platens in the same manner as in a wall. The average compressive strength of bricks was

14.6MPa (2114 psi). For design purpose, it is recommended to use average brick strengths.

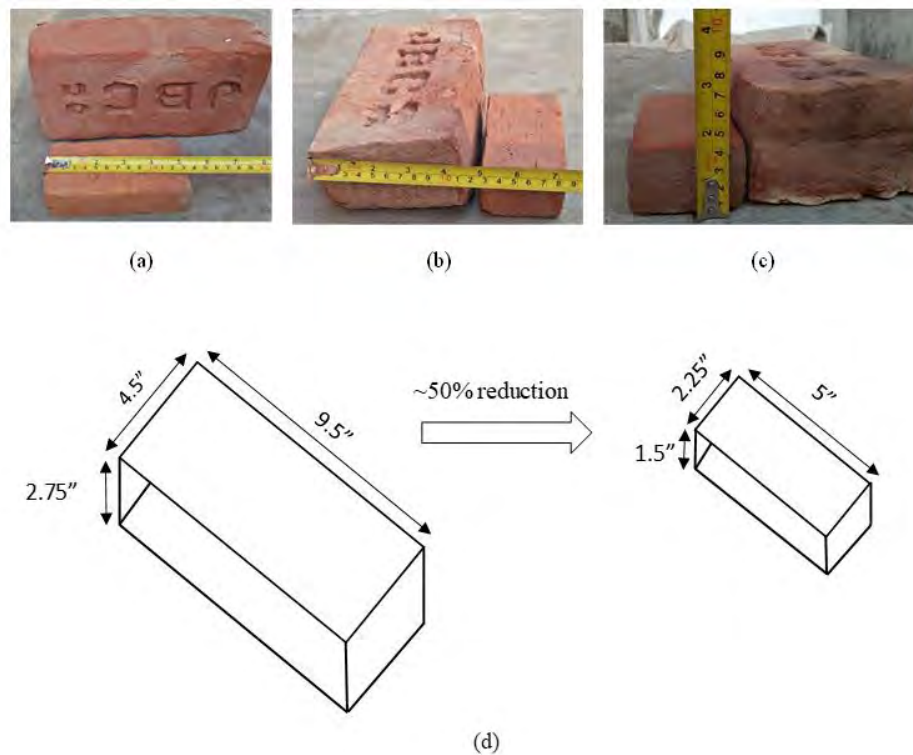


Figure 3.1 Dimensions of reduced scale brick

Table 3.1 Compressive strength of reduced scale brick (127mm x 57mm x 38mm)

Applied Load (kN)	Area (mm ²)	Compressive Strength, MPa	Average Compressive Strength, MPa
130.14	7239	17.98	14.6 (2114 psi)
66.33	7239	9.16	
120.17	7239	16.60	

3.2.2 Properties of sand

Sand composed of naturally occurring granular material of finely divided rock and mineral particles. It is defined by size, being finer than gravel 2mm - 100mm and coarser than silt 0.002mm - 0.05mm. Sand can also refer to a textural class of soil or soil type; i.e. a soil containing more than 85% sand-sized 2mm - 0.05mm particles (by mass). Physical and chemical properties of the sand influence the strength and durability of concrete. Local sand has been used for masonry wall constructions and Sylhet sand has been used for slab and base construction. Figure 3.2 and Figure 3.3 show the

gradation curve of local sand and Sylhet sand respectively. Table 3.2 shows the properties of sand used in the construction of slab, base and in joining of bricks. Local sand was used for the construction of wall (brick joining) and Sylhet sand was used for base and slab construction.

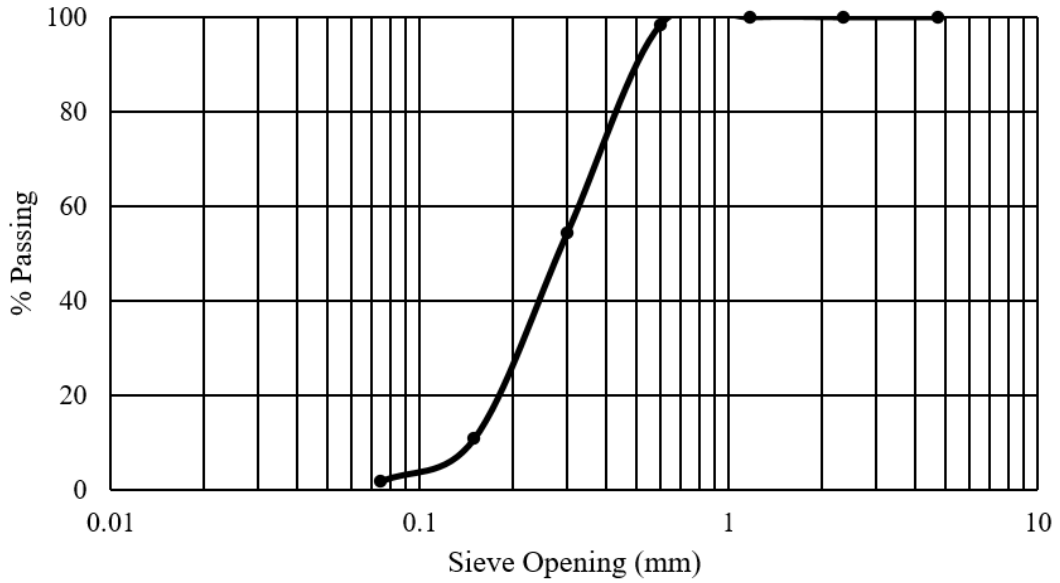


Figure 3.2 Gradation curve of Local Sand

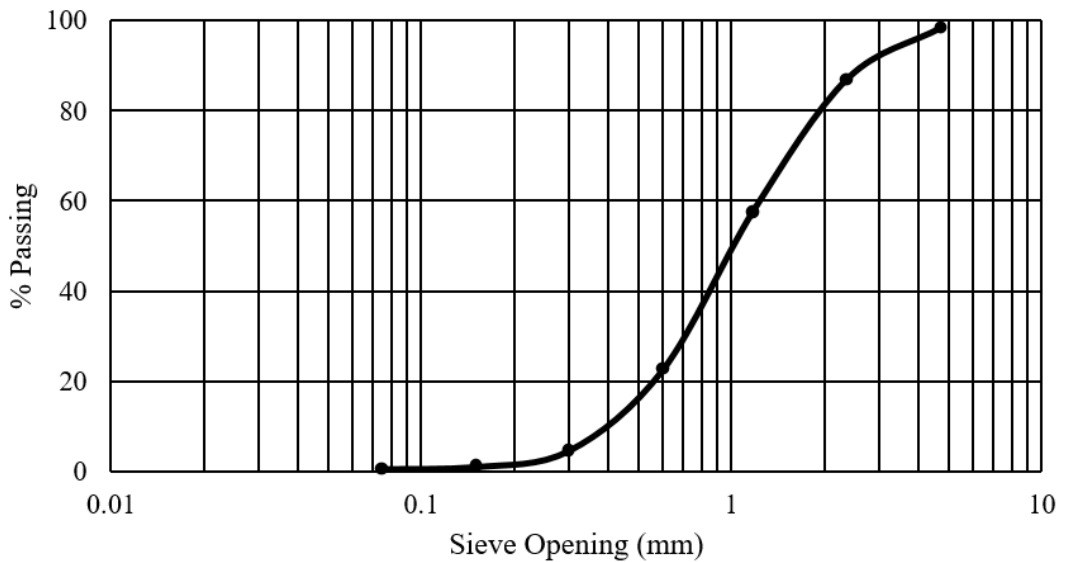


Figure 3.3 Gradation curve of Sylhet Sand

Table 3.2 Properties of Sand used for the construction purpose

	Sand (%)	Fines (%)	F.M.	Cu	Cz
Local sand	98	2	1.37	2.12	0.84
Sylhet sand	99.6	0.4	3.29	3.38	0.91

3.2.3 Properties of cement

Cement is a substance that sets and hardens and bind others materials together. Cement is used as a component of mortar which is used to bind bricks. Cement is also used with aggregate for the preparation of concrete, to form a strong building material.

3.2.4 Properties of mortar

According to the BNBC 2015, Type-M2 mortar with cement : sand in 1:4 proportions were used in the construction of the model. This type of mortar is used in the local construction practice in Bangladesh. Compressive strength of mortar was determined in the concrete laboratory of civil engineering department, BUET. 50mm x 50mm x 50mm (2" x 2" x 2") cubes were made for this testing purpose. Table 3.3 illustrates the compressive strength of mortar for 7, 14 and 21 days (as per BNBC 2015, minimum compressive strength at 28 days is 7.5 MPa).

Table 3.3 Compressive Strength of Mortar

Days	Applied Load (kN)	Area (mm ²)	Compressive Strength, MPa	Average Compressive Strength, MPa
7	16.36	2499	6.55	5.6 (816 psi)
	14.06	2652	5.30	
	13.36	2652	5.04	
14	21.74	2397	9.07	9.0 (1310 psi)
	22.24	2500	8.90	
	22.84	2499	9.14	
21	25.63	2499	10.26	10 (1445 psi)
	24.44	2601	9.40	
	24.64	2401	10.26	

3.2.5 Prism test

During construction of the model structure, brick prisms (127mm x 57mm x 191mm) were constructed. These prisms consisted of five bricks stacked with four mortar (bed) joints in between. The prisms were tested in compression to determine the strength of the masonry. Each end of the prism was coated with hydrocal to provide a uniform bearing surface. The prisms were then compressed until failure, with the highest load resisted recorded. This load was divided by the plan area of the prism to determine the strength. At the same time, compressive strength of full scale masonry unit were

determined. Compressive strength of scaled masonry unit and full scale masonry unit were presented in Table 3.4 and Table 3.5 respectively.

Table 3.4 Compressive Strength of scaled masonry unit (127mm x 57mm x 191mm)

Applied Load (kN)	Area (mm ²)	Compressive Strength (MPa)	Average Compressive Strength, MPa
51	7258	7.02	6.8 (979 psi)
53	7258	7.29	
43	7258	5.93	

Table 3.5 Compressive Strength of real size masonry unit (241mm x 114mm x 349mm)

Applied Load (kN)	Area (mm ²)	Compressive Strength (MPa)	Average Compressive Strength, MPa
100	27580	3.63	4.4 (632 psi)
120	27580	4.36	
140	27580	5.09	

3.3 Specimen Preparation

Systematically process of model preparation is described in this section. Following subsection will cover the process of specimen preparation.

3.3.1 Foundation pad casting and curing

A reinforced concrete foundation pad was designed and constructed on which to build the model structure. The foundation pad was designed to serve as an interface between the earthquake simulator platform and the structures, and to provide a lifting element for transportation of the structures via the overhead crane. The pad formed the shape of a rectangular ring and had dimensions of 7' x 6' with 8" thickness. The rectangular ring was 16" wide. To serve the interface requirements, the pad had 24 holes for bolting to the simulator platform (shaking table) and was roughed on its top surface along the footprint of the structures to increase the bond with the base mortar joint. Amount of reinforcement was more than required to prevent the premature failure of the foundation pad before the failure of structure. Both in the long and short side of the ring had 4 -16 mm bars top and 4 -16 mm bars bottom with 1-12 mm bars along the both vertical sides of the base beam. 6mm bars @ 100 mm center to center was used as tie. To hold the intermediate (nos 2) bars, extra tie was used with same diameter and spacing. There are

total 24 holes in staggered position to anchor (to provide precise positioning) the foundation pad to the shake table. Six 12 mm loops positioned near the inside corners provided means for lifting. Figures 3.4 shows the foundation pad detailing and cross section and Figure 3.5 shows the foundation pad on shake table. Total weight of the foundation pad is 1.24 ton.

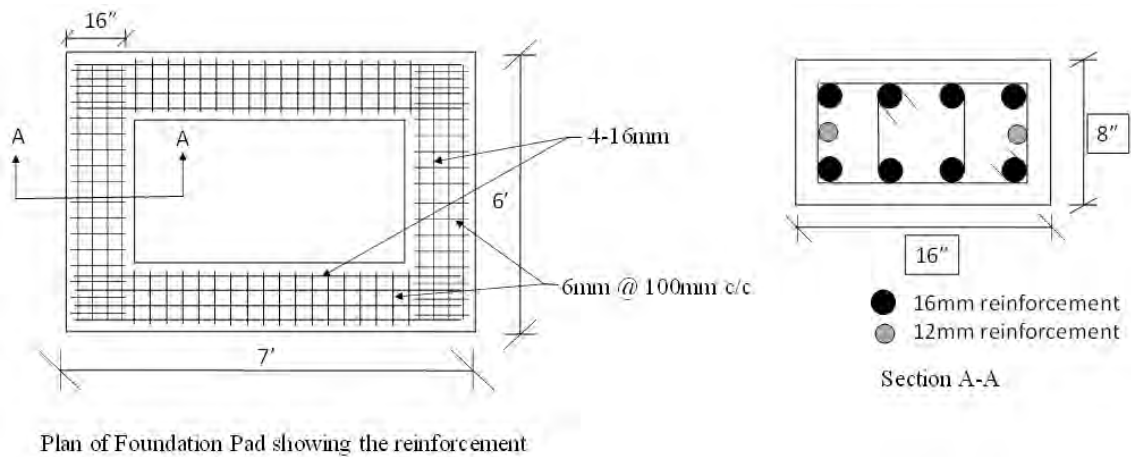


Figure 3.4 Detailing of foundation pad and cross section



Figure 3.5 Foundation pad on shake table

3.3.2 Masonry room construction

Masonry room was constructed on the foundation pad after placing the foundation pad on the shake table. Due to the size and payload of the shaking table, the experimental model was built using a 1:2 reduced scale, taking in account Cauchy's law of similitude

law. Table 3.6 shows the scale factors of the Cauchy similitude law. The geometric properties of the experimental model result directly from the application of the scale factor to the prototype. The material properties of the experimental model should be equal to the prototype, namely in terms of compressive strength, shear strength and modulus of elasticity. The mortar used fine sand to comply with the reduced scale of the bed joints and also in local practice fine sand is commonly used for mortar preparation. A cement mortar of a mix 1:4 (cement : sand) with a water/cement ratio of 0.7 was used so that appropriate flow ability and workability was achieved. The model represents the typical room size of the Bangladeshi masonry structure. The prototype was 12' x 10' (length x width) with 10' height. Typical wall thickness of a masonry building in Bangladesh is 5". Keeping this dimensions in mind, the size of model was kept 6' x 5' (length x width) with 5' height and 2.5" wall thickness. Walls were constructed in stretcher bond. The thickness of mortar used in the construction is 10mm. No openings were kept because opening in one or two side may create torsion and stiffness degradation. Walls were constructed in three days, one-third in a day. In future, author have intention to perform shake table test of masonry building keeping window, door and lintel. Figure 3.6 illustrate the constructed masonry model. Total weight of the masonry model is 1.24 ton.

3.3.3 Diaphragm design

The original intent of the research program was to study the dynamic, in-plane and out of plane response of unreinforced brick buildings with concrete floor/roof diaphragms. Size of the slab is 6' x 5' (length x width) with 3" thickness. The slab was design considering 20 psf (20 nos weight =20*20 kg/weight=400 kg) live load on the slab and 220 lb/ft (100kg/ft) load on the wall as axial compression and those loads was calculated according to the rules of scaling. The model was tested considering two storey building and 220 lb/ft comes from the upper storey.

Figure 3.7 shows the reinforcement detailing of the slab. 6 mm reinforcement was provided at 4" c/c in both direction. This reinforcement is more than calculated reinforcement as per the rules of scaling. This is because, the purpose of this test is to see the performance of masonry building not the slab. The reinforcement is cranked at L/4 distance from the edge of the slab. The extra top is 6" more than the calculated length. Total weight of the slab is 0.52 ton.

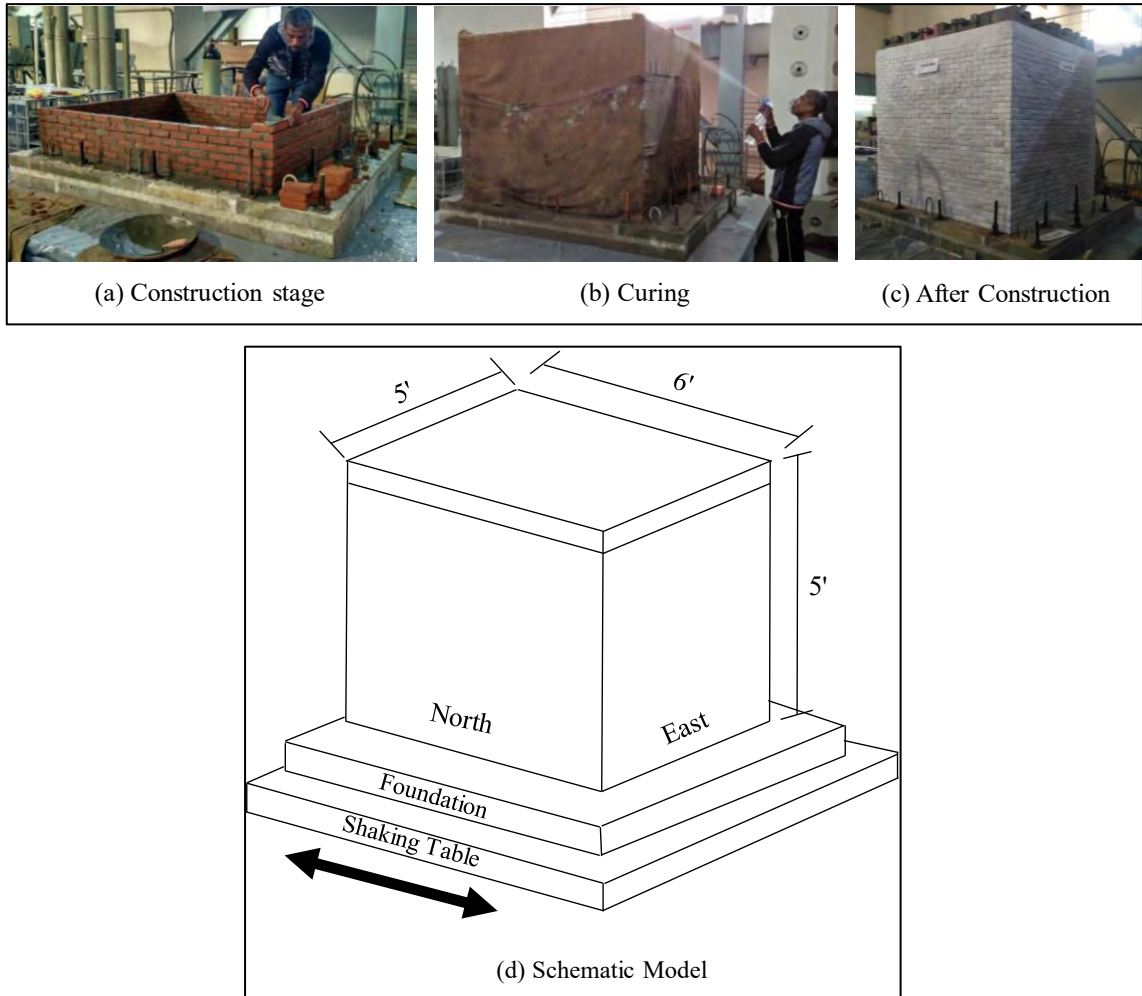


Figure 3.6 Unreinforced Masonry Room

3.3.4 Retrofitting of the masonry model

At first, the bare URM specimens (reference specimen) were tested without allowing collapse. Then, the reference specimen was upgraded using wire mesh and retested. For upgradation or retrofitting purpose 18 gauge wire mesh with 12mmx12mm (1/2" x 1/2") opening was used. To retrofit the model, firstly the previous cracks were sealed by epoxy grout and then the white wash of the model was removed. The wire mesh was wrapped along the whole length of the wall. Wire mesh was applied to the all four walls. The wire mesh was attached to the wall with royal bolt. After that, plaster was applied on all four walls. For rapid strength gain of the plaster, cement grout was used with chemical. After eight days retrofitted sample was retested. Figure 3.8 shows the application process of wire mesh and plastering. Wire mesh was applied only on the wall. Wire mesh was not extended to connect with the base.

Table 3.6 Scale factors of the Cauchy similitude

(where p and m designate prototype and experimental model, respectively)

Parameter	Symbol	Scale Factor
Young's Modulus	E	$E_p/E_m=\lambda=1$
Specific Mass	ρ	$\rho_p/\rho_m=\lambda=1$
Stress	σ	$\sigma_p/\sigma_m=\lambda=1$
Strain	ε	$\varepsilon_p/\varepsilon_m=\lambda=1$
Length	L	$L_p/L_m=\lambda=2$
Area	A	$A_p/A_m=\lambda^2=4$
Volume	V	$V_p/V_m=\lambda^3=8$
Mass	m	$m_p/m_m=\lambda^3=8$
Displacement	d	$d_p/d_m=\lambda=2$
Velocity	v	$v_p/v_m=\lambda=1$
Acceleration	a	$a_p/a_m=\lambda^{-1}=1/2$
Weight	W	$W_p/W_m=\lambda^3=8$
Force	F	$F_p/F_m=\lambda^2=4$
Moment	M	$M_p/M_m=\lambda^3=8$
Time	t	$t_p/t_m=\lambda=2$
Stiffness	K	$k_p/k_m=\lambda=2$
Damping	C	$C_p/C_m=\lambda^2=4$
Frequency	f	$f_p/f_m=\lambda^{-1}=1/2$

3.4 Experimental Setup

Before testing, estimated loads were placed on the roof. Instruments were placed on proper position. Following sections describes the axial load estimation, instrumentation, specification of earthquake simulator and selection of time history.

3.4.1 Axial load estimation

Considering two storey building, axial load on the bottom storey's wall was calculated and scaled down according to the rules of the scaling. Scaled live load (20 psf) on the

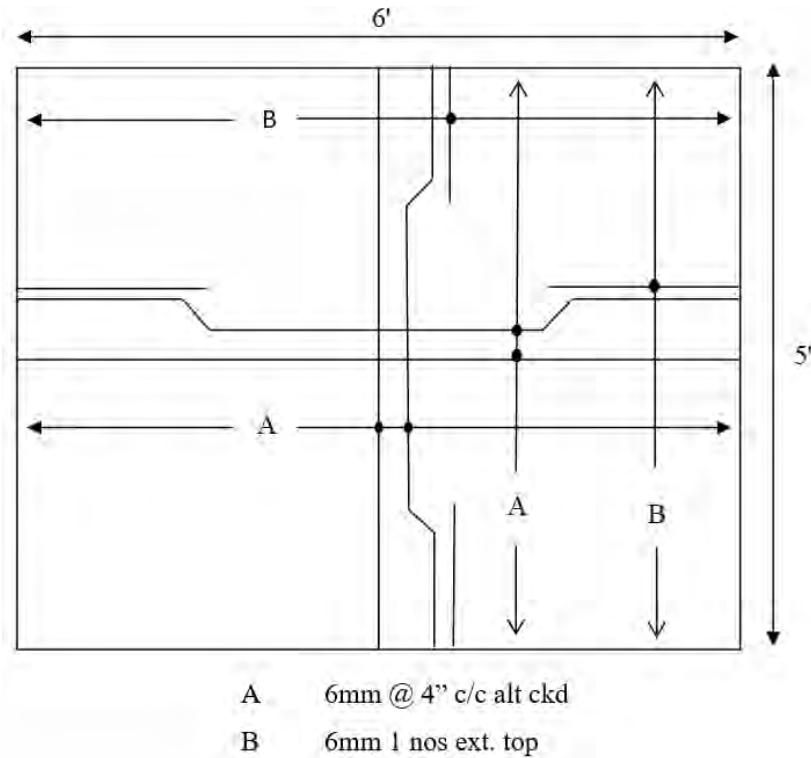


Figure 3.7 Reinforcement in Slab

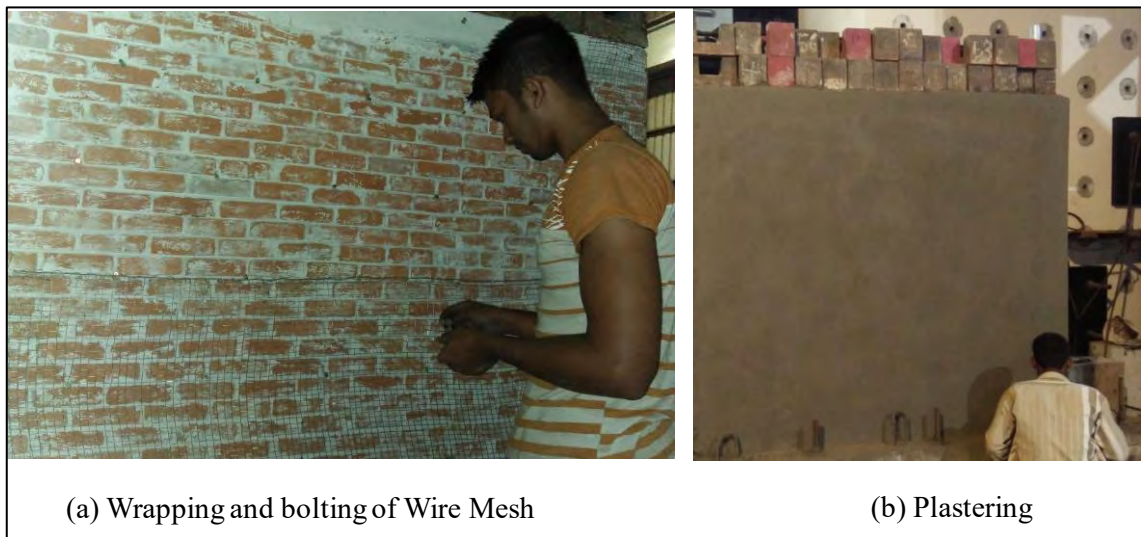


Figure 3.8 Retrofitting Procedure

ground floor slab was used and it is 400 kg. One hundred and four weights were used which were rectangular in shape and nominally weighed 45 pounds (20 kg) each. Of the One hundred and four weights used, eighty four weights (84 nos*20 kg=1680 kg) were kept along the periphery of the building to simulate the axial compression of the wall and remain twenty weights (20 nos*20 kg = 400 kg) were kept at the central area of the building to simulate the live load on the slab. Hence total surcharge weight acting on the slab is 2080 kg that is equal to 2.08 ton. This weight will help to generate inertia force.

Same amount of weight was used for both reference model and for retrofitted model. Therefore, total weight acting on the shake table is 5.08 ton. Figure 3.9 shows the weights used in the slab. A rope was used to tight the weights together. Four anchors of the slab were used for stronger tightening so that those weights cannot fall during the test. Despite this, a rectangular box made by wood was used around the weights so that those weights cannot fall. The model is anchored to the shake table with 20mm bolt. Total 12 bolt is to anchor the model to the table. After every test run all bolts were tighten so that no shear failure of the bolt can occur.



Figure 3.9 Weights on the slab

3.4.2 Instrumentation

An overview of the instrumentation wiring regarding the different types of instruments used are outlined in Sections 3.4.2.1, and 3.4.2.2.

3.4.2.1 Accelerometers

Two piezo-resistive accelerometers (500mV/g) were used during the dynamic testing of masonry building. One accelerometer mounted to the earthquake simulator while the other was attached to the slab of the building. The accelerometers were positioned to

record motions in the direction of testing. Table 3.7 summarizes the accelerometer locations and their sign conventions.

Table 3.7 Accelerometer locations

Accelerometer No.	Location	Direction of Positive Acceleration
1	Attached on Shake Table	Loading Direction (W-E)
2	At top of the model	Loading Direction (W-E)

3.4.2.2 Laser displacement sensors (LDSs)

The displacement response of the models at critical locations was measured using laser displacement sensor (LDSs) and acquired in data-acquisition system at a sampling rate of 200 Hz to capture deformation in the direction of loading and. One LDSs was built into the hydraulic actuator that drove the earthquake simulator. Two LDSs were positioned to the building to record motions of the wall in the direction of testing while two additional LDSs were added to measure out of plane displacements of the wall. Table 3.8 summarizes the LDSs capacity and Figure 3.10 illustrates their locations on reference sample and on retrofitted sample. Figure 3.11 shows the Laser Displacement Sensors (LDSs) and Accelerometer used in the test.

Table 3.8 Accelerometer locations

LDSs No.	Range, mm
1	150-2000
2	150-800
3	150-800
4	150-2000

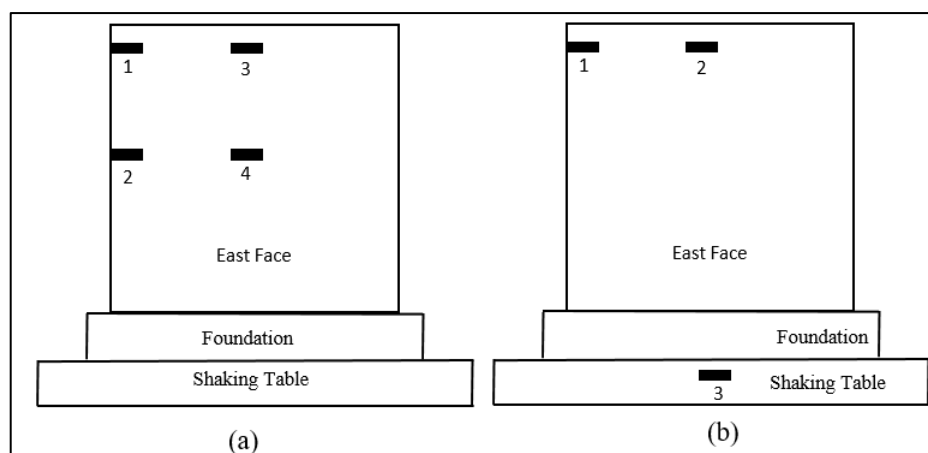


Figure 3.10 Locations of LDSs



Figure 3.11 Instruments used in the test

3.4.3 Earthquake simulator

The earthquake simulator used in this dynamic testing of masonry room is resident in the Earthquake Engineering Laboratory of BUET-JIDPUS, BUET. The platform measures 3mx3m (10' x 10') and is supported by six bearing pad for the movement of shaking table. Total platform height of the shaking table is 15". The platform itself is a 38mm solid MS plate supported by/welded with six (6) nos longitudinal T-beam and three (3) nos transverse T-beam in multiple bay. Platform are threaded which form an $7\frac{3}{3}'' \times 7\frac{3}{3}''$ center to center bolting pattern. The hole of the shake table is 20mm in diameter. An instrumentation datum is attached to one end of the simulator platform for collecting measurements relative to the platform base. The simulator is driven by a 25 ton hydraulic actuator driven hydraulic power system (HPS) attached to three-stage electro-hydraulic servo-valve with a total capacity of 200 gallon per minutes (gpm). Table 3.9 shows the specification of shake table. The simulator is controlled via DANCE (Version 632.2) software which was supplied by ANCO Engineers Inc. DANCE is also capable of providing rapid graphical display of the data once the test is complete. After a test had been completed, the data from the various channels was exported in a text format.

3.4.4 Selection of time history

Before selection of time history, ambient vibration of the masonry model were measured using microtremor for the purpose of assessing the dynamic parameters. Ambient vibration can be from sources of micro-seismic tremors (incessant agitation of earth surface) which cannot be controlled but instead considered as a stationary random process. Collection of ambient vibration data was based on in-situ records, with highly

Table 3.9 Specification of Shake Table of BUET-JIDPUS

Shake Table Specification
Size: 3m x 3m (10'x10')
Actuator: 25 ton\$ Servo Hydraulic Actuator
Acceleration Capacity: 1.6g maximum acceleration with 10ton payload
Bare table Acceleration: 4.0g
Velocity Capacity: 100 cm/s (40 inch/sec)
Displacement Capacity: +/- 100mm (± 4 inch)

sensitive dynamic tri-axial sensors located at the top of the model. Acceleration data were separately copied into MS Excel files for further use. The time history plot of ambient vibrations does not resemble a periodic pattern. Thus the OriginPro 8.5.0 was used to calculate Fast Fourier Transforms (FFT) of the obtained acceleration data. Then data were analyzed using resulted frequency spectrum. In the frequency spectrum the plot of Fourier amplitude versus structural vibration frequencies are clearly presented which is shown in Figure 3.12. Then, Fast Fourier Transforms (FFT) of different recorded earthquake time history (e.g. Kobe earthquake, Imperial Valley earthquake etc.) were done and pre-dominant frequencies of model structure were then compared with the pre-dominant frequencies of different recorded earthquake time history. Since first pre-dominant frequency of model structure is around 6 Hz. The pre-dominant frequency of Scaled Imperial Valley earthquake is 5 Hz which is close to the model's frequency and time history of Imperial Valley earthquake was taken as input motion so that the model can collapse due to resonance. Figure 3.13 shows the time history and pre-dominant frequency of Imperial Valley earthquake. Same earthquake time history was for both reference model and retrofitted model.

3.5 Simulation of the Seismic Action and Procedure

The ground motion produced by an earthquake can be represented by three components, namely two horizontal and one vertical. There are unidirectional, bidirectional and three-dimensional shaking tables that can reproduce only one, two or the three components respectively. The shaking table at BUET-JIDPUS has one degree of freedom.

Time history of Imperial Valley earthquake is selected as an input seismic load of the shaking table which is describe in section 3.4.4. Taking into account the Cauchy

similitude law, the artificial accelerograms should be compressed in time by a factor of 2 and the acceleration should also be multiplied by the scale factor 2. The standard response spectrum and response spectrum obtained from the compressed artificial accelerograms are shown in Figure 3.13.

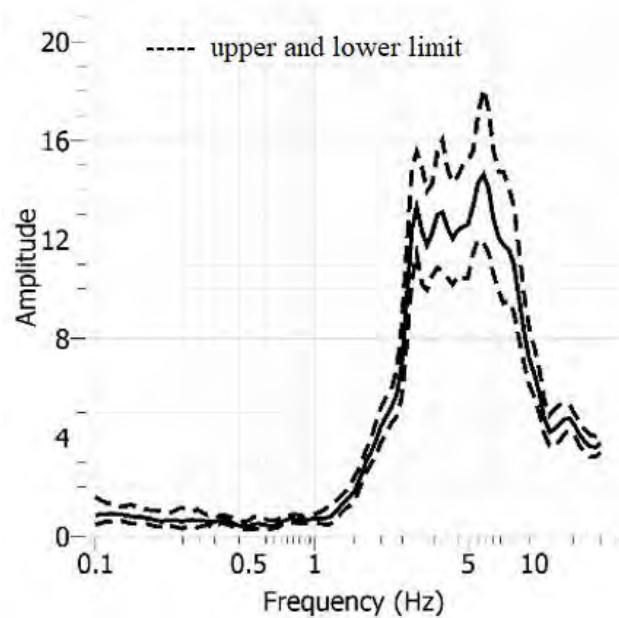


Figure 3.12 Pre-Dominant Frequencies of model structure

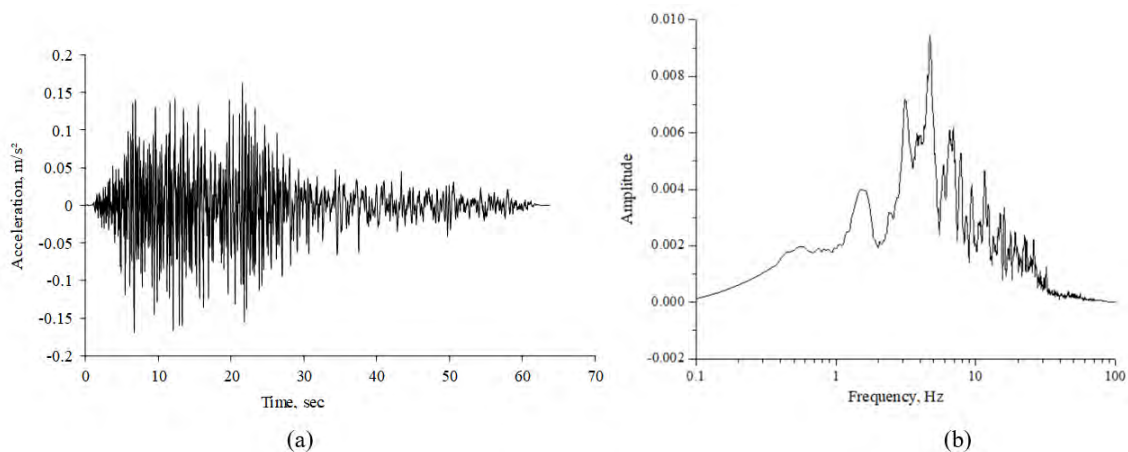


Figure 3.13 time history and Pre-Dominant Frequencies of scaled Imperial Valley earthquake

The shaking table motion has been displacement controlled and to obtain the displacement time history, the artificial accelerograms were processed by double integration and this was done for reference model. For retrofitted model displacement time history of the table was directly recorded. The seismic action was applied to the

models in a phased procedure, with a sequence of incremental amplitude levels of accelerograms imposed.

Severe damage of the model or limit of the shaking table in term of actuators displacement capacity was the parameters for defining the last test run. This procedure of applying load, common in literature, enables to follow the damage and deformation patterns for increasing seismic action, even if it is accepted that nonlinear behavior can be influenced by the phased seismic action and that damage accumulates in the tests.

3.6 Dynamic Testing

The complete experimental setup for model structure is shown in Figures 3.14. A total of twelve earthquake simulations were performed for reference model. The first three runs were sine wave with low frequency (1Hz, 2Hz, 3Hz) and low acceleration (0.05g) which were run without damaging the structure. Then the test was conducted with incremental acceleration ranging from 0.27g to 1.05g using Imperial Valley Earthquake. Between each earthquake simulation, visible damage was noted and recorded. Prior to their testing, model structure was painted white to facilitate crack identification and marking. Cracks were marked with colored pens, with a different color used for each run that induced new cracks. These crack patterns are discussed in Section 4.2.2. A large number of photographs were taken between tests to record characteristics such as dislodged bricks, missing mortar, misalignment across cracks etc.



Figure 3.14 Complete Experimental Setup

The retrofitted model was tested in the same procedure. Same as reference model testing, first three runs were sine wave with low frequency (1Hz, 2Hz, 3Hz) and low acceleration (0.05g). Those sine wave excitaiton were run in such a way that the masonr model cannot undergo any kind of damage. After this sine wave excitaion the rest of the test were conducted with incremental acceleration ranging from 0.195g to 1.49g using Imperial Valley Earthquake. The Imperial Valley Earthquake was used because this earthquake history was used for reference model. The crack patterns developed in the retrofitted model are also discussed in Section 4.2.2. Cracks were observed in between two run. A large number of photographs were taken to record characteristics of cracks.

Chapter 4

EXPERIMENTAL RESULTS AND DISCUSSION

4.1 Introduction

This chapter will discuss the overall dynamic behavior, in-plane and out of plane behavior of URM wall observed and recorded through the total dynamic test runs of both reference model and retrofitted model. Among the dynamic test, three input motion was sine wave with 1 Hz, 2 Hz, and 3 Hz frequencies to determine the dynamic characteristics of the wall. In addition, rest of them was Imperial Valley earthquake motion. Visual observations were made through eyewitnesses and recording devices which will be described, followed by a detailed account of the recorded acceleration and displacement histories. Of the data channels collected, all of them are used to describe the dynamic behavior of structure in this chapter. All acceleration or related data mentioned in this chapter, are for scaled model tested for this research purpose.

4.2 Observations

In-plane, out of plane and overall behavior of URM model was observed through eyewitnesses and recording devices. During the testing, notes were made on the visually-observed behavior of the test structures. The seismic action was applied to the structure in a phased procedure, with a sequence of incremental amplitude levels of accelerograms imposed. Table 4.1 summarizes the test sequence with the actual Peak Ground Acceleration (PGA) measured from the base of the models, corresponding to distinct acceleration value of the seismic input.

The shaking table motion was displacement controlled type. Displacement time history was found by double integration of artificial accelerograms. All necessary correction and calculations (offset correction, filtering, and integration) of the raw data were made in Origin Lab software. The global behavior of the model structure was analyzed in terms of deformations and damage patterns for all the seismic inputs. Obtained results are related to the scale model and therefore in order to obtain the prototype's values Cauchy similitude law presented in Table 3.6 should be implemented. The measurements made at the base allow assessing the correct accelerations and displacements that was imposed to the model, for further analysis of the results. For the adequate analysis of the seismic response of the buildings, evaluation of the base

ground motions of models is essential. Therefore, the masonry model will be evaluated from the motions recorded in the base.

Table 4.1 Seismic Input and corresponding Peak Acceleration at Shake Table

Run	Table Acceleration (g) of Reference Model	Table Acceleration (g) of Retrofitted Model
1	0.27	0.195
2	0.36	0.25
3	0.41	0.328
4	0.59	0.38
5	0.66	0.52
6	0.76	0.77
7	0.83	0.9
8	0.92	1.02
9	1.05	1.15
10	-	1.24
11	-	1.34
12	-	1.45
13	-	1.49
14	-	1.45

4.2.1 Input acceleration comparison

Table 4.1 shows the seismic input to the reference model and retrofitted model. It is clear from the recorded acceleration that retrofitted mode can sustain more than 1.4 times acceleration than reference model. First crack was initiated at 0.83g in reference model while in retrofitted model first crack was initiated at 1.49g, which is approximately 1.8 times more than 0.83g. The reference model was not able to sustain an acceleration of 1.05g without any collapse, although it is 1.49g for retrofitted model. Figure 4.1 and Figure 4.2 depicts the maximum acceleration and displacement history of reference model and retrofitted model respectively. All Input time history for reference model and retrofitted model is presented in Appendix A. Summary of the largest acceleration peaks are shown in Appendix A in Table A.1.

4.2.2 Damage pattern

Observed damage pattern of the walls are presented in the following subsection.

4.2.2.1 Damage pattern of reference model

Total four laser sensor was attached to the east face (perpendicular to the direction of loading) of the model to observed in-plane and out of plane response and two

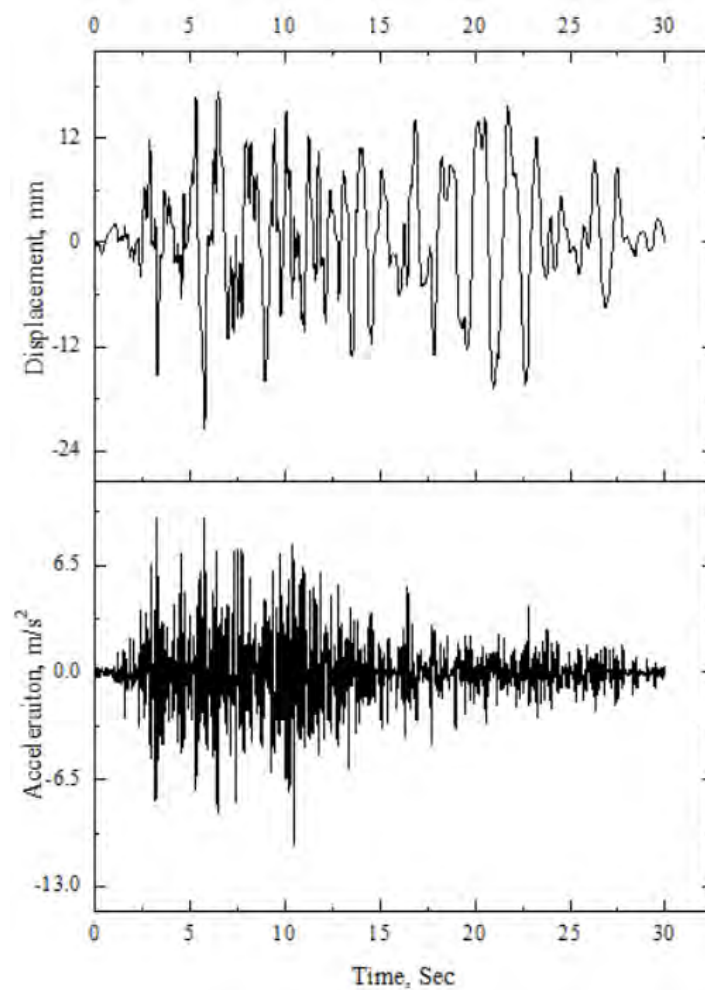


Figure 4.1 Input Motion in Reference Model (1.05g)

accelerometer were attached to the roof and shake table to record the acceleration of at roof and base respectively. Figure 4.1 shows the acceleration and displacement of last input (1.05g) and time history of the input motion (both acceleration and displacement) is summarized in Appendix A.

Total nine seismic motion were run and the visible cracks were summarize in Table 4.2. No crack was observed in the first seven run in which acceleration range was from 0.27g to 0.76g. First horizontal crack was observed at 0.83g in east wall which is the out of plane wall. It should be mentioned that the crack was initiated at the lower south-east corner along the bed joint in the east wall (out of plane wall) which is depicted in Figure 4.3. This crack was developed at the second course with almost the one third-length of the wall. No crack was observed in any other wall at this acceleration. At 0.92g acceleration, horizontal crack along the bed joint in east face was observed. This crack

was along the same course as was at 0.83g. At north-east corner, cracks were developed along the head joint in north wall as well as along the bricks which indicate that mortar

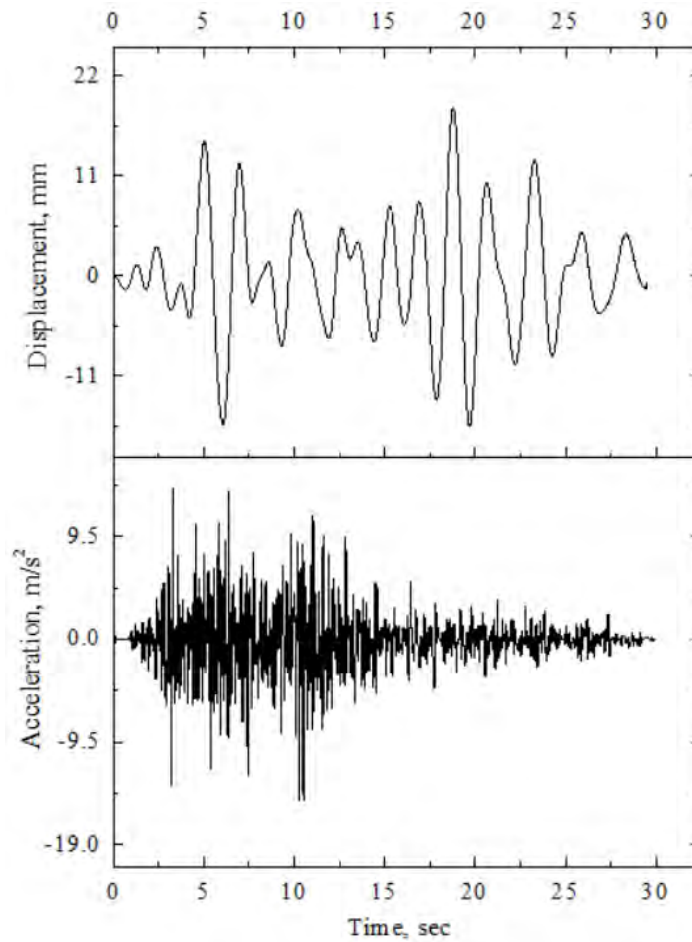


Figure 4.2 Input Motion in Retrofitted Model (1.49g)



Figure 4.3 First crack develop at 0.83g in east wall (out of plane wall)

was stronger than the brick. Cracks were also observed at north-west corner in north wall along the head and bed joint (zigzag). Horizontal cracks along the bed joint and brick were observed in south wall in the lower first course. These cracks are figure out in Figure 4.4 and 4.5. Cracks observed at 0.83g were expanded in this stage.

Table 4.2 Crack Distribution in different acceleration of Reference Model

Run	Table Acceleration (g) of Reference Model	Crack Distribution
1	0.27	no crack
2	0.36	no crack
3	0.41	no crack
4	0.59	no crack
5	0.66	no crack
6	0.76	no crack
7	0.83	visible crack in out of plane wall (east) in bed joint
8	0.92	visible crack in out of plane wall (east), in-Plane wall (north, south) along the head and bed joint
9	1.05	visible crack in out of plane wall (east), in-Plane wall (north, south) along the head and bed joint. Previous cracks were extended



(a) North-East Corner

(b) North-West Corner

Figure 4.4 Cracks develop at 0.92g ((a) horizontal crack in out plane wall
(b) horizontal and zigzag cracks in-plane wall)

Visible cracks mostly developed at 1.05g acceleration and greatest amount of cracks were also developed in this run. It should be stressed that almost all cracks developed along the unit-mortar interface, even if some concrete units were also affected with minor cracks. Horizontal cracks appear to be the result of lack of in-plane flexural resisting mechanism associated with low values of vertical pre-compression. All stair-

stepped cracks are localized in the corner of the walls. At this stage, the cracks developed in east, west, north and south walls covering the whole lower half of the walls.



Figure 4.5 Horizontal Cracks develop at 0.92g (south wall)

Shear diagonal stepped cracks developed at the unit mortar interface even in the bricks, starting from the corner of the wall. The walls did not slide relative to their footings or the shake table during the tests. In the east wall, both horizontal and stepped cracks developed at the lower part. This wall is the out of plane wall, aligned along the perpendicular direction of the loading. The two cracks (developed at 0.83g and 0.92g) near the bottom of the east out-of-plane wall were linked by a new crack during this run. A horizontal cracks also developed at the height of $L/4$ of height from the bottom. Mostly all the cracks developed along the unit-mortar interface, some bricks also were also cracked. Due to the lack of low flexural resistance and low vertical compression, These horizontal cracks were developed. This is depicted in Figure 4.6. Due to this low vertical compression, sliding occur in the in-plane wall (north and south). This is presented in Figure 4.7. Shear diagonal stepped diagonal cracks were developed in the in-plane wall which were initiated from the lower corners along the unit mortar interface and also along the brick, which indicate the lower brick strength than that of mortar. A horizontal crack also developed at the wall-base interface. This is depicted in Figure 4.7. Same type of cracks were developed in the west wall which is shown in Figure 4.9. In the south wall face, a horizontal crack along the bed joint was developed at the lower first course. At the south-east corner of south wall, there are some stepped cracks along the brick and unit-mortar interface which is shown in Figure 4.8. Slide torsion, with an angle of 0.22 degree, of the east wall was occurred with a displacement

of 6mm in the east-north corner. It can be inferred that the global condition of the model was much notorious and did not collapsed, in spite of heavy damage. It will not be able to sustain any of acceleration after this final run. The model is not intended collapsed because of further testing.

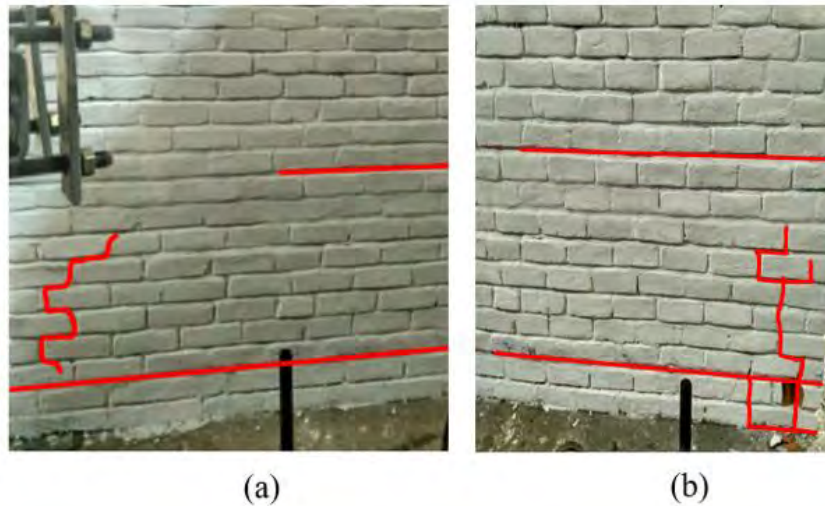


Figure 4.6 Cracks developed at 1.05g in east wall (out-of-plane wall)
 ((a) south-east face (b) north-east face)

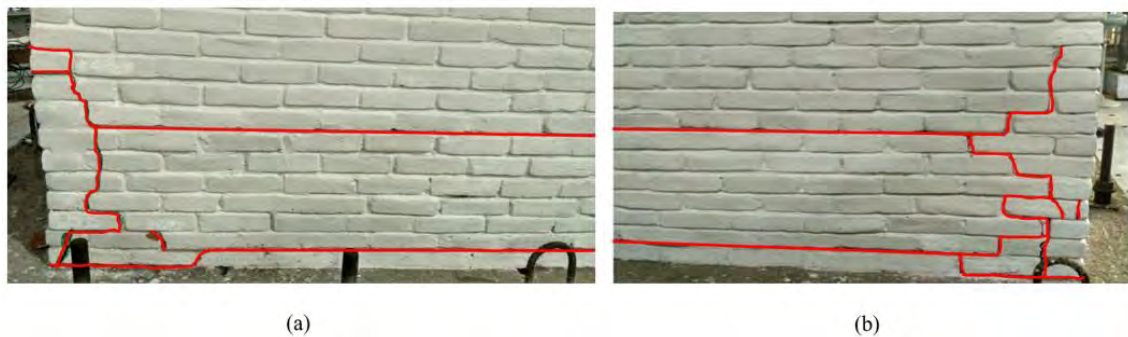


Figure 4.7 Cracks developed at 1.05g in north wall (in-plane wall)
 ((a) north-east face (b) north-west face)

4.2.2.2 Damage pattern of retrofitted model

Total three laser sensor was attached to the east face (perpendicular to the direction of loading) of the retrofitted model to observed in-plane, out of plane and table response and two accelerometer were attached to the roof and shake table to record the acceleration of at roof and base respectively. Figure 4.2 shows the acceleration and displacement of last input (1.49g) and time history of the input motion (both acceleration and displacement) is summarized in Appendix A.

Total fourteen seismic motion were run and no visible cracks were observed in the wall for the first eleven run in which acceleration range was from 0.27g to 1.45g. In twelve run at an acceleration of 1.49g, which is the maximum acceleration, cracks develop at the base of the model in all wall. This is due to the sliding of the wall. After retrofitting, model become stiff- this stiffness as well as low vertical compression accelerate the sliding of the wall. In the next following run, a vertical crack developed at the bottom of north-west corner of the north wall and no other visible cracks were observed in any other wall. The cracks along the base was further extended and the model was totally separated from the base. In Figure 4.10, crack in base and crack in north wall are shown.

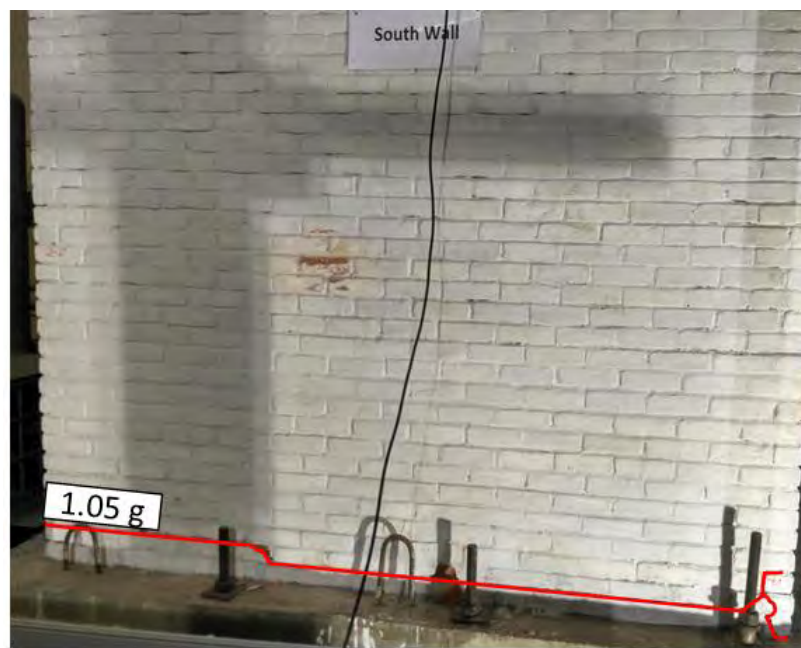


Figure 4.8 Cracks developed at 1.05g in south wall (in-plane wall)



Figure 4.9 Cracks developed at 1.05g in west wall (out of plane wall)



Figure 4.10 Crack developed in Retrofitted Model ((a) vertical crack in north wall
(b) separation of wall from base)

4.3 Displacement Characteristics

Displacement characteristics of reference model and retrofitted model are described in the following subsections.

4.3.1 Displacement characteristics of reference model

For each test run, displacements at four points of the structure were measured by the laser sensors; two at mid heights of the two walls (In-plane and Out of plane) and two at the top of the two walls (Figure 4.11). It is to be noted that all the values of the displacements were relative to the base of the structure. This relative displacement was measured by subtracting base displacement from the recorded displacement at top.

The displacements for the in-plane wall was plotted by joining the displacement readings of point 0 and point 2 at the instantaneous time when the top displacement (Point 0) was maximum, where maximum corresponds to absolute maximum. Joining these points eventually lead to a deflected shape of the wall. The same thing was done for the Out of plane wall joining displacements of point 3 and point 1 when absolute value displacement of point 3 was maximum.

Through this process the approximate deflected shapes of both the in-plane and out of plane wall during the time of peak displacement at top can be depicted for different test runs. The results are shown in Figure 4.12 and 4.13.

However, due to presence of equipment's capable of taking not more than two readings along the height of the walls the displacements of points other than the two measured cannot be estimated.

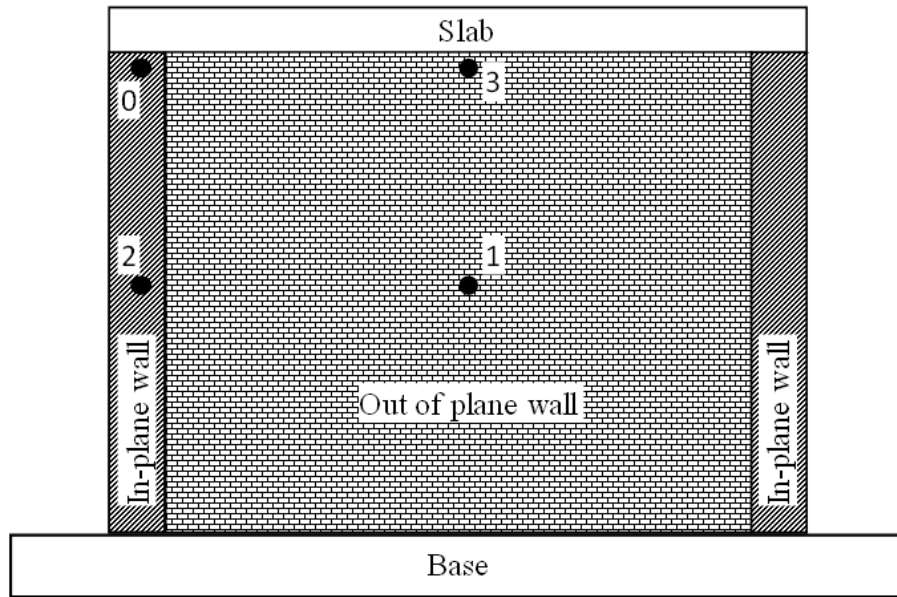


Figure 4.11 Position of Sensors measuring displacements of walls

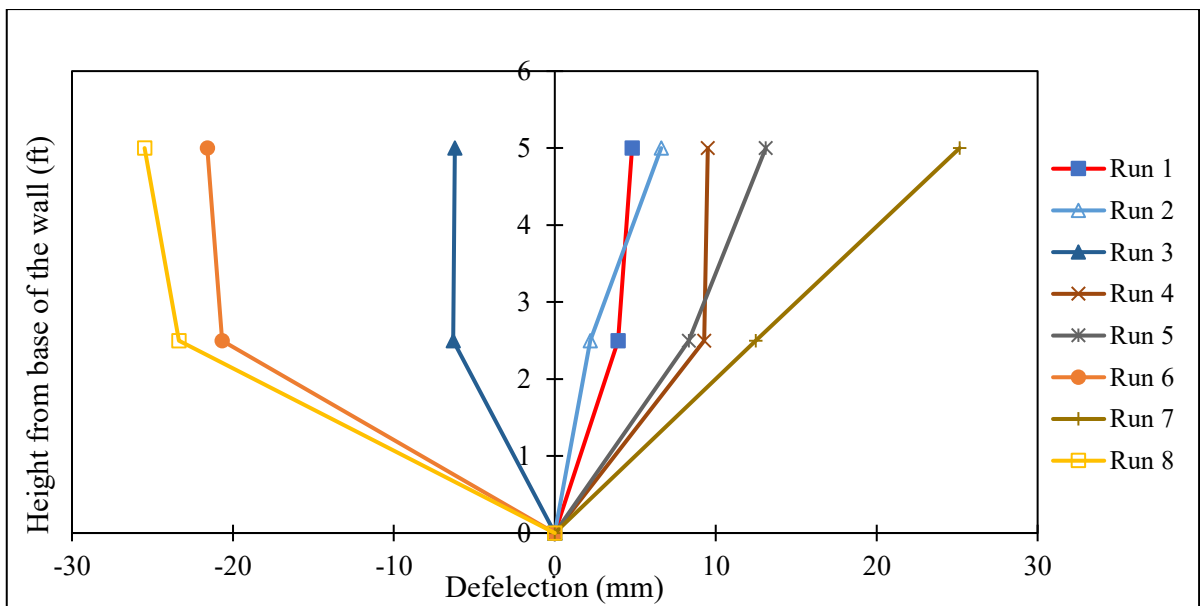


Figure 4.12 Approximate deflected shape of In-Plane wall for maximum top deflection

Table A.2 in Appendix A lists the two largest displacement peaks recorded for each laser sensor and at the table during Test Runs 1-10, along with their occurrence times. It is seen that displacement increase as the acceleration of the excitation increases for the in-plane, out of plane and table displacement. Only for the last excitation when the acceleration was maximum, the displacement decrease. Out of place wall experienced more displacement, which is 34.7 mm for the excitation of 0.92g (Run 8). At the same excitation, in-plane wall also experienced maximum displacement, which is 25.5mm.

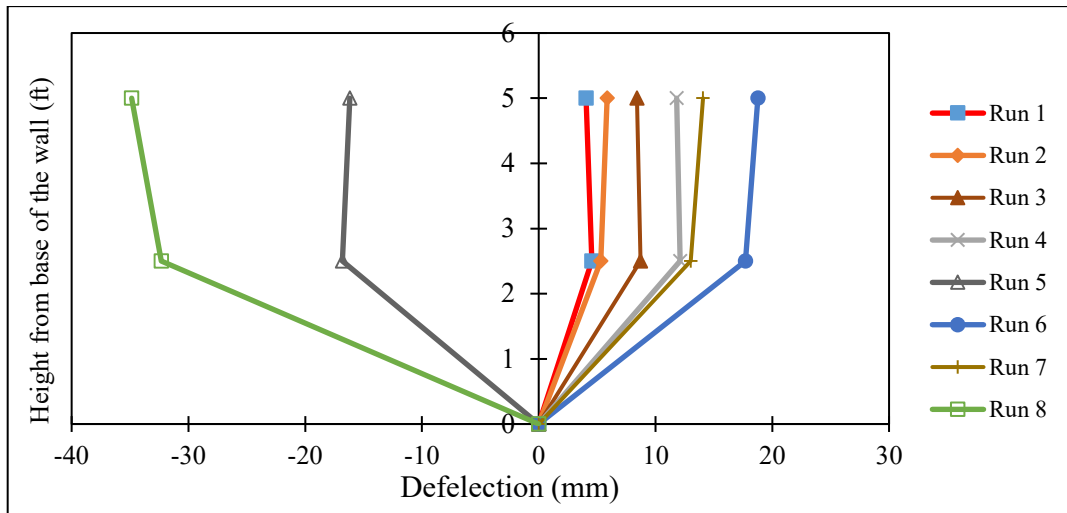


Figure 4.13 Approximate deflected shape of Out-of-Plane wall for maximum top deflection

4.3.2 Displacement characteristics of retrofitted model

During the tests conducted after retrofitting, the displacement data of walls were taken with one laser sensor for each wall. Two sensors were placed to record the wall top displacements, each at the top of one In-plane and one Out of Plane walls; one sensor was placed to record the displacement of the shake table. The displacements of one wall top relative to the table was found by subtracting the table displacement from the recorded displacement at wall top. Afterwards, the maximum displacement at wall top of in-plane and Out of plane wall for each run are plotted in Figure 4.14 and Figure 4.15 respectively.

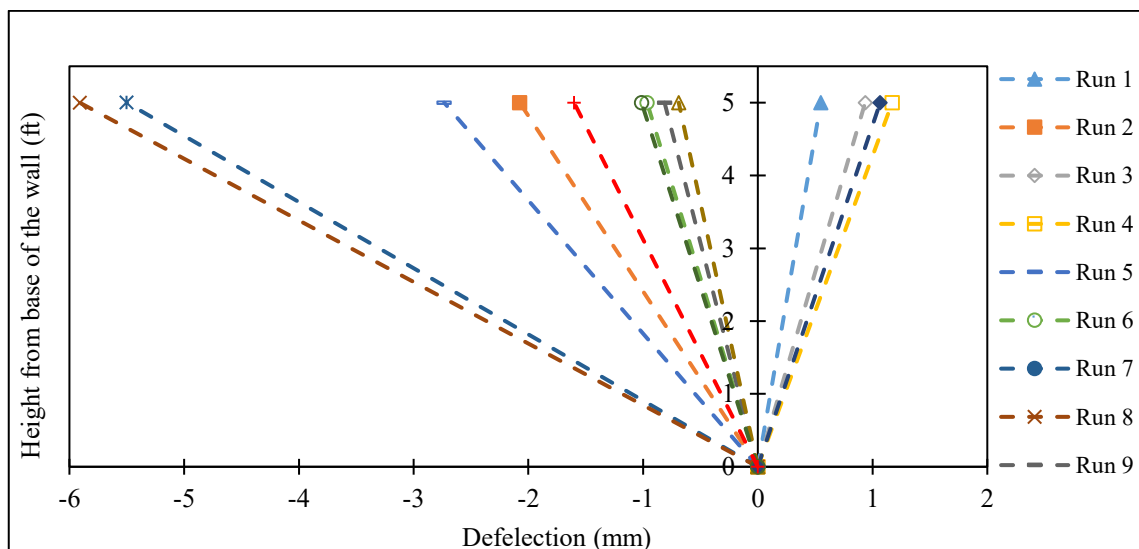


Figure 4.14 Approximate Deflected shape of In-Plane wall for maximum top deflection

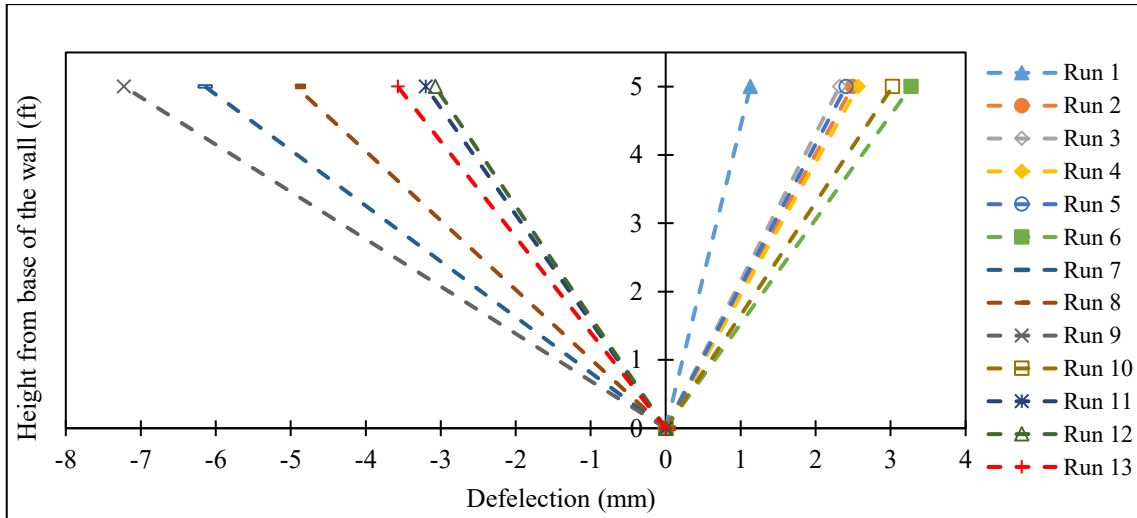


Figure 4.15 Approximate Deflected shape of Out-of-Plane wall for maximum top deflection

It is to be noted for both the In-plane and Out-of-Plane walls that the maximum displacement for all the test runs combined is found to be greater in value for runs before retrofitting than after it. It is due to the fact that, the stiffness of the structure increased after retrofitting and thus the deflection of the walls were lower than the ones obtained before retrofitting.

For instance, at an approximate PGA of 1.03g the maximum displacement of the In-plane wall after retrofitting reduced to around one-third of its value before retrofitting and for out of plane wall the displacement reduced to one-seventh of the value obtained before retrofitting.

4.4 Load Characteristics

Lateral load resistance capacity of the tested models are presented in the section 4.4.1, 4.4.2 and 4.4.3.

4.4.1 Load characteristics of reference model

Lateral force

The lateral force was computed as a multiple of the roof mass (2.08-tons), slab weight and upper half of the walls times the measured roof acceleration/total acceleration ignoring damping force. Since the motion is unidirectional, the lateral force will mostly be carried by in-plane wall. Therefore the force is divided by two. The maximum and

minimum lateral force, for one in-plane wall, for each test run is listed in the Tables 4.3. It is to be noted that all displacement mentioned here is relative displacement. The peak lateral force values are normalized by 25.8 kN, the weights sum of the 2.08-ton mass, and the weight of the slab (0.50ton). The drift is normalized by dividing the measured lateral relative displacement by the height of the specimen. Figure 4.16 shows the normalized force and displacement of the wall.

Table A.3 in Appendix A, the largest input forces are shown. It is seen that during the first crack which were initiated at run 7, the input force is 42.29 kN which were in the negative direction. The visible horizontal and some stair-steeped cracks were developed at input force of 46.65 kN which were also in the negative direction at run 8. The severe crack were developed at a negative input force of 53.12 kN. Up to a maximum input force of 40.5 kN, no visible cracks were develop in any of the wall. Input acceleration and corresponding roof acceleration as well as in-plane and out of plane displacement histories are presented in the Appendix A.

Table 4.3 Maximum displacement and maximum lateral force of Reference Model

Test Run	F _{max} , kN	F _{min} , kN	In-plane wall		Out of plane wall	
			d _{max} , mm	d _{min} , mm	d _{max} , mm	d _{min} , mm
1	1.89	-2.5	6.41	-5.59	3.91	-2.63
2	2.61	-3.03	6.51	-5.59	5.77	-4.4
3	3.21	-3.45	4.56	-6.22	8.42	-7.67
4	3.39	-3.81	9.51	-7.71	11.73	-7.39
5	6.26	-9.14	12.98	-13	12.31	-16.17
6	8.08	-10.09	16.32	-21.55	18.38	-17.36
7	8.96	-10.8	24.71	-22.96	13.96	-9.46
8	11.17	-14.07	18.11	-25.48	26.82	-34.76
9	12.75	-13.61	16.4	-17.5	30.4	-27.1

Hysteresis loops

The lateral force is plotted versus the measured relative lateral displacement producing what are commonly referred to as hysteresis loops. By examining different aspects of the hysteresis loops, many of the visual observations were confirmed. As an example, samples of the hysteresis loops of model are shown in Figure 4.17, which is derived from the in-plane wall displacement data. It is worth to note the following:

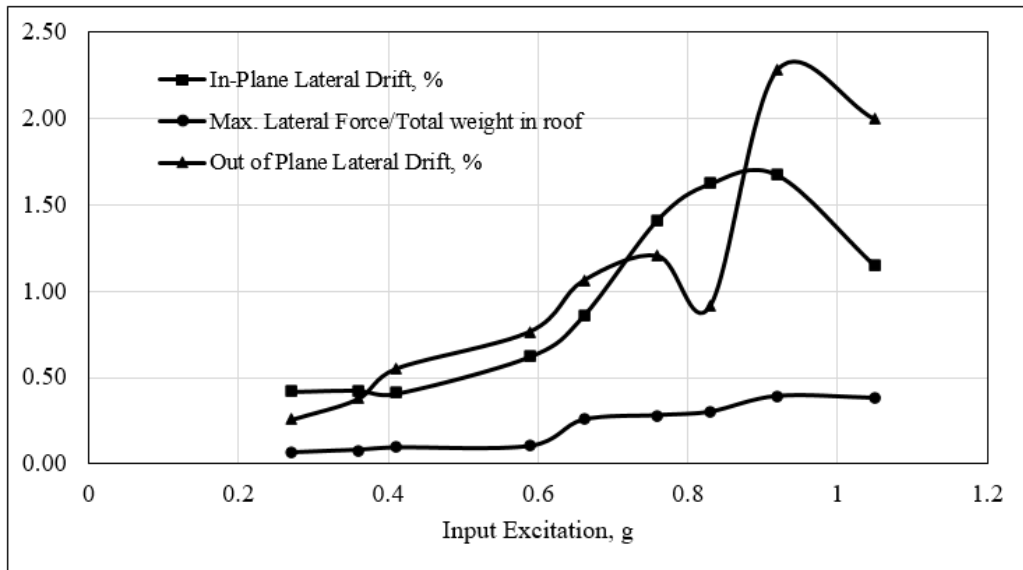


Figure 4.16 Input acceleration vs normalized lateral force and displacement of Reference Model

- From hysteresis loop, it is clear that the behavior of the specimen is not linear. Since masonry is non-homogeneous and anisotropic composite structural material, so it is not unexpected result.
- As the acceleration of the excitation increase the area enclosed by the hysteresis loop increase. This indicate the more energy dissipation than previous excitation.
- The cracking observed in test Run 7 (0.83g) and later on, and it is clearly visible form the hysteresis loop because sample suddenly experienced a large displacement which is not visible in the previous run.
- There was relatively high-energy dissipation in the test run 7, 8, and 9 due to initiation and expansion of cracks. However, for other test runs there was little energy dissipation. This energy dissipation increased slightly with increasing earthquake intensity due to mortar grinding, friction and sliding.
- Shape of hysteresis loop of Run 9, reflect the brittle failure of the specimen.

Same type of hysteresis loops are constructed for out of plane wall displacement, which is shown in Figure 4.18. Roof acceleration is taken to build hysteresis loops because lateral force mostly carried by in-plane wall. It is worth to note the following conclusion from the hysteresis loop:

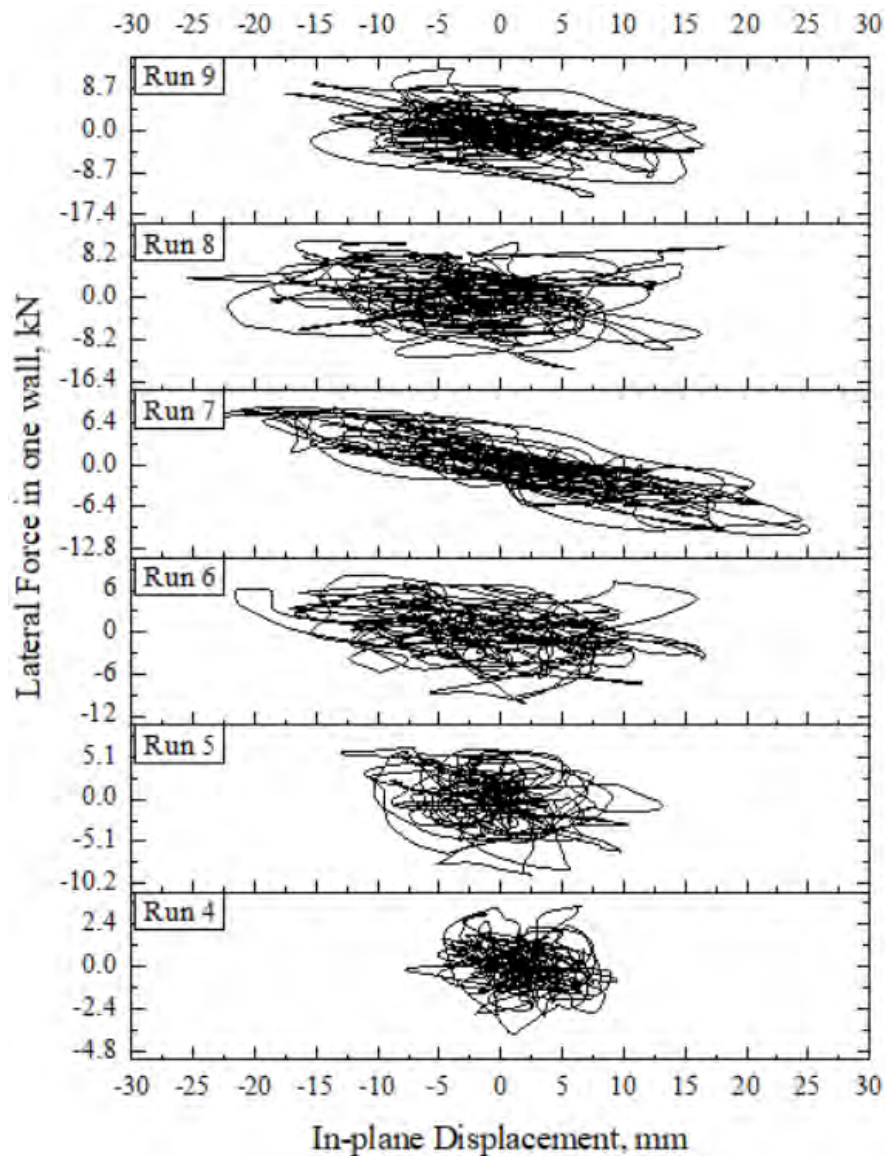


Figure 4.17 Lateral Force vs. Relative Lateral Displacement of in-plane wall for different input acceleration

- Characteristics of hysteresis loop is very much similar to the hysteresis loop of in-plane wall. The behavior of the specimen is not linear.
- As the acceleration of the excitation, increase the area enclosed by the hysteresis loop increase, except at Run 7 (0.83g) excitation. This indicate the more energy dissipation than previous excitation.
- Sample experienced much out of plane deformation than in-plane wall. Out of plane deformation is more at Run 8 (0.92g) and cracks mostly developed at this acceleration.

- There was relatively high-energy dissipation in the test run 8, and 9 due to initiation and expansion of cracks. Cracks mostly developed in the out of plane wall at run 8 and 9.

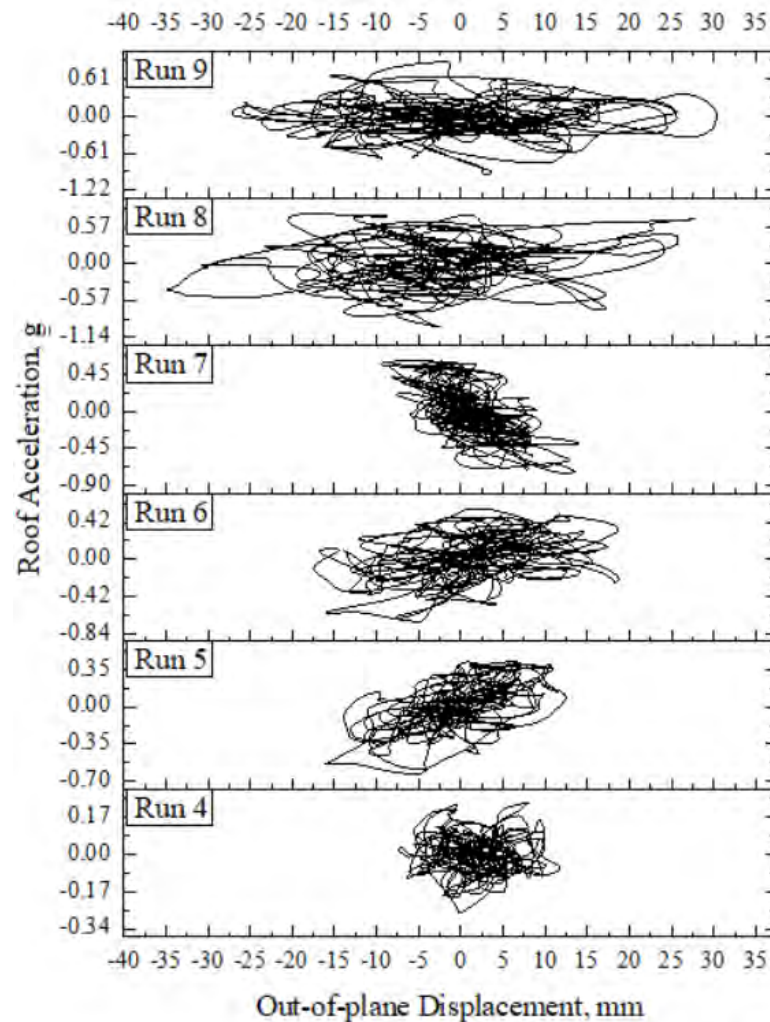


Figure 4.18 Roof Acceleration vs. Relative Lateral Displacement of out-of-plane wall for different input acceleration

4.4.2 Load characteristics of retrofitted model

Lateral Force

For the retrofitted model, lateral force is calculated multiplying the load of the upper half of the model with roof acceleration ignoring damping force. The maximum and minimum lateral forces for one wall are summarize in Table 4.4 for each test run. In-plane and out of plane lateral drift were calculated and the maximum inertia force was normalized by dividing 25.8 kN (sum of slab weight and additional load on roof).

Figure 4.19 depicts the lateral drift and normalized inertia force against input acceleration. Therefore, the comparison of the lateral force was not done.

Table A.4 in Appendix A, the largest input forces are summarized. It is to be noted from the list, the retrofitted model was able to sustain a maximum input force of 75.9kN which is more than 1.4 times greater than the reference model and first crack at base was initiated at this stage (1.49g). All four wall of the model was separated from the base at this stage of run (Run 13).

Table 4.4 Maximum displacement and maximum lateral force of Retrofitted Model

Test Run	F _{max} , kN	F _{min} , kN	In-plane wall		Out of plane wall	
			d _{max} , mm	d _{min} , mm	d _{max} , mm	d _{min} , mm
1	1.41	-2	0.53	-5.09	1.104	-1.02
2	1.7	-1.74	1.88	-2.07	2.42	-2.43
3	1.85	-2.5	0.403	-0.42	2.28	-2.05
4	1.91	-2.59	1.01	-1.04	2.54	-2.46
5	0.98	-1.07	2.41	-2.72	2.3	-2.41
6	3.15	-3.66	0.87	-0.96	3.23	-2.88
7	3.08	-3.95	5.13	-5.49	5.11	-4.79
8	4.76	-4.91	5.55	-5.91	4.85	-4.92
9	4.36	-4.48	0.704	-0.81	6.88	-7.22
10	5.88	-5.43	0.658	-0.689	3.02	-2.88
11	5.93	-5.59	1.053	-0.966	2.98	-3.2
12	7.21	-6.68	0.93	-1.011	2.799	-3.038
13	6.04	-7.6	1.504	-1.6	3.08	-3.57
14	8.11	-6.77	1.36	-1.259	3.04	-3.55

Hysteresis loops

Lateral force at roof level is computed multiplying roof acceleration by roof mass, weight of slab and half of walls weight. The lateral force is then plotted versus measured relative displacement. Using in-plane wall displacement data following hysteresis loop was derived which is depicted in Figure 4.20 following conclusions are derived from the hysteresis loop:

- Although wire mesh is used for the retrofitting purpose, it is clear from the hysteresis loop is that the behavior of retrofitted in-plane wall is not linear.
- From the hysteresis loop reference and retrofitted model, it is clear that wire mesh contributed to increase some linearity of the wall.

- Top deflection at Run 7 and 8 (0.90g and 1.02g) is more than all other excitation. Although no visible cracks were observed until 1.45g (Run 12) acceleration.
- The area enclosed by the hysteresis loop is larger at Run 7 and 8, which indicate more energy dissipation. This is due to the failure of the bricks at internal surface.

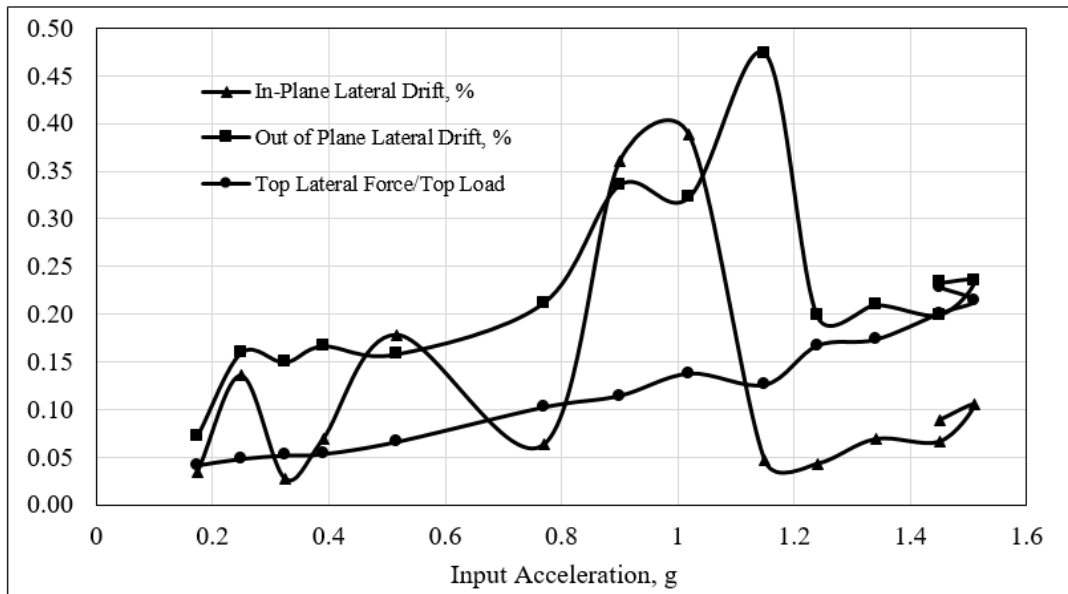


Figure 4.19 Input acceleration vs normalized lateral force and displacement of Retrofitted Model

Same type of force-displacement relationship also derived for out of plane wall, which is shown in Figure 4.21. Roof acceleration versus out-of-plane displacement is constructed because the lateral force will mostly be carried by in-plane wall. It is worth to note the following conclusions from the hysteresis loop:

- The behavior of retrofitted out of plane wall is not linear which is clear from the hysteresis loop. Although it is clear from the comparison of hysteresis loop reference and retrofitted model, wire mesh helps to increase linearity of the wall.
- Maximum deflection of out of plane is seen at Run 7, 8 and 9 (0.90g, 1.02g, 1.15g respectively), which is due to out of plane bending and failure of the bricks at inner surface.

- As the acceleration of the excitation increase, area of the hysteresis loop also increase but rate of increase in not much more (except for the acceleration of 0.90g, 1.02g and 1.15g). Which indicate much energy dissipation than previous excitation.

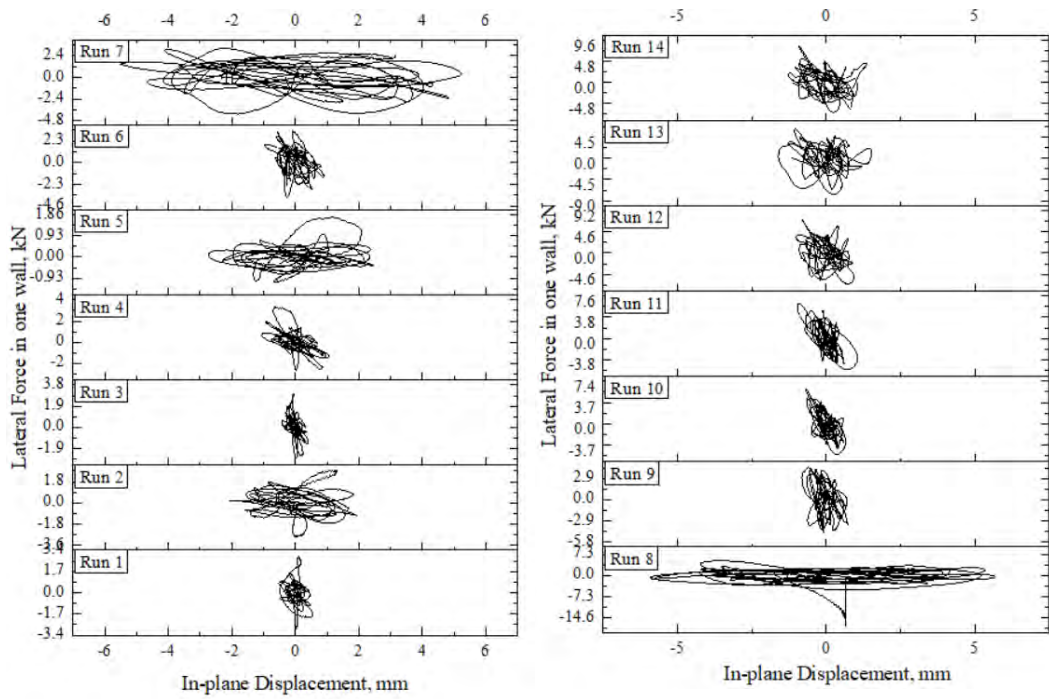


Figure 4.20 Force-Displacement relationship for in-plane wall of Retrofitted Model

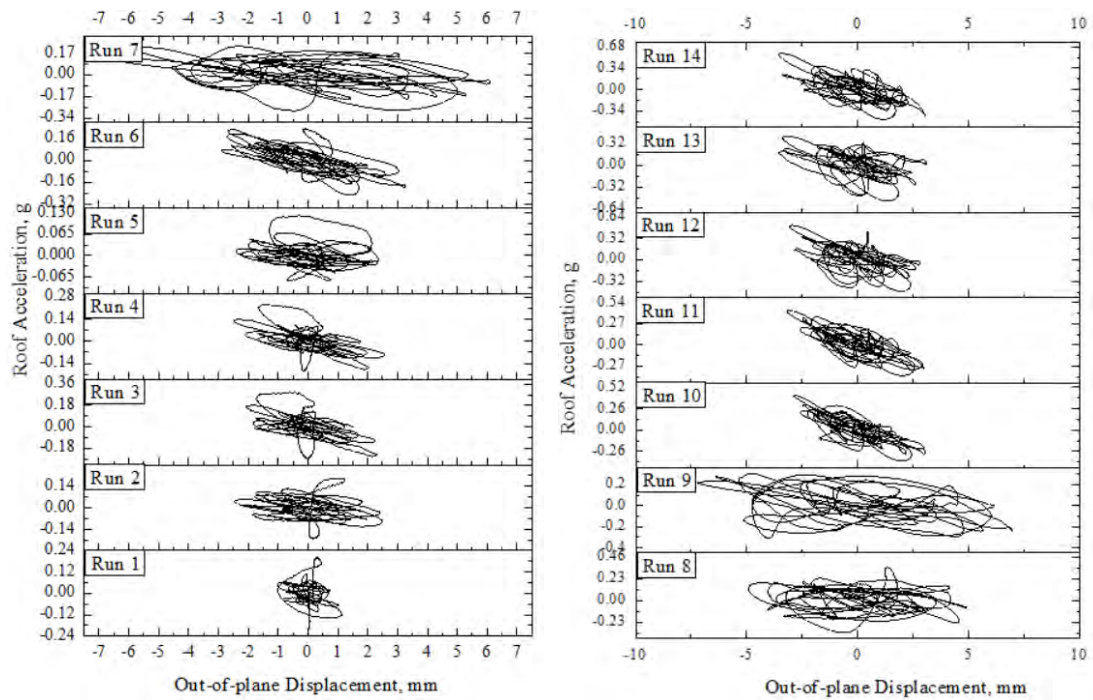


Figure 4.21 Force-Displacement relationship for out-of-plane wall of Retrofitted Model

4.4.3 Tested lateral force and calculated lateral force comparison

For reference model, which is bare structure, maximum calculated lateral force for a in-plane wall is presented in Table 4.3, which is calculated from test data. The maximum lateral force (14.07kN) the bare model structure undergoes at Run 8 (0.92g). From BNBC 1993, the shear force for both in-plane and out-of-plane wall is calculated, which is presented in Appendix A. The lateral load for a in-plane wall is 6.77 kN and for an out of plane wall, it is 5.64 kN. Lateral force calculated from test data will mostly be carried by in-plane wall. The cracks initiated at Run 7 with lateral shear force of 10.8kN, which this is more than the capacity (prescribed value calculated from code). Therefore, it can be concluded that the code is conservative in terms of lateral load resisting capacity.

4.5 Sine Wave Excitation

Sinusoidal signal was selected as the input excitation, which is commonly applied dynamic excitation but is a simple one. Three type of sinusoidal inputs comprising 1Hz, 2Hz, and 3Hz, were designed with low amplitudes (0.5 m/s²) in order to avoid quick collapse, and to obtain a stable response during the whole process. A 30-second excitation was applied in each test to maintain a complete respond process. In Figure 4.22, the acceleration at roof level during the each subsequent test is shown. It is visible that the acceleration decreases as the frequency of the excitation increase. For reference/bare model, the amplification of acceleration was more for 1Hz excitation this is because of resonance. The calculated natural frequency of the model is shown in Appendix A.

4.5.1 Sine wave excitation of reference model

Displacement behavior of the reference model is depicted in Figure 4.23 for sine wave excitation. Lateral displace of the model decrease as the frequency of the sine wave excitation increase. At 1Hz excitation, the lateral displacement is much more than for the 2Hz and 3Hz excitation. This is due to the resonance of the model during 1Hz excitation. The frequency of model is calculated using secant stiffness and considering single degree of freedom system. The calculated natural frequency of the model is shown in Appendix A. For this type of excitation in-plane displacement is slightly more than out of plane displacement.

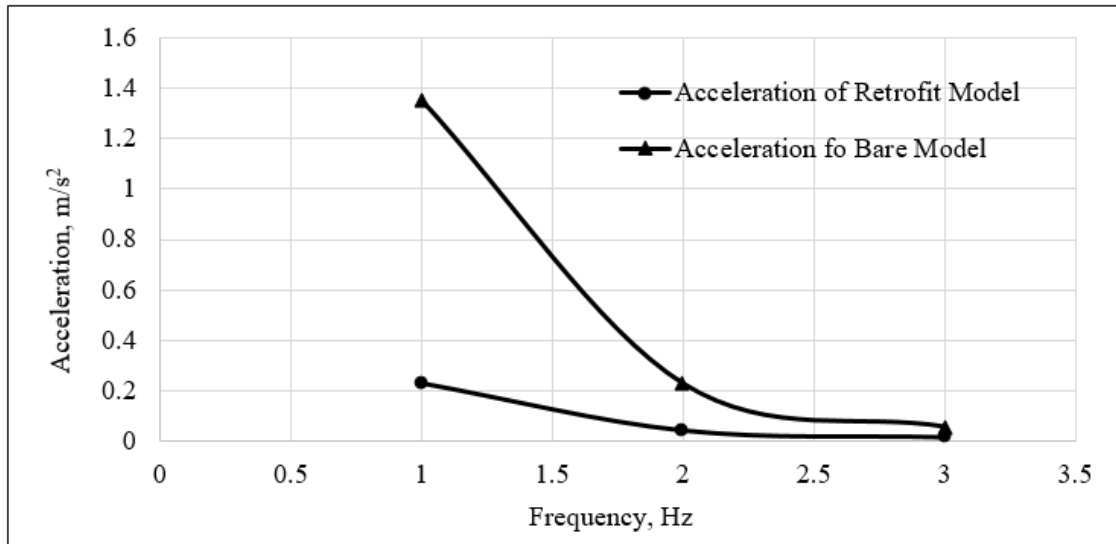


Figure 4.22 Acceleration at Roof Level for Sine Wave Excitation

4.5.2 Sine wave excitation of retrofitted model

Same type of sine wave excitation is used for the retrofitted model. In Figure 4.24 the displacement of the retrofitted model is shown. Decreasing displacement response with the increase of frequency is found for both in-plane and out of plane wall. Displacement for out of plane wall is more than in-plane wall. Frequency of the model was 1Hz during the 1Hz sine wave excitation. That's why the response is more at 1Hz than for the 2Hz and 3Hz excitation. This is also because of resonance. The FFT result of the velocity data of the model for various sine wave excitation is shown in Appendix A.

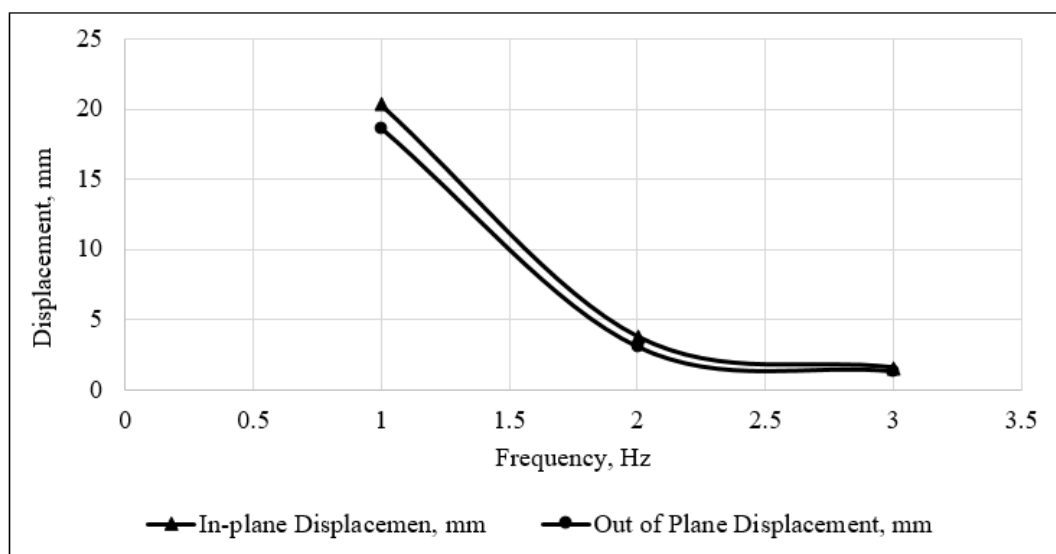


Figure 4.23 In-plane and Out of plane displacement of Reference Model for Sine wave excitation

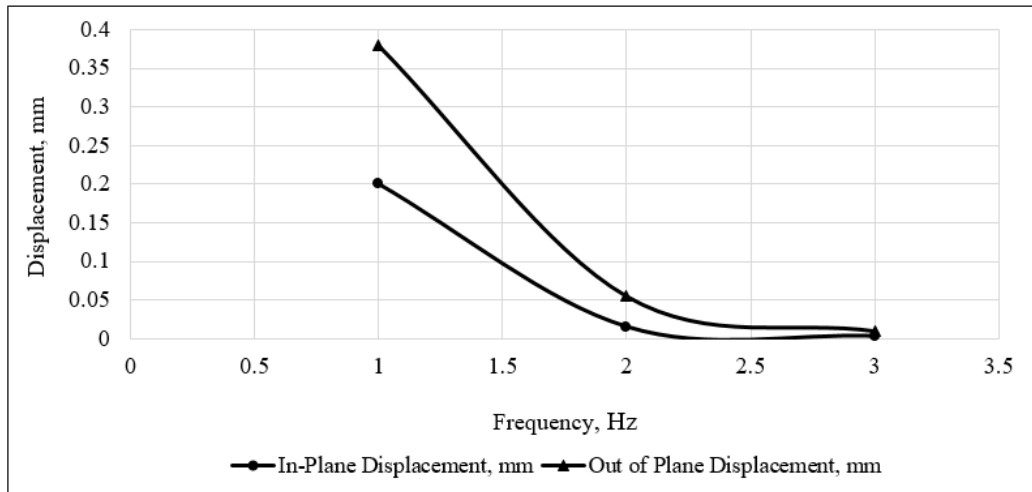


Figure 4.24 In-plane and Out of plane displacement of Retrofitted Model for Sine wave Excitation

Chapter 5

CONCLUSIONS AND SUGGESTIONS

5.1 Introduction

This chapter summarizes the major findings of the present study. The main objective of this study was conducting shaking table test of typical masonry structure of Bangladesh to see the overall response, in-plane wall behavior, out of plane wall behavior, load and deformation characteristics of the walls. In addition, the masonry model was retrofitted using wire mesh to see how the retrofitting increase its behavior. Since dynamic experimental study of masonry structure is not done yet in Bangladesh, only some cyclic test is done so far, it is the demand of time to do some experimental research in this field. Force-displacement relationship of the walls are studied and a normalized lateral drift and lateral force against acceleration is presented. Bangladesh is located in the seismically active region and there are many historical heritage, masonry houses in rural area even in the major cities, which are made by masonry, therefore, the study of dynamic behavior of masonry is important to increase the performance of those buildings in earthquake. Keeping this in mind, the performance of masonry structure retrofitted with locally available material-wire mesh- is studied. It is expected that this research will make a useful help to understand the dynamic behavior of a nonhomogeneous and anisotropic structure. This research will also help to understand how useful a locally available material to increase the performance of structure in an earthquake.

5.2 Conclusions

Behavior of unreinforced masonry room (bare and with retrofit) under dynamic loading were investigated in this study. Based on the results obtained from the experiment of the specimens, the following observations can be drawn:

- i. The cracks in the bare sample are mostly localized in the corner of the wall and those are stair-stepped cracks. Lateral sliding along the bed joints are also visible in the in-plane and out of plane wall. Cracks are mostly generated in the lower 1/3 length of the walls (both in-plane and out of plane wall). Therefore, corners are mostly vulnerable in earthquake.
- ii. First crack was observed in the out-of-plane wall. So special consideration need to be taken in case of design of masonry buildings.

- iii. In retrofitted sample, no visible cracks was observed in the wall except a vertical crack in the in-plane wall. The failure was initiated along the intersection of base. So proper precautionary measures should be taken in the base-wall connection.
- iv. The retrofitted model masonry structures was able to sustain 1.42 times more acceleration than bare model structure.
- v. Retrofitting using wire mesh decrease the deformation of the structure around 4.3 to 4.8 times and increase the capacity of the structure to undergo more acceleration.
- vi. Maximum lateral force at the top of the bare model structure is 14.07kN, which will be carried by one in-plane wall. According to BNBC 1993, shear force limit for this type of model structure is 6.77kN (in-plane wall) and 5.64kN (out of plane wall). The model failed after reaching the capacity. Therefore, the code is conservative or under designed.
- vii. From sine wave excitation, it is clear that both acceleration and lateral force decrease with the increase of frequency (for both bare and retrofitted model) of the excitation.

5.3 Suggestions

The present study was focused on dynamic behavior of unreinforced masonry structure made of Bangladeshi indigenous material. Some recommendations for future studies are presented below:

- i. In this research, dynamic behavior of in-plane and out of plane wall (5" wall thickness) without opening are studied. For better simulation of a typical masonry building of Bangladesh, it is better to perform dynamic test of a masonry structure keeping opening e.g. door, window as per rules of BNBC as well as normal practice.
- ii. Validation of experimental results can be done with numerical simulation.
- iii. Dynamic behavior of masonry structure with 10" wall thickness can be studied.

- iv. Reinforced masonry is also common in Bangladesh. Therefore, it is suggested to see dynamic behavior of reinforced masonry building made indigenous materials.

5.4 Limitations

The additional weights that are put on the slab was not possible to provide inertia force perfectly. The weights did not move monolithically and provided frictional resistance. Moreover, those weights acted as a damper. Therefore, weights should be placed in such a way that it can provide the inertia force.

REFERENCES

- Asif, M. M., Alam, M. Z. and Ahsan, R., “Cyclic Load Test on Ferrocement Retrofitted Masonry Wall Units,” *Proceedings, International Conference on Disaster Risk Mitigation*, Dhaka, Bangladesh, September 23 - 24, 2017.
- Ansary, M.A., “HOUSING REPORT: Single-storey brick masonry house (EMSB1)” *World Housing Encyclopedia*, Report No. 91, March 2003.
- Al Zaman, M.D.A., and Monira, N.J., “A Study of Earthquakes in Bangladesh and the Data Analysis of the Earthquakes that were generated In Bangladesh and Its’ Very Close Regions for the Last Forty Years (1976-2016).” *Journal of Geology and Geophysics*, Vol. 6, pp. 300, 2017.
- Ali, Q., Khan, A.N., Ahmad, N., and Alam, B., “In-Situ Dynamic Testing of Masonry Structure by Means of Underground Explosions Simulating Earthquake Motions, a Unique Case Study.” *Internal Journal of Earth Science and Engineering*, Vol. 05, No. 05, pp 1196-1207, 2012.
- Abrams, D. P., and Lynch, J. M. 2001. “Flexural behavior of retrofitted masonry piers.” *Korea Earthquake Engineering Research Center (KEERC)–Mid America Earthquake Center (MAE) Joint Seminar on Risk Mitigation for Regions of Moderate Seismicity*, Urbana, Ill.
- Bothara, J.K., Dhakal, R.P., Mander, J.B., “Seismic performance of an unreinforced masonry building: An experimental investigation”. *Earthquake Engineering and Structural Dynamics*, Vol. 39(1), pp. 45–68, 2010.
- Benedetti, D., Carydis, P. G., and Pezzoli, P., “Shaking table tests on 24 simple masonry buildings”, *Earthquake Engineering and Structural Dynamics*, Vol. 27, pp. 67–90.
- Benedetti, D., Carydis, P., and Limongelli, M. P., “Evaluation of the seismic response of masonry buildings based on energy functions.” *Earthquake Engineering and Structural Dynamics*, Vol. 30(7), pp. 1061–1081.
- CDMP (2009), “Time-Predictable Fault Modeling of Bangladesh” Comprehensive Disaster Management Programme (CDMP), Ministry of Disaster Management and Relief, Dhaka.

CDMP (2009), “Earthquake Vulnerability Assessment of Dhaka, Chittagong and Sylhet City Corporation Area” Comprehensive Disaster Management Programme (CDMP), Ministry of Disaster Management and Relief, Dhaka.

Candeias, P., Costa, A. C., and Coelho, E., “Shaking table tests of 1:3 reduced scale models of four unreinforced masonry buildings.” *13th World Conference on Earthquake Engineering*, Vancouver, Canada. August 1-6, 2004, Paper No. 2199.

Capozucca, R. “Experimental Analysis of Historic Masonry Walls Reinforced by CFRP Under In-Plane Cyclic Loading,” *Composite Structures*, Vol. 94, pp-277-289, 2011.

Chakravorti, B. K., Kundar, M., Moloy, D. J., Islam, J., and Faruque, S. B., “Earthquake Forecasting In Bangladesh and Its Surrounding Regions.” *European Scientific Journal*, June 2015 edition, vol.11, No.18, pp. 238-244, ISSN: 1857 – 7881 (Print) e - ISSN 1857- 7431

Calderini C, Cattari S, Lagomarsinol S (2009) “In-plane strength of unreinforced masonry piers”, *Earthquake Engineering and Structural Dynamics*, Vol. 38(2), pp. 243–267.

Costa, A. A., Arêde, A., Costa, A., & Oliveira, C. S., “In situ cyclic tests on existing stone masonry walls and strengthening solutions”. *Earthquake Engineering & Structural Dynamics*, Vol. 40(4), pp. 449-471. John Wiley & Sons, Ltd. doi:10.1002/eqe.1046.

Dolce M., Ponzo F.C., Goretti A., Moroni C., Nigro D., Giordano F., De Canio G., Marnetto R., “3D dynamic tests on 2/3 scale masonry buildings upgraded with different systems”, *Proc. 14th World Conference on Earthquake Engineering*, October 12-17, 2008, Beijing, China.

Derakhshan, H., and Ingham, J. M., “Out-of-plane testing of an unreinforced masonry wall subjected to one-way bending”. *In Australian Earthquake Engineering Conference*, AEES 2008. Ballarat, Victoria, Australia.

Derakhshan, H., Ingham, J. M., & Griffith, M. C., “Tri-linear force-displacement models representative of out of-plane unreinforced masonry wall behaviour.” *11th Canadian Masonry Symposium*, May 31-June 3. Toronto, Ontario, 2009.

- Das, T., “Behaviour of Masonry Wall Retrofitted With Ferrocement Under Lateral Cyclic Loading,” *M. Sc Engg. Thesis*, Dept. of Civil Engineering, Bangladesh University of Engineering and Technology, 2016.
- Da Porto, F., Guidi, G., Garbin, E., Modena, C., “In-Plane Behavior of Clay Masonry Walls: Experimental Testing and Finite-Element Modelling”, *Journal of Structural Engineering*. Vol. 136, pp. 1379-1392, 2010.
- Elgawady, M.A., Lestuzzi, P., Badoux, M., “Dynamic In-Plane Behavior of URM Wall Upgraded With Composites,” *3rd ICCI’02*, San Francisco, USA, 2002, Paper No. 009.
- Ersubasi, F. and Korkmaz, H. H., “Shaking Table Tests on Strengthening of Masonry Structures Against Earthquake Hazard,” *Natural Hazards and Earth System Sciences*, Vol. 10, pp-2009-2020, 2010.
- El Gawady, M. A., Lestuzzi, P., and Badoux, M. “Static cyclic response of masonry walls retrofitted fiber-reinforced polymers.” *Journal of Composites for Construction*, Vol. 11(1), pp. 50–61, 2007.
- FEMA P-774 (2009) “Unreinforced Masonry Buildings and Earthquakes”, *Applied Technology Council (ATC)*, California, October 2009.
- Ferreira, T.M., Vicente, R. and Varum, H., and Coar, A.A., “Out-of-plane seismic response of stone masonry walls: an analytical study of a real pier”. *15th World conference on earthquake engineering*, Lisbon, Portugal, 4-28 Sept 2012.
- Fam, A., Musiker, D., Kowalsky, M., and Rizkalla, S., “In-Plane Testing of Damaged Masonry Wall Repaired With FRP,” *Advanced Composite Letter*, Vol. 11, No. 6, 2002.
- Guerrini G., Graziotti F., Penna A., Magenes G., “Dynamic shake-table tests on two full-scale, unreinforced masonry buildings subjected to induced seismicity”, *Proc. of the 7th Int. Conf. on Experimental Vibration Analysis for Civil Eng. Structures*, paper No. 060, San Diego, La Jolla, CA, USA.
- Griffith, M.C., Lam, N.T.K., Wilson, J.L. and Doherty, K., “Experimental investigation of URM walls in flexure”, *Journal of Structural Engineering*, Vol. 130, No. 3, March 1, 2004.

Gautam, D., Rodrigues, H., Bhetwal, K.K., Neupane, P., Sanada, Y., “Common structural and construction deficiencies in Nepalese buildings”, *Innovative Infrastructures Solutions* (2016), <http://dx.doi.org/10.1007/s41062-016-0001-3>.

Hong, N.K., Kim, J. and Mosalam, K., “Seismic Performance of Unreinforced Masonry Building in Low Seismicity Region” *13th World Conference on Earthquake Engineering*, Vancouver, Canada. August 1-6, 2004, Paper No. 953.

Hanazato, T., Minowa, C., Narafu, T., Imai, H., Qaisar Ali, Kobayashi, K., Ishiyama, Y. and Nakagawa, T., “Shaking Table Test of Model House of Brick Masonry For Seismic Construction,” *The 14th World Conference on Earthquake Engineering*, Beijing, China, 12-17 October 2008.

Hamed, E., Rabinovitch, O., “Nonlinear dynamic behaviour of unreinforced masonry walls subjected to out-of-plane loads.” *Journal of Structural Engineering* 2008; Vol. 134(11), pp. 1743–1753.

Hui Su, Jian Wang, Xinpei Jiang, “Shaking table test on building in masonry structure with construction waste recycled brick”, *World Journal of Engineering*, 2014,11(4):357-364.

Islam, M. M., Huda, M. M., Al-Noman, M. N., & Al-Hussaini, T. M., “Attenuation of Earthquake Intensity in Bangladesh”. Proceedings, *3rd International Earthquake Symposium*, Bangladesh, Dhaka, pp. 481-488, 5-6 March 2010.

Kasparik, T., Tait, M. J., and El-Dakhkhni, W. W., “Seismic performance assessment of partially-grouted nominally-reinforced concrete masonry structural walls using shake table testing.” *Journal of Performance of Construction Facilities*, 10.1061/(ASCE)CF.1943-5509.0000416, pp. 217–226.

Kit Miyamoto, H., and Amir S.J.G., “Urban Earthquake Damage Assessment and Reconstruction: 2010 Haiti Earthquake.” *World Conference on Earthquake Engineering*, Lisboa, 2012.

Lang, K., “Seismic vulnerability of existing buildings.” *PhD dissertation*, Institute of Structural Engineering, Department of Civil, Environmental and Geomatics Engineering, Swiss Federal Institute of Technology, Zurich, Switzerland, 2000.

- Lourenço, P.B., Avila, L., Vasconcelos, G., Alves, J.P., Mendes, N., and Costa, A.C., “Experimental investigation on the seismic performance of masonry buildings using shaking table testing”. *B. Earthq. Eng.*, Vol. 11(4), pp. 1157-1190.
- Macabuag, J., Guragain, R., and Bhattacharya, S., “Seismic retrofitting of non-engineered masonry in rural Nepal,” *Proceedings of the Institution of Civil Engineers-Structures and Buildings*, Vol. 165, Issue 6, pp. 273-286, 2012.
- Moon, F. 2004. “Seismic strengthening of low-rise unreinforced structures with flexible diaphragms.” *Ph.D. dissertation*, Georgia Institute of Technology.
- Moffet, P., “Report: The Sustainability of Masonry in Construction Today” *Masonry Worx*, April 2016.
- Nakagawa, T., Narafu, T., Imai, H., “Collapse behavior of a brick masonry house using a shaking table and numerical simulation based on the extended distinct element method.” *Bulletin of Earthquake Engineering*, Vol. 10, pp. 269–283, 2012.
- Ohsumi, T., Mukai, Y., and Fujitani, H., “Investigation of damage in and around Kathmandu Valley related to the 2015 Gorkha, Nepal earthquake and beyond”, *Geotechnical and Geological Engineering*, Vol. 34, pp. 1223–1245, 2016.
- Russell, A.P., Mahmood, H. and Ingham, J.M., “Pseudo-Static In-Plane Testing of Typical New Zealand Unreinforced Masonry Walls,” *8th Pacific Conference on Earthquake Engineering (8PCEE)*, Singapore, 2007, Paper No. 100.
- Shaw, R., Mallick, F., and Islam, A., “*Disaster Risk Reduction Approaches in Bangladesh*”. Springer, pp. 103, 2013.
- Shawa, Al. O, de. Felice, G., Mauro, A. and Sorrentino, L., “Out-of-plane seismic behaviour of rocking masonry walls”. *Earthquake Engineering and Structural Dynamics*, Vol. 41, pp. 949–968. doi: 10.1002/eqe.1168.
- Shi, Y., D'Ayala, D., & Prateek, J., “Analysis of Out-of-Plane Damage Behaviour of Unreinforced Masonry Walls”. *Paper presented at 14th International Brick & Block Masonry Conference*, Sydney, Australia, 2008.
- Simsir, Can. C., Aschheim, M.A., Abrams, D.P., “Out of Plane Dynamic Response of Unreinforced Masonry Bearing Walls Attached to Flexible Diaphragms,” *13th World*

Conference on Earthquake Engineering, Vancouver, B.C., Canada, Paper No. 2045, 1-6 August 2004.

Tondelli, M., Petry, S., Peloso, S. and Beyer, K., "Shake-table test on a four-storey structure with reinforced concrete and unreinforced masonry walls" *Vienna Congress on Recent Advances in Earthquake Engineering and Structural Dynamics (VEESD 2013)*, 28-30 August 2013, Vienna, Austria, Paper No. 346.

Wight, G. D.; Kowalsky, M. J.; Ingham, J. M. (2007). "Shake Table Testing of Posttensioned Concrete Masonry walls with Openings." *Journal of Structural Engineering*, Vol. 133 (11), pp. 1551–1559.

Yeats, R. S., Sieh, K. and Allen, C. R., "*The geology of earthquakes.*" Oxford University Press, pp. 568, 1997.

Appendix A

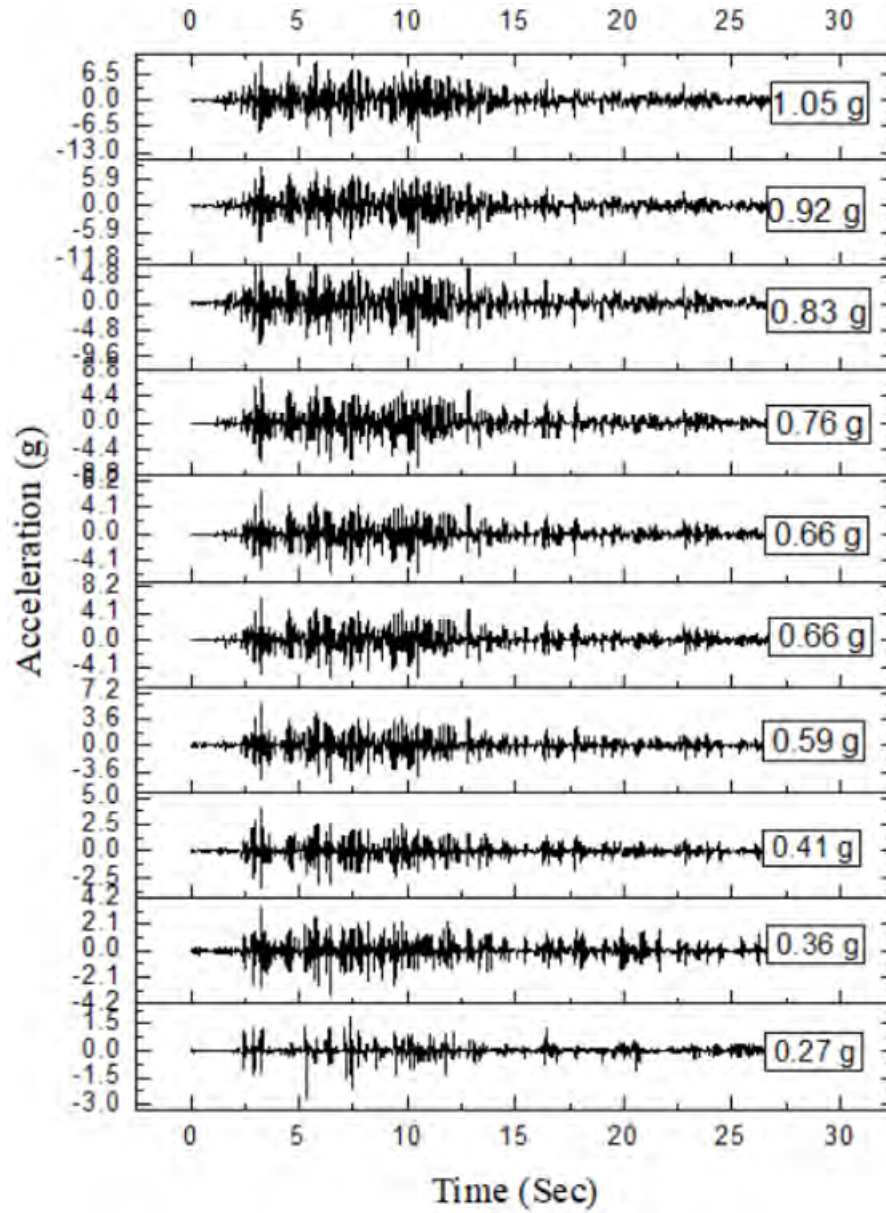


Figure A.1: Input Motion for Reference Model (table acceleration in g)

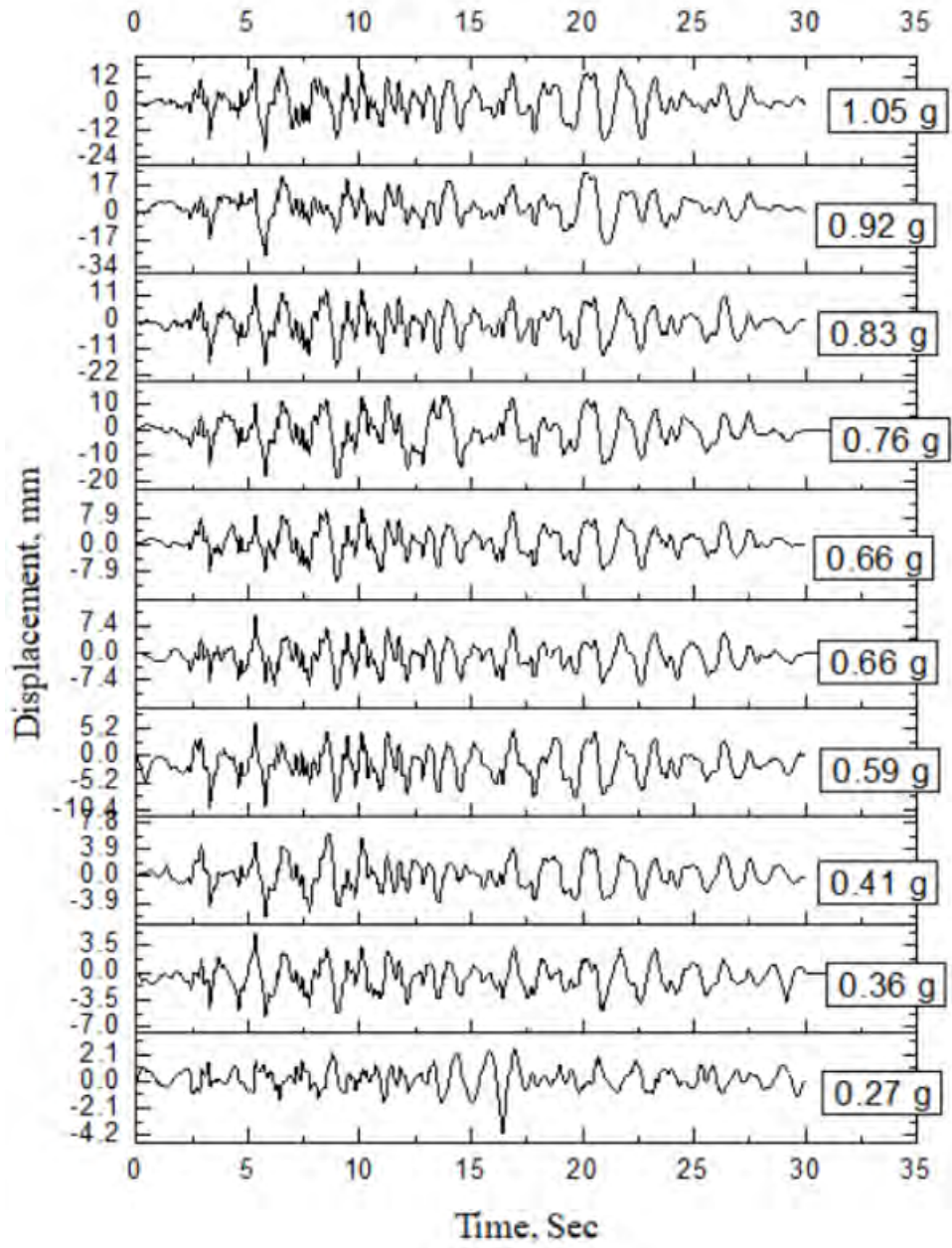


Figure A.2: Corresponding Displacement value of Input Motion for Reference Model

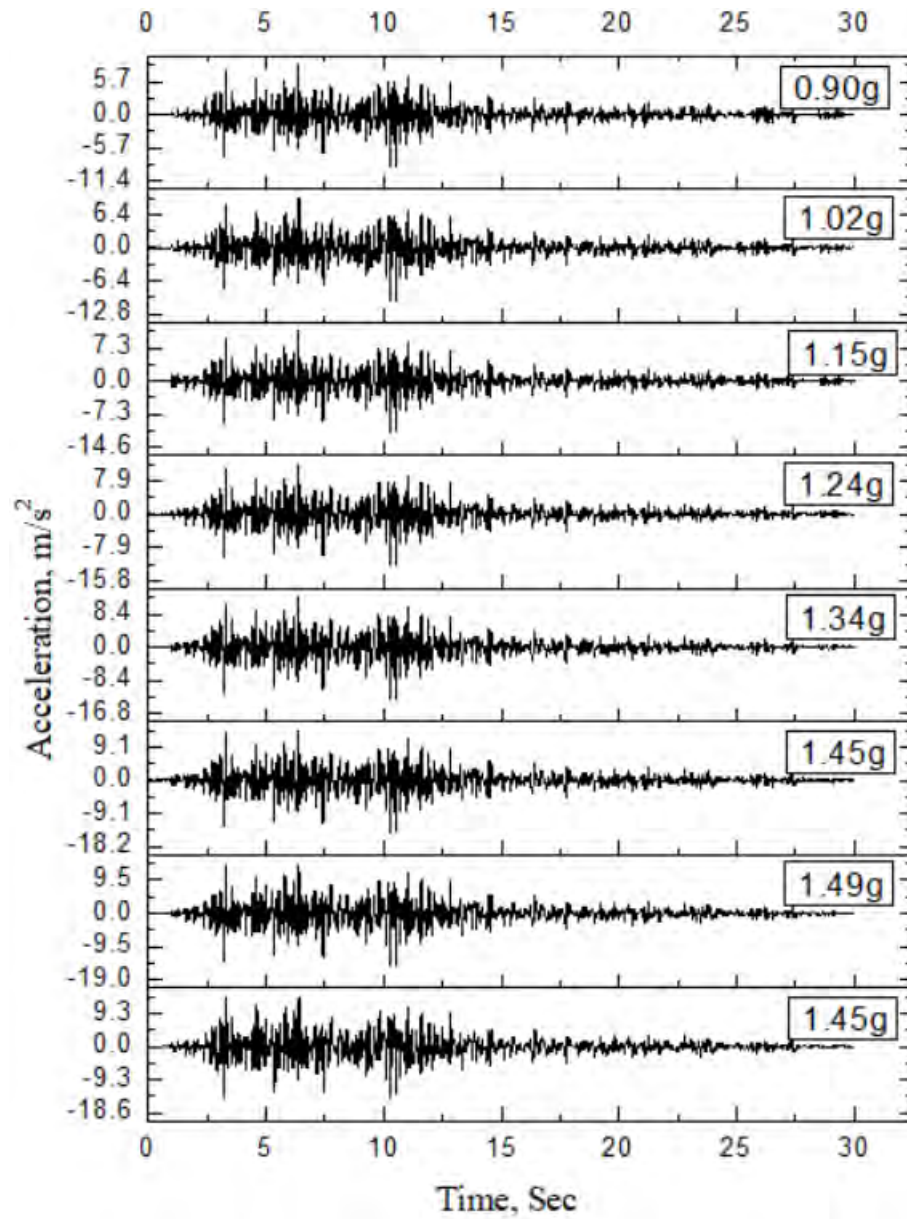


Figure A.3: Input Motion for Retrofitted Model

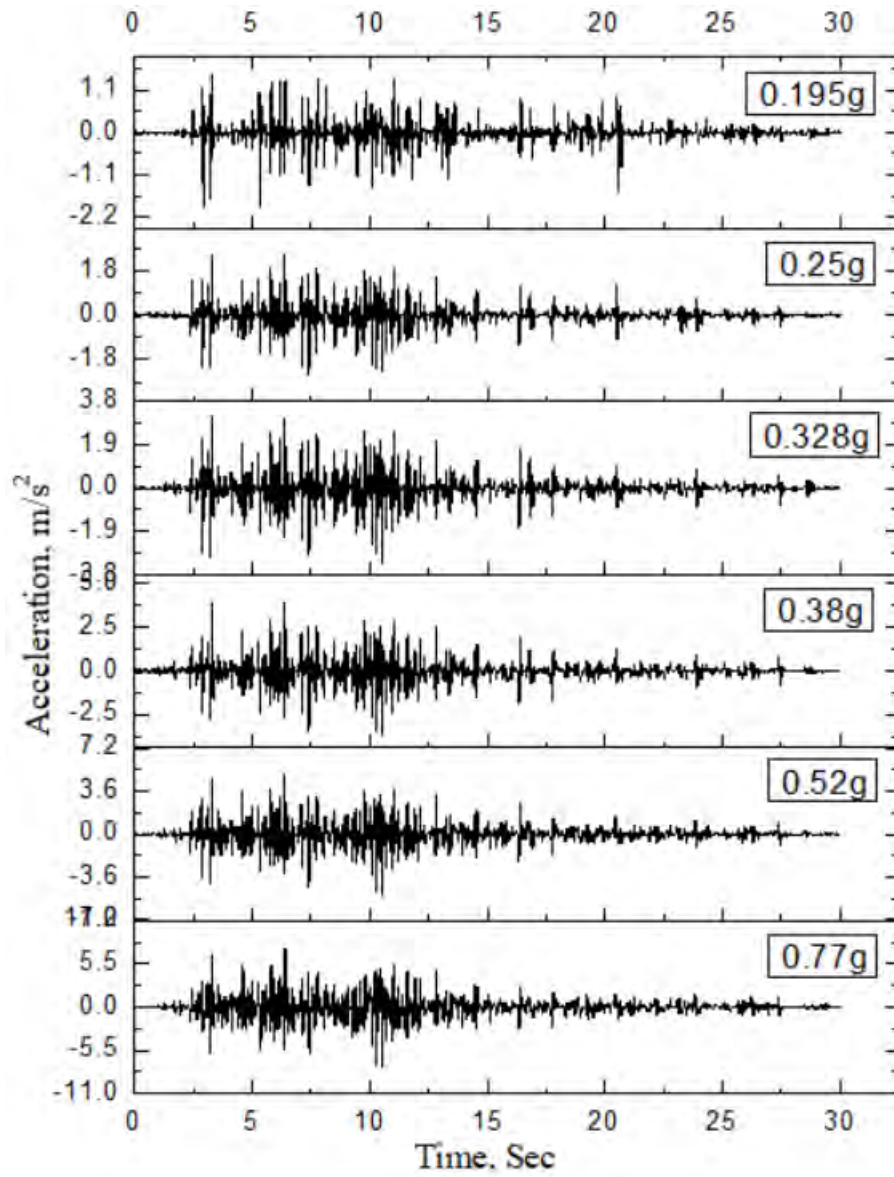


Figure A.4: Input Motion for Retrofitted Model

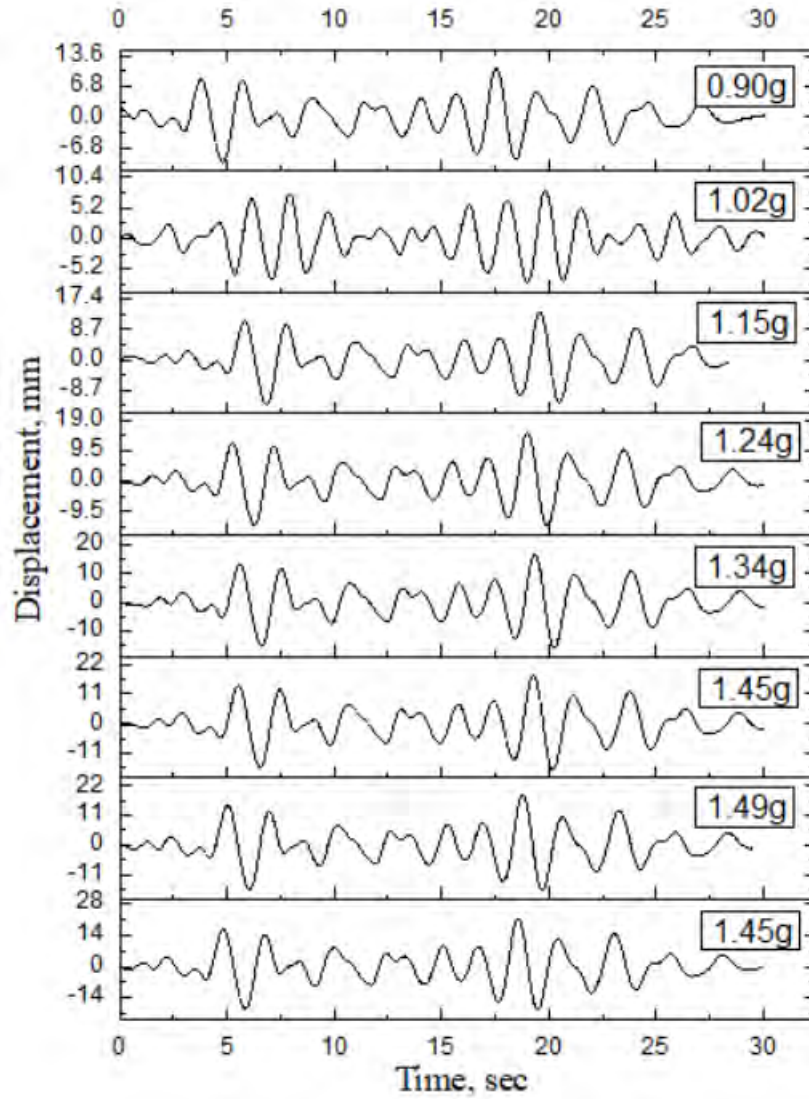


Figure A.5: Corresponding Displacement of Input Motion for Retrofitted Model

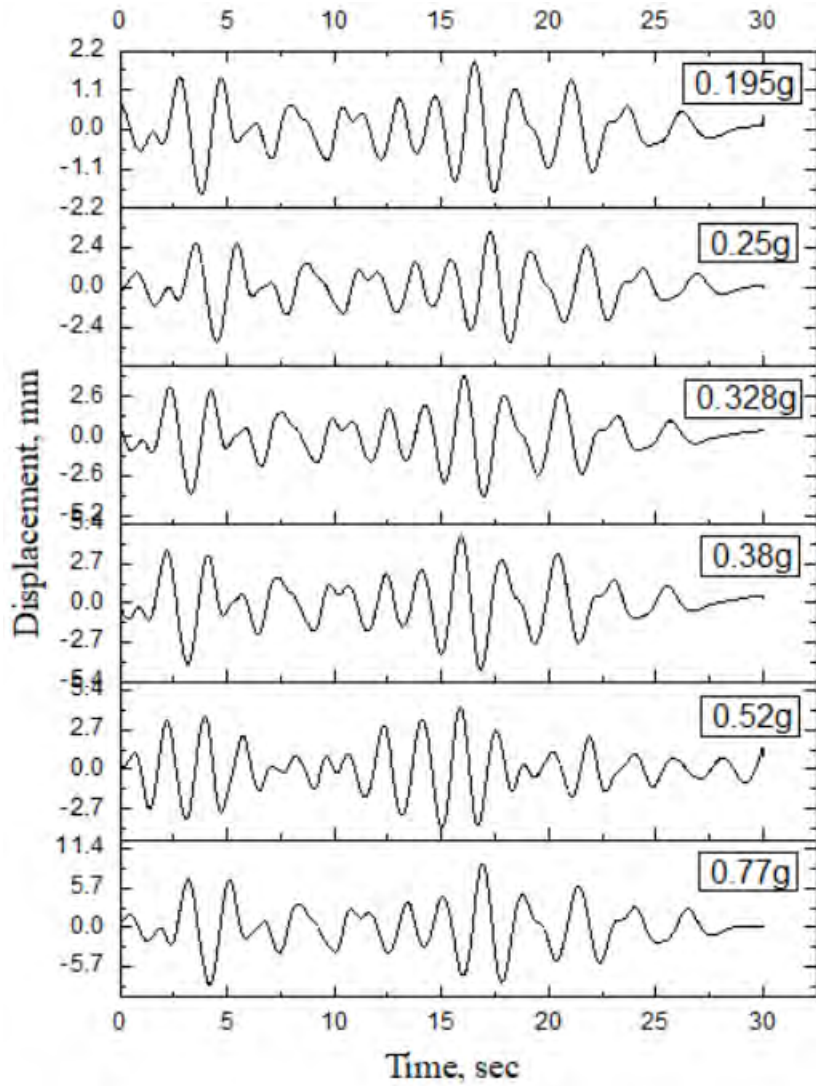


Figure A.6: Corresponding Displacement of Input Motion for Retrofitted Model

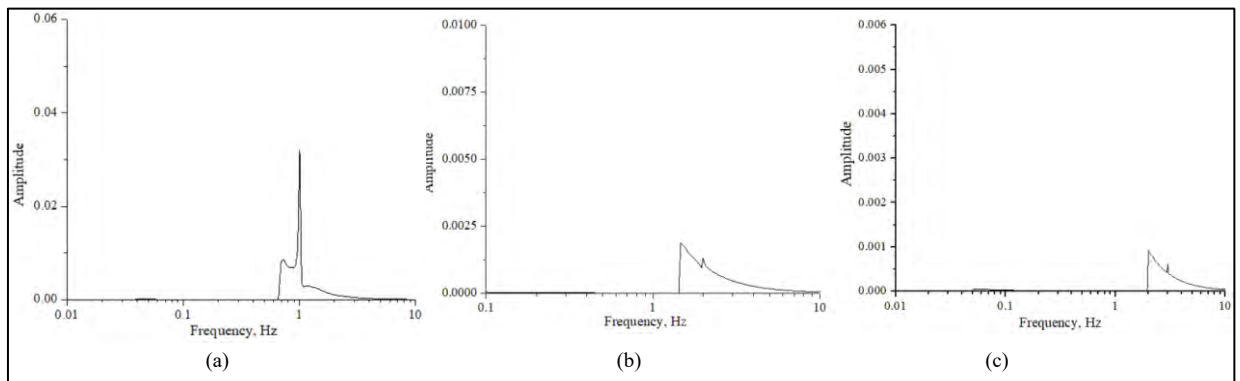


Figure A.7: FFT of Sine wave excitation for Retrofitted Model ((a) 1Hz, (b) 2Hz, (c) 3Hz)

Table A.1: Largest two acceleration pecks and occurrence time of Reference Model

		Base		Top	
Run 1	Time, sec	5.35	7.46	8.44	15.4
	Acceleration, g	-0.265	-0.216	0.13	-0.17
Run 2	Time, sec	3.275	6.46	6.68	9.94
	Acceleration, g	0.354	-0.356	-0.202	-0.21
Run 3	Time, sec	3.225	3.28	4.38	7.99
	Acceleration, g	0.35	0.41	0.22	-0.24
Run 4	Time, sec	3.28	6.465	8.4	8.72
	Acceleration, g	0.59	-0.51	0.23	-0.27
Run 5	Time, sec	3.275	10.49	9.94	11.9
	Acceleration, g	0.66	-0.588	-0.64	-0.59
Run 6	Time, sec	3.29	10.5	5.19	7.16
	Acceleration, g	0.72	0.76	-0.703	-0.66
Run 7	Time, sec	5.78	10.485	8.91	13.52
	Acceleration, g	0.75	0.83	-0.75	-0.705
Run 8	Time, sec	3.285	10.49	8.15	10.12
	Acceleration, g	0.86	-0.92	-0.98	-0.82
Run 9	Time, sec	3.275	10.48	10.39	13.84
	Acceleration, g	0.94	1.05	-0.95	0.88

Table A.2: Largest two displacement and occurrence times of Reference Model

		In-plane		Out of Plane		Base	
Run 1	Time, sec	15.74	16.42	16.41	16.93	16.42	16.96
	Displacement, mm	2.93	4.34	3.85	3.25	4.05	2.56
Run 2	Time, sec	20	20.9	5.29	5.77	5.37	5.78
	Displacement, mm	5.54	6.13	4.44	5.64	4.8	5.56
Run 3	Time, sec	2.89	8.62	5.8	7.76	5.79	8.61
	Displacement, mm	5.3	6.22	8.35	8.25	5.86	6.17
Run 4	Time, sec	3.3	13.6	3.275	5.79	3.28	5.78
	Displacement, mm	9.34	8.89	10.04	11.58	9.84	9.56
Run 6	Time, sec	6.47	16.8	8.51	10.07	8.97	10.07
	Displacement, mm	17.06	21.5	13.82	16.1	10.83	10.69
Run 7	Time, sec	9.04	16.82	5.795	9.01	5.79	8.97
	Displacement, mm	16.31	21.6	18.475	18.23	18.22	18.57
Run 8	Time, sec	9.015	16.81	3.29	8.94	5.78	8.96
	Displacement, mm	16.385	21.5	13.79	13.27	18.54	19.24
Run 9	Time, sec	9.45	20.01	6.54	20.09	5.78	20.23
	Displacement, mm	25.5	21.54	30.59	34.7	26.78	24.68
Run 10	Time, sec	9.25	9.75	21.01	21.73	5.78	6.52
	Displacement, mm	17.45	16.28	30.35	27.09	21.84	16.71

Table A.3: Largest two input forces and occurrence time of Reference Model

Run	Time, Sec	Input Forces, kN
1	5.34	-13.4
	7.425	-11.0
2	3.275	18.0
	6.46	-18.1
3	3.285	21.1
	3.225	-17.75
4	3.28	29.9
	6.465	-26.0
5	3.275	33.7
	6.465	-29.8
6	3.28	38.4
	10.495	38.36
7	5.775	40.5
	10.485	-42.29
8	3.285	43.67
	10.485	-46.65
9	10.48	-53.12
	3.275	47.89

Table A.4: Largest two input forces and occurrence time of Retrofitted Model

Run	Time, Sec	Input Forces, kN
1	2.925	-9.86
	5.34	-9.88
2	6.38	12.6
	7.41	-12.6
3	3.298	15.9
	10.50	-16.7
4	6.38	19.9
	3.29	-19.5
5	6.38	25.4
	10.5	-26.2
6	6.40	38.4
	10.51	-39.0
7	10.26	-45.6
	10.5	-45.6
8	10.52	-51.7
	10.275	-51.3
9	10.259	-58.10
	10.5	-57.0
10	10.501	-52.8
	10.263	-61.4
11	10.499	-67.9
	10.259	-66.9
12	10.259	-73.5
	10.498	-70.9
13	10.263	-75.9
	10.505	-75.7
14	3.215	73.66
	3.32	71.63

Shear Stress for Shear Walls

Unreinforced masonry walls,

For clay units $F_v = 0.025\sqrt{f'_m} \leq 0.40 \text{ N/mm}^2$

Where, f'_m = specified compressive strength of masonry at the age of 28 days

For In-plane wall,

Length, $L=6'$ =1828 mm; thickness, $t=2.25'$ =57 mm

$F_v = 0.025\sqrt{f'_m}$

$=0.025*\sqrt{6.75} = 0.06495 \text{ N/mm}^2 = 0.0565*104196 = 6.77 \text{ kN}$

For Out of Plane wall,

Length, $L=5'$ =1524 mm; thickness, $t=2.25'$ =57 mm

$F_v = 0.025\sqrt{f'_m}$

$=0.025*\sqrt{6.75} = 0.06495 \text{ N/mm}^2 = 0.0678*86868 = 5.64 \text{ kN}$